SANDIA REPORT
SAND2017-0414
Unlimited Release
Printed January 2017

UFD Expert Panel on Chloride Induced Stress Corrosion Cracking of Interim Storage Containers for Spent Nuclear Fuel

Moderated and Assembled by D.G. Enos (Sandia National Laboratories)

C.R. Bryan (Sandia National Laboratories)
P.L. Andresen (GE Global Research Center)
R.G. Kelly (University of Virginia)
J.R. Scully (University of Virginia)
A. Turnbull (National Physical Laboratory, United Kingdom)

Prepared by
Sandia National Laboratories
Albuquerque, New Mexico 87185 and Livermore, California 94550

Sandia National Laboratories is a multi-mission laboratory managed and operated by Sandia Corporation, a wholly owned subsidiary of Lockheed Martin Corporation, for the U.S. Department of Energy's National Nuclear Security Administration under contract DE-AC04-94AL85000.

Issued by Sandia National Laboratories, operated for the United States Department of Energy by Sandia Corporation.

Available to DOE and DOE contractors from
U.S. Department of Energy
Office of Scientific and Technical Information
P.O. Box 62
Oak Ridge, TN 37831

Telephone: (865) 576-8401
Facsimile: (865) 576-5728
E-Mail: reports@osti.gov
Online ordering: http://www.osti.gov/scitech

Available to the public from
U.S. Department of Commerce
National Technical Information Service
5301 Shawnee Rd
Alexandria, VA 22312

Telephone: (800) 553-6847
Facsimile: (703) 605-6900
E-Mail: orders@ntis.gov
Online order: http://www.ntis.gov/search

SAND2017-0414
Unlimited Release
Printed January 2017

UFD Expert Panel on Chloride Induced Stress Corrosion Cracking of Interim Storage Containers for Spent Nuclear Fuel

D.G. Enos
Materials Reliability

C.R. Bryan
Storage and Transportation Department

Sandia National Laboratories
P.O. Box 5800
Albuquerque, New Mexico 87185-MS0888

Abstract

This report summarizes the outcome of an expert panel review of a key degradation phenomenon identified for atmospherically exposed austenitic stainless steel containers used for the interim dry storage of used nuclear fuel – specifically, chloride induced stress corrosion cracking due to the presence of atmospherically deposited salts. The expert panel consisted of Dr. Peter Andresen (GE Corp Research & Development), Dr. Robert G. Kelly (University of Virginia), Dr. John R. Scully (University of Virginia), and Dr. Alan Turnbull (National Physical Laboratory) and was moderated by Dr. David G. Enos (Sandia National Laboratories). In addition to the above subject matter experts, participants from Sandia National Laboratories, Savannah River National Laboratory, Pacific Northwest National Laboratory, and the Southwest Research Institute will be present. Input from the panel members for a series of preliminary questions dealing with the subject area, along with the meeting minutes, presentation materials, and final recommendations are included here.

CONTENTS

NOMENCLATURE

ASME	American Society of Mechanical Engineers
ASTM	ASTM International
B&PVC	Boiler and Pressure Vessel Code
CISCC	Chloride Induced Stress Corrosion Cracking
CGR	Crack Growth Rate
CoC	Certificate of Compliance
CRIEPI	Central Research Institute of Electric Power Industry
CT	Compact Tension
DCPD	Direct Current, Potential Drop
DOE	Department of Energy
EPRI	Electric Power Research Institute
IGSCC	Intergranular Stress Corrosion Cracking
ISFSI	Independent Spent Fuel Storage Installation
K	Stress Intensity
NRC	Nuclear Regulatory Commission
SCC	Stress Corrosion Cracking
SENT	Single Edge Notched Tension
SKP	Scanning Kelvin Probe
SNF	Spent Nuclear Fuel
SNL	Sandia National Laboratories

1. INTRODUCTION

In the US, spent nuclear fuel is likely to remain in interim dry storage until a permanent disposal solution has been developed and placed into operation. The majority of current dry storage systems consist of a welded 304 stainless steel container located within a concrete or steel overpack. The welded container serves as the primary confinement barrier, protecting the fuel from the outside environment. The containers are passively cooled, utilizing ambient air drawn through the overpack and across the container surface. A portion of the atmospheric aerosols carried by the air are deposited on the container surface. These include soluble salts, the composition of which varies with geographic location, but which is some cases are chloride bearing. With time, as the canister surface cools, these salts will deliquesce to form potentially corrosive chloride-rich brines. As austenitic stainless steels are prone to chloride-induced stress corrosion cracking (CISCC), the concern exists that SCC may significantly impact long-term canister performance, particularly for systems located in marine environments.

Presently, there is a rather poor understanding of what governs this cracking process under atmospheric conditions, and how best to characterize each step of the process (localized corrosion nucleation and growth, the pit to crack transition, and the crack growth process) such that the information could be incorporated into a predictive model that might be used to assess the risk of SCC at various spent fuel storage installations. To begin to address this data gap, a panel of world recognized subject matter experts in the area of stress corrosion cracking and atmospheric corrosion was assembled to discuss and make recommendations as to the path forward on the evaluation of this complex corrosion phenomenon.

The panel consisted of:

Dr. Peter Andresen (GE Global Research Center)

Dr. Robert Kelly (University of Virginia)

Dr. John Scully (University of Virginia)

Dr. Alan Turnbull (National Physical Laboratory)

The panel was tasked with addressing three primary areas of concern for atmospherically exposed, austenitic stainless steel interim storage containers – (1) Localized corrosion initiation and growth, (2) Processes that govern crack initiation, and (3) The crack propagation process. The panel provided input on each of these areas (enclosed in the following sections) as well as participating in the panel review. The meeting was moderated by David Enos (Sandia National Laboratories). The meeting attendees included (in addition to the panel):

David Enos (Sandia National Laboratories) – Moderator

Charles Bryan (Sandia National Laboratories)

Sylvia Saltzstein (Sandia National Laboratories)

Ken Sorenson (Sandia National Laboratories)

Peter Swift (Sandia National Laboratories)

Darrell Dunn (Nuclear Regulatory Commission)

Brady Hansen (Pacific Northwest National Laboratory)
Mychailo Tolozcko (Pacific Northwest National Laboratory)
Andrew Duncan (Savannah River National Laboratory)
Brenda Garcia-Diaz (Savannah River National Laboratory)
Jim Dante (Southwest Research Institute)
Todd Mintz (Southwest Research Institute)

2. PRELIMINARY QUESTIONS

The focus of this expert panel review is atmospheric CISCC of austenitic stainless steels. Prior to the panel review, a series of questions were provided to each panel member. The purpose of these questions was not to assemble an extensive document prior to the meeting, but rather to enable each panel member to organize their thoughts prior to beginning discussions. The three topics are localized corrosion nucleation and propagation, the transition from localized corrosion to stress corrosion cracking – or more specifically, the nucleation and early growth of stress corrosion cracks, and finally, the stable propagation of stress corrosion cracks.

1. Localized Corrosion. SCC in atmospherically exposed stainless steels has typically been observed to initiate from localized corrosion sites, and as such, understanding the processes that govern localized corrosion initiation and growth is critical in assembling any predictive model for fielded structures. In your opinion, what are the key processes that govern localized corrosion under atmospheric conditions in terms of the induction period prior to pit nucleation, the sites from which meaningful/stable pits nucleate, and the growth of stable pits? Please include your view both on what processes and microstructural features are important, and on how they might be captured experimentally.
2. Crack initiation. In the literature, SCC crack initiation on austenitic stainless steels under atmospheric conditions is believed to take place from localized corrosion sites. In your opinion, what are the key factors that determine when a pit is likely to result in the nucleation of a crack in terms of its size, internal chemistry, and relation to the underlying microstructure and stress field? In addition, what are your thoughts on how the pit to crack transition might be captured/observed experimentally?
3. Crack Propagation. Once an SCC crack has initiated, understanding the rate at which it will propagate as a function of environmental conditions is critical, particularly for aging management programs/inspection plans, the development of the ASME B&PVC code case, and so on. Chloride driven SCC cracks in austenitic stainless steels observed in the field tend to be highly branched in nature, hindering effective evaluation of their depth, or assessment of their geometry simply by observing the surface. In the corrosion literature, many different views have been expressed in terms of the required surface chemistry, salt load or brine layer characteristics, location of the cathode supporting crack propagation, and underlying microstructural features of importance. In your opinion, what are the critical conditions and processes that govern atmospheric SCC crack propagation? In addition, given the documented difficulties in determining accurate crack growth rate measurements for atmospheric SCC cracks, how might this issue be attacked experimentally?

2.1 Response from Peter Andresen (GE Global Research Center)

The brief background initially provided, and several questions that we were asked to respond to, are listed at the end. My exposure to the details of this issue is limited, but it shares may things in common with problems that have long occurred in stainless steels exposed to chlorides. In particular, there have been extensive problems with cracking in stainless steel piping at nuclear plants exposed to the atmosphere. Many of these problems are aggravated by the direct exposure of the piping to the atmosphere, but I believe some occur in semi-protected areas that perhaps have many things in common with spent nuclear fuel (SNF) canisters.

Analysis, understanding, experimental evaluation, and prediction of these atmospheric corrosion problems are complicated by variability and ambiguity in the salt level and composition, the air flow rate, the changing relative humidity and outside temperature, other atmospheric contaminants (in addition to salt), the heat flux from the SNF canister, the orientation (e.g., vertical vs. inverted vs. horizontal) of the surfaces, the nature of the surface (cold work, grinding, contaminants, etc.), etc. While deliquescence can create liquid films on the surface, they may not be stable/permanent. Even when the salt composition on the surface is known, the composition and pH of the solution that is formed can vary with relative humidity. The thickness of the liquid film and its ability to provide sufficient liquid and salt to drive pitting and cracking poses additional experimental and modeling challenges.

A primary challenge in addressing this problem is the 'environment scenario'. There are few measurements of the salt loading on the canisters, and also limited understanding of the aqueous film chemistry that develops at low relative humidity (i.e., very concentrated salt solutions). A further challenge is the transient nature of the conditions – changing temperature, changing relative humidity, changing atmospheric conditions and contaminant, etc. Without a well-defined boundary on the 'environment scenario', there will forever be challenges in the acceptance of the corrosion and SCC data and models.

More specific comments on each of the questions posed to the panel are summarized below.

1. Localized Corrosion. There is little question that pitting and crevice corrosion can occur in stainless steels in environments high in chloride. The exact conditions under which pitting and crevice corrosion will develop vary with chloride concentration, pH, temperature, oxygen concentration, metal surface condition including exposed MnS inclusions, etc. While MnS inclusions are often a preferred initiation site, there are typically a myriad of surface defects from machining, welding, grinding, etc. that are often pit initiation sites.

   The need to model both the surface chemistry and the probability and density of pitting depends on how critical these processes are to predicting through-wall penetration. For example, it seems very unlikely that pitting can proceed through-wall given the dimensions of the wall of the SNF canister. So the primary value of a pitting model may be to help predict the onset of SCC. As noted in the response to the third question, this is very valuable provided it is not viewed as the only possibility scenario for SCC initiation and growth – that is, SCC should occur more rapidly under such circumstances, but could also occur in the absence of pitting.

2. Crack initiation. The history of SCC studies is that most focus on high SCC susceptibility situations using relatively simplistic and short-term tests, and such studies fail to capture the

moderate and subtle conditions that become important after 5+ years of exposure. There is no question that SCC can develop from the base of pits, and a common approach to estimating the transition to SCC uses the stress intensity factor at the base of a pit, which might not be hemispherical and might include some intergranular morphology. The growth rate of the pit is at least as important as the internal chemistry, because high pitting corrosion rates blunt an incipient cracking tendency. SCC might develop from smaller pits as the pit growth slows for any of various reasons.

This is an area where aqueous experiments are valuable – it can be very difficult to address issues such as chemistry and pit-to-crack transitions in an experimentally complex system involving water films at varying relative humidity. The SNF canister benefits from being a very statically stressed system – it seems reasonable to assume that there are no cyclic stresses present. Experiments might employ a tapered specimen tested at constant load that is both pre-pitted and pitted under load to identify the stress and pit size that lead to SCC, and perhaps characterize whether the transition to SCC is inhibited in an actively growing (high corrosion rate) pit, which can be measured independent of the development of cracking.

3. Crack Propagation. SCC is challenging to study well, and there is a historical tendency to perform experiments that are sensitive only to relatively severe SCC, then assume SCC will not occur under less aggressive conditions. This has been a major problem in high temperature water, and increasingly sophisticated experiments with very high crack length resolution have been needed to understand the vulnerability to SCC over long times. Such experiments have been conducted at temperatures near and below 100 °C, and show quite high growth rates in sensitized stainless steel and other materials even in pure, deaerated water – conditions that are dramatically less aggressive than those needed for pitting and crevice corrosion. The contribution of stress and dynamic strain can create a dramatically different 'environment' that supports SCC than is the case with pitting and crevice corrosion, which rely solely on the chemical and metallurgical 'environment'.

Nonetheless, SCC usually initiates and grows faster under such aggressive conditions, with the exception of blunting when the corrosion rate exceeds the nominal SCC growth rate. Thus, experiments should employ the techniques and sophistication developed to study moderate and subtle forms of SCC in higher temperature water, and should scope out the spectrum of environments from pure water to high chloride, varying pH, varying aeration environments, varying temperature, etc. Many of these scoping experiments can be done in fully aqueous conditions, but experiments must also be done under varying relatively humidity conditions to evaluate how differently SCC develops under the same nominal conditions, but with water films and limited surface salt loading potentially affecting how fast SCC growth can occur. The supply of water to the crack may be less challenging because capillary condensation tends to promote formation of liquid water at lower relative humidity levels. The supply of salt could retard SCC growth rates, but since many cracks are very tight (low liquid volume) and SCC might not require the severe chemistry associated with pitting, salt-supply may not be a controlling factor.

SCC testing must recognize that there are times when SCC slows and stops, but if the crack is re-activated, it can be sustained for very long periods of time. So one or two observations –

especially those showing crack retardation or arrest – have to be more extensively evaluated and reproduced to have confidence in the result. Engineering structures have thousands or millions of opportunities for cracks to develop and grow, and one laboratory observation on a single specimen is almost certain to be misleading. Conversely, it is certainly possible that cracking is not sustained with changing temperature, relative humidity, etc. from day-to-day and month-to-month.

2.2 Response from Dr. Robert Kelly (University of Virginia)

1. Localized Corrosion. With respect to the long-term performance of the dry casks, I don't think induction time is relevant because of the length of the time considered. No defensible technical argument can be made based on initiation NOT occurring without having exposures for times GREATER than the time period of interest that exactly mimic the conditions to which the canisters are exposed. It would seem that understanding limitations on pit growth rate/extent could form the basis for such an analysis. The type of microstructural/geometry sites of importance would be: (a) MnS inclusions, (b) surface roughness, (c) deposits, and (d) physically occluded regions. Characterization of the effects of (a) and (b) would be straightforward using controlled laboratory testing (described below). Characterization of (c) and (d) is more challenging as there is little true knowledge of the chemistry and geometry of the deposits, and the geometry of the occluded regions. Some effort should be made to try to mimic the evolution of the deposit chemistry by controlled laboratory experiments.

With respect to growth, the use of the maximum pit size model would seem to provide a framework for capturing the regions of parameter space in which the largest pits would be expected. The model was developed for a uniform, thin electrolyte layer. The effects of droplet formation also need to be assessed. It is not obvious whether the loss of cathode area will be compensated for by a decrease in the ohmic drop. If the area loss dominates, than the thin film case will be bounding, whereas if the ohmic drop decrease is sufficient, the droplet could be more aggressive. If the cathodic reaction is under diffusion control, my expectation is that the thin film would be the more conservative approach, but this assumption needs to be run to ground.

The range of chemical composition of the solution layers on the surfaces of the dry casks needs to be assessed in order to develop the parameter space of plausible extremes. The oxidizing strength of the environments may be the most critical aspect of that environment and one that is least understood. The oxidizing strength of the environment will likely overwhelm the range of chemistry because the diurnal cycles will likely lead to the formation of highly concentrated brines independent of the starting composition. The loading density will affect the water layer thickness, but the oxidizing strength will dominate the potential of the surface. Even low loading densities will very likely have sufficient chloride concentrations at low RH to initiate and grow pits **if** the oxidizing power is high enough.

How to capture experimentally

Three aspects need to be addressed experimentally: (a) surface environment chemistry parameter space, (b) surface deposit parameter space, and (c) electrochemical kinetics of atmospheric pitting.

Surface Environment: It is critical to expand the understanding of the actual field conditions to which these casks are exposed. Although there are substantial engineering challenges involved, without exposures of stressed stainless steel components and silver coupons at or near the inlets of the cask containers, the technical basis for the selection of environmental conditions for laboratory studies will be difficult to defend. Ideally the exposures would be

sheltered from outside rain as the casks are. The exposure time periods would not need to be extremely long (although the longer the better), because the insights gained on pitting locations (e.g., surface roughness vs. occluded site vs. MnS inclusions) and oxidizing power (from the amount of AgCl formed) would be of great benefit even for short exposures. These data would allow plausible extremes for deposit composition and oxidizing power (i.e., potential) to be determined.

Surface Deposit: The nature of the surface deposits could be important in either leading to crevice attack or in mitigating damage by increasing the ohmic drop between a pit and the surrounding cathodic surface. Characterizing the ionic conductivity of deposits formed in the lab under conditions meant to mimic the range of temperature/loading density/deposit composition plausible on dry casks would be useful as input to the maximum pit size model.

Electrochemical kinetics of atmospheric pitting: There are two sets of electrochemical kinetics needed for the maximum pit size model. The anodic kinetics of the pit surface can be determined via the use of artificial pit measurements. Recent work has shown that the repassivation potential and the critical stability product in the same measurement. Both values depend (to different degrees) on the bulk solution composition, but such dependencies as well as that on temperature, are straightforward to determine. The cathodic kinetics needed are those that are relevant to the unpitted surface surrounding the pit. Thus, they should be generated in solutions without chloride that have the same oxygen solubility and diffusivity as do the chloride solutions present. The absence of chloride is important to prevent localized corrosion occurring which would mask the actual cathodic behavior.

2. Crack initiation. Key factors include not only the pit size, but also the microtopography within the pit. I think the microstructure is of less importance. The stress field is obviously also key. The presence of physical occlusion will also be key in order to maintain the critical chemistry. As I mentioned above with respect to pitting, any integrity argument based on the absence of crack initiation is doomed. Such an approach is now gospel in the fracture mechanics community.

3. Crack Propagation. In addition to the obvious factors listed (size, chemistry, microstructure, stress field), the importance of the location and extent of the cathodic reaction needed to support crack growth should be considered. It should be determined the extent to which the crack communicates with/requires a cathodic surface outside the crack (as opposed to along the crack flank). A combination of full immersion work and (the more difficult) atmospheric cracking work should be pursued. The full immersion work will allow a more controlled assessment of the importance of the factors whereas the atmospheric testing is obviously more relevant to the situation of interest. As noted above for pit growth, cracking kinetics are strongly dependent on potential, so this parameter needs to be connected to the oxidizing power of the environment to which the casks are exposed.

2.3 Response from Dr. John Scully (University of Virginia)

1. Localized Corrosion. The key processes include salt deposition, deliquescence, gas absorption, and establishment of an oxidizing potential on the stainless steel surface as we have observed with the scanning Kelvin probe (SKP). The initiation process is less clear at the molecular scale, but is favored at sites such as scratches or roughness, phases or zones depleted in Cr or other chemical and structural heterogeneities. It should be noted that it is easy for a chemical heterogeneity such a MnS inclusion to serve this purpose. Moreover, at MnS inclusions, cracking of the interface between the particle and matrix has been observed and can create a confined space between the inclusion and the matrix that provide a local site that helps stabilize localized corrosion. Surface roughness may help serve the same purpose other than the lack of sulfide chemistry and the likely greater difficulty of attaining stabilization. The stabilization and propagation process may indeed be under cathodic control and this tends to be supported by the fact that in cases where the electrolyte exists as droplets on the active metal surface, only one pit is often seen per droplet. However, much more needs to be learned about how a pit might be sustained such in copper pitting where stifling occurs instead of true repassivation. The role of wetting/drying must be better understood in the light of cathodically limited pits. In other alloying systems, evaporative concentration of the environment accelerates pit initiation as Cl^- contents increase. However, cathode limitation eventually limits pit growth. This process must be better understood. The role of relatively benign environments and whether or not HCl can provide a release mechanism for Cl^- must be clarified. Other microstructural features such as delta ferrite in welds, potential carbides induced sensitization, and potential martensite formation may change pitting susceptibility from a metallurgy point of view. The assumption that high carbon grades won't form deformation induced martensite may be incorrect as more modern low carbon grades may be more susceptible. Recent experiments on BT Super 13 Martensitic steels with variations in alloying element partitioning in alloys containing martensite, ferrite and austenite show unusual effects of phases on pit formation and growth where simple notions such as a pitting resistance equivalent number (PREN) does not predict phases which pit in chloride environments. These can be characterized in low tech are well as high tech experiments where low tech experiments might involve rack exposures and high fidelity experiments might be heavily instrumented with multi-electrode arrays or SKPFM measurements. Plausible extremes are worth exploring in terms of environments and alloy conditions.

2. Crack initiation. The first aspect to be realized is that both low temperature hydrogen embrittlement and Cl^- induced SCC must both be considered as pertinent SCC mechanisms. It is incorrect to think of this phenomena only as due to as Cl^- induced SCC only, although this mechanism may dominate this class of materials at temperature above 120°C. (The threshold temperature must be determined as well). In light of this, many aspects of the way to think about each variable might be altered. For instance what environments promote hydrogen uptake besides those that promote pitting. The report summary covers many aspects of this that I think are important. Since the source of hydrogen is the cathodic reaction (one of several) in acid stabilized pits, much must be understood about this process

and the factors that control the manner in which a crack is initiated. Luckily some of the factors that drive acid pitting, Cl- SCC and hydrogen embrittlement are common such as acids with high Cl- content. There are differences though. At high temperature cracking might be transgranular but could occur by IGSCC if sensitized. On the other hand hydrogen controlled cracking might be intergranular. Testing must carefully include a range of metallurgical conditions such as martensite and austenite that could produce these different mechanisms and rates. HE rate might be hydrogen diffusion controlled to the fracture process zone and susceptibility, critical hydrogen levels and crack growth rate would be a strong function of microstructure. The crack path should be carefully inspected after the tests. Post-exposure hydrogen analysis would add in interpretations.

I think there is value in low tech bent beam or 3 point load samples with salt deposited, drops or designer pits. These specimens would be valuable for high throughput screening. In fact there are advantages in that cracking from an array of pits can be investigated by examining the pit at each droplet to catch the crack transition at various stages (all drops with pits would not experience pitting and crack initiation at the same time). Moreover, highly instrumented SENT specimens with salt deposition and crack initiation and propagation are recommended to be monitored by methods such as DCPD and load pulse marking. A range of environments and microstructures must be considered. I think that this method is perfectly suitable for such screening but should not be relied upon for crack growth measurements and accurate rate determination – given the number of assumptions needed. Careful attention must be given to microstructure in plausible extremes. I also recommend full immersion tests in NaCl solution at the pit repassivation potential or SKP determined droplet OCP as well as full immersion tests after hydrogen charging at various hydrogen levels. I would argue that this condition is quite pertinent until proven otherwise. The idea would be to test a range of H levels and to try to determine the levels seen at actual pits via rescaling methods or via local measurements with an SKP or SKPFM.

The pit to crack transition will become better understood by this full set of experiments. Our approach has been to test individual droplets that transition to SCC in the various manners described above.

3. Crack Propagation. My comments on the report summary and the answers above cover much of this. The crack branching can be addressed with the load pulse marking method with high probability. This must be checked, however. The K field trajectory must be investigated to see if crack arrest can occur as residual stress is dissipated by cracking. The effect of wetting and drying on crack growth must be much better understood. In some systems cracks start and stop with the wetting and drying. This must be verified. Moreover, the source of hydrogen and the hydrogen concentration field is most assuredly disturbed by the wetting and drying. There may be some enhancement in uptake just before drying but what happens after that and through this process is unclear. I remain concerned that the K trajectory differs between three point loaded. SENT and actual canisters leading to differences in results.

2.4 Response from Dr. Alan Turnbull (National Physical Laboratory)

1. **Localized Corrosion:** Issues to consider in localized corrosion: environmental conditions (including temperature and thermal gradients) on the metal surface and how it changes with time; initiation sites on the metal surface; factors controlling pit growth.

   In relation to the environment, we make the reasonable assumption first that marine environments are inherently the most aggressive and that inland environments will be relatively benign unless their location is near to any facility spewing out nasty chemicals. There is no consistent view of what constitutes the water chemistry at the surface with atmospheric exposure in marine environment; we "believe" that simple $MgCl_2$/NaCl models that make up the bulk of laboratory testing are not representative and recognize that water chemistry associated with evaporated seawater and atmospheric exposure is complex and may not be as aggressive as simple salts. It is also not clear in relation to dynamic atmospheric conditions how the metal-solution interface is changing with time; for example, droplets, thin liquid layer, drying out combinations, T variation, all of which will impact on pit initiation, pit growth and crack development. In that context, we need some data from service as to the nature of deposits, the time variation of temperature, moisture content and particulate matter content and composition. Can we define a suitable laboratory simulation that is practically relevant; e.g. with seawater deposits in controlled humidity (constant and variable) and also complement it with a test system at site that allows observation and analysis. Extreme laboratory test conditions are not helpful.

   The solution around deposited particles on the surface will concentrate but it is possible also that under-deposit attack with changes in local chemistry induced by constrained transport could be the additional factor creating the environment necessary for pit initiation.

   Initiation sites for pits can be MnS inclusions, physical defects with the latter often more significant for ground surfaces in our experience (are there any unused/discarded containers available for evaluation of surface state?). Need to consider whether crevice/crack-like defects may exist at welds and pre-empt the need for pitting.

   The fundamental question is whether to consider the initiation stage at all. While there can be much discussion about factors leading to pit initiation, I would take the view that it has occurred early in life and is of the order of the largest defect and concentrate on what factors control propagation from some assumed initial pit/defect size. In that context, we have observed that pits may arrest and not re-start when the environment is transiently changed to a benign environment (unpublished work for EPRI). A controlled experiment to evaluate that possibility and thus give insight into the effects of varying the humidity may be merited.

   In relation to propagation, the Kelly model is educational in highlighting the cathodic limitations to growth but need to consider droplets, wetting and drying, physical deposits which would provide a challenge in modelling. I would suggest that there is too much uncertainty in relation to pit propagation and the complex and dynamic nature of environment to allow confidence in any quantitative prediction except under limiting

conditions (e.g. thin liquid layer with established salt concentration to predict possible maximum pit depths.

Pit growth rates will be inherently variable not just from pit to pit because of different size (and for the same pit size from statistical variation) but primarily because of the dynamic nature of the environment. We can only measure the distribution with exposure time to get the rates but from a statistical perspective the period of measurement has to be representative and include variation with all four seasons. Hence, short term tests would not be representative and reliance on published data in a similar climatic region would be required in the short term (should reliable data exist).

2. **Crack Initiation:** Combination of factors that affect transition including stress concentration associated with micro-topography and macro-topography, local environment, pit growth rate (strain rate effect) and Kondo criterion. Very hard to predict pit distribution and what constitutes crack initiation without actual exposure data as a baseline. Modelers, including myself, use the Kondo criteria as it has to be satisfied but site of initiation can vary around the pit and defining the initial crack depth on initiation becomes very difficult.

   In my view, it will be very hard to capture the pit-to-crack transition and I would advocate focus on measuring growth from a prepared defect - could be a specially grown pit of controlled size or physical notch (I prefer pit). As the pit-to-crack transition is so variable we grow a very small fatigue crack from the pit to kick-start the process!

3. **Crack Propagation:** The key questions are what is the rate of crack growth as a function of crack depth as measured from the exposed surface; how to define crack depth when cracks are irregular/branched; how does the crack growth rate change with dynamic changes in environmental variables such as humidity.

   As noted in previous section I am biased towards using a previously grown pit of controlled depth as a crack starter with a small fatigue crack then grown from that since that is closest to the real situation. The challenge then is how to measure the growth rate with time. There is no automated way that can deal with crack branching as techniques such as DCPD are sensitive only to the change in resistance from whichever source. Nevertheless, such techniques are useful in indicating crack activity and in the context of fluctuating exposure conditions that in itself is helpful though only for a particular focused experiment, to explore threshold humidity for example. Inevitably, multiple specimen testing for different environments may be necessary with specimens removed at different times and fractured to determine the deepest crack. However, if constant load is used then there is the option of adopting specimens with multiple cracks of varying initial depth. However, final crack depth for each crack would have to be determined by layer removal in this case. In view of overall potential drop in crack and external solution a crack size effect on growth rate is projected and readily evaluated by this method. For the case of a thin liquid layer of defined salt content we can model some aspects of that depth dependence (we are doing this currently) as can Kelly. For droplets it is more of a challenge and would require significant development (incorporation of chemistry changes from effluent from pit/crack, surface tension driven convection..)

In terms of exposure conditions I am moving away from fully immersed conditions as they may be considered so poorly representative with regard to potential drop in the solution, with an uncertainty also in defining what the environment should be, as to be approaching guesswork. That means setting up the relevant SCC tests as proposed above in controlled humidity and temperature conditions with initial deposited seawater as the preferred route.

3. MEETING MINUTES

What follows are the minutes from that panel review. The minutes have been grouped into five specific topic areas that were discussed during the meeting.

3.1 Inspection

The first dry spent fuel storage system was fielded in 1986 at the Surry reactor, with a number of reactors following shortly thereafter. The expanded use of dry storage systems was necessary for operating reactors to maintain full core off load capability in spent fuel pools. Initially a specific ISFSI license and a Certificate of Compliance (CoC) for a storage systems that could be used by any general licensee were approved for a period of 20 years. As a result, many specific ISFSI licensees and CoCs are approaching the point at which the specific license or CoC must be renewed.

The concern exists that stress corrosion cracking of fielded interim storage containers could take place, potentially leading to a breach of the container wall. As a result, the NRC is requesting that ISFSI owners identify a lead system and inspect at least one of their fielded storage containers to determine the current condition of the canisters as part of the license renewal process. The NRC regulations require the development and implementation of Aging Management Programs (AMPs) for important to safety (ITS) structures, systems and components (SSCs) susceptible to credible aging effects that may affect their intended safety function(s). The aging management activities including AMPs must be included in a license or certificate of compliance (CoC) renewal application and implemented during the period of extended operation. AMPs for the management of localized corrosion and stress corrosion cracking have relied on periodic inspections of at least one canister at an ISFSI site.

Darrell Dunn (NRC) led a discussion on the need for inspections, and the rationale behind the currently proposed inspection interval of 5 years. As everyone is aware, there is a limited quantity of high quality data available on the atmospheric stress corrosion cracking of austenitic stainless steels such as 304 in chloride-containing environments, particularly in the ranges of temperature and relative humidity of relevance to interim storage systems. The majority of that data has been obtained at combinations of temperature, absolute humidity, and contaminant loading which are more aggressive than the conditions that could occur on the surface of fielded containers. Because of this, the data may over-predict the occurrence of crack initiation, or yield crack growth rates significantly faster than would occur on the container. However, despite the limitations of the available data, it must be taken into account. Given these data, then, once initiated and actively propagating, a crack progressing at the highest rate could penetrate an 0.5 to 0.625 inch thick container wall in as little as 17 years at temperatures where deliquescence of chloride salts may be possible. The inspection interval was set such that, based upon the available data, if a crack were to initiate and be continuously propagate at the maximum rate based on the aforementioned literature data, then an ISFSI licensee would have at least two inspection cycles during which they could potentially catch the crack before it had penetrated the container wall.

Several panel members inquired as to what needed to be inspected, and if found what size of a crack would be a problem? Darrell indicated that the regions where there was most interest were welds, as they are typically associated with high residual stresses. However, which welds are of

importance varies depending on the design. While all of the fielded designs in the US are single shell vessels, and thus the welds along the sides of the container are of interest for all designs, there are substantial differences in the top and bottom welds. For some containers designs, the container lid incorporates a second cover such that the outermost weld is not the confinement weld (i.e., the weld that is exposed to the external environment is not the confinement weld). In other cases, the outermost weld is the confinement barrier. For the base of the container, some of the welds are constructed such that the base weld is a side-penetrating weld, similar to a side circumferential weld, while in other cases the base plate of the container is inserted as a plug, and the weld at the bottom of the canister is not. To summarize, the specific welds of greatest importance vary from design to design.

In terms of what constitutes a failure, the container licenses stipulate that the container must be leak-tight. While the fielded canister designs may be able to handle a substantial crack and maintain their mechanical integrity, and, radionuclide releases from cracks, should they occur, would likely be small or negligible, that is not what forms the basis of the license. Any crack that penetrates through the entire wall, irrespective of its size, would constitute failure in terms of compliance with the license.

Several viewpoints were raised as to the nature of the potential for stress corrosion cracking and the ability to address it. One view, expressed by Sylvia Saltzstein, was that this was, in part, a public perception issue. The issue has been raised that stress corrosion cracking may be a plausible mechanism through which fielded storage containers may fail, eroding public confidence in the ability of the fielded systems to maintain confinement of the spent nuclear fuel that they contain. As such, any approach taken to evaluate this phenomenon must be evaluated in terms of how it would help alleviate the perception of public health issues – the question must be asked "how is this work going to answer the questions or concerns that the public has?" Ken Sorenson presented a slightly different assessment, stating that this appeared to be a licensing issue, and that understanding the cracking process is critical if a licensee is going to be able to build a sound technical basis for extended dry storage of spent nuclear fuel – in other words, the research is necessary to build the justification for extended use of existing and future spent fuel canisters, and to support the development of sound aging management programs. The question was then posed to Darrell as to how the information would fit into a licensing scheme. Darrell indicated that there is significant value in understanding all aspects of the cracking process – from localized corrosion to the pit to crack transition, to crack propagation. As mentioned already, better crack propagation information is needed to inform/refine inspection intervals, and help both the NRC and its licensees understand the significance of a crack of a particular size. In terms of localized corrosion and the pit-to-crack transition, industry representatives have expressed that they anticipate pitting to not be uncommon on the surface of the containers, though to date, this has not been verified via visual or other inspection methods. An understanding of when and how localized corrosion initiates, the rate and extent of propagates, and under what conditions a localized corrosion site would result in the initiation of an SCC crack is critical to determining when canister surface inspections should be initiated.

3.2 Environment

The environment discussion began with a presentation by Charles Bryan on the anticipated salt chemistry on the surface of fielded containers. First, the results of the EPRI sampling program were reviewed. The first site sampled was Calvert Cliffs, a near-marine site located approximately a half mile inland from the Chesapeake Bay (a sheltered bay containing brackish water) with a horizontal Areva-TN NUHOMS system. While a significant dust load was visible on the top of the container, due to issues associated with the implementation of the sampling system, only samples from the side of the container were obtained. The soluble salts within these samples were calcium- and sulfate-rich, with gypsum ($CaSO_4 \cdot 2H_2O$) being the dominant phase present. A small fraction of chlorides was also present, with the dominant phase being NaCl. The second site sampled was Hope Creek, located approximately 0.25 miles from the shore of the Delaware River, 15 miles upstream from the Delaware Bay (but within the tidal zone), again being adjacent to brackish water and sheltered from the open ocean, with a vertical Holtec HiStorm system. The canister top was much more heavily loaded than the sides, and the dust was dominated with insoluble materials such as quartz, clays, and aluminosilicates. The soluble salts that were present consisted primarily of gypsum and carbonates. A small quantity of chloride-bearing salts was also present, primarily as isolated grains of NaCl. The final site sampled was Diablo Canyon, a marine site located 0.35 miles away from and 400 feet above the ocean, utilizing a vertical Holtec HiStorm system. As with the other locations, the dust load was higher on the upper surface than the sides. The deposit was again dominated with insoluble materials such as quartz, clays, and aluminosilicates, however, in this case a higher quantity of chloride rich materials were present. The chlorides were present as sea-salt aggregates rich in sodium, chloride, magnesium, and sulfate, consistent with deposition at a marine site.

Next, the results of thermodynamic models of brine composition upon evaporation of sea water was presented. At low relative humidities (e.g., RH < ~60%), predicted deliquescent brine compositions are rich in Mg^{2+} and Cl^-, and somewhat less enriched in Br and B (it should be noted that the thermodynamic database utilized for these calculations is not qualified for use to predict borate species and contains few borate salts, so the enrichment in B may not be real). Under these conditions, other seawater components have been removed by precipitation, and are minor in the remaining brine. Salt minerals that are predicted to precipitate out during evaporation, in order of occurrence, include calcite ($CaCO_3$), and then gypsum ($CaSO_4 \cdot 2H_2O$), which converts to anhydrite ($CaSO_4$) at a concentration factor of about 9 (where the concentration factor is equal to the ratio of substance concentrations in the concentrated solution to the concentration in the initial solution). Halite (NaCl) precipitates at a concentration factor of about 11. Other minerals precipitate, and in many cases redissolve, as the seawater evaporates. The final salt assemblage at dryout consists mostly of halite, with lesser amounts of bischofite ($MgCl_2 \cdot 6H_2O$) and kieserite ($MgSO_4 \cdot 2H_2O$) and trace amounts of anhydrite, carnallite ($KMgCl_2:6H_2O$), and hydromagnesite ($Mg_5(CO_3)_4(OH)_2 \cdot 4H_2O$). As sea-spray aerosols dry out, these salts are precipitated, and salts, or a mixture of salts and brine, may be present on the canister surface. As the RH rises over time, the salts redissolve and the composition of the deliquescent brine follows the path of evaporation in reverse order. It is the highly deliquescent $MgCl_2 \cdot 6H_2O$ that is believed to control the deliquescence behavior of sea salts, determining when an aqueous phase is present.

During the ensuing discussion, the suggestion was made that chloride might be lost by degassing as HCl from the acidic pit solutions, based on the observation of Na-bicarbonate precipitation at

the cathode in NaCl corrosion experiments by Schindelholz et al. (2014). The observed reaction essentially converts NaCl to $NaHCO_3$, and a balancing reaction to consume the chloride seems necessary. This expectation is supported by observations of Cl-depleted Na-K bicarbonate and carbonate salts associated with corrosion on storage canisters at the Diablo Canyon ISFSI. Alan Turnbull disagreed with the statement that chloride would degas when associated with a pit, noting that oxygen reduction at the cathode (external to the pit) would result in the production of hydroxyl ions, and that chloride would be driven by electromigration to the anode site within the pit. While the discussion presented regarding degassing considered the chemical reactions/thermodynamics for their determinations, the electrochemistry was left out. In order to capture what is taking place at an active localized corrosion site, the electrochemical reactions (and their impact on the local chemistry) must be considered.

The discussion then moved to the nature of the evaporatively concentrated brine on the container surface. Thermodynamics, along with a field study at the Morton Salt facility in Inagua (the Bahamas), some laboratory studies, and geological evidence from salt evaporate deposits indicate that as seawater evaporates, the brine chemistry should evolve to a magnesium chloride rich brine. This result is consistent with many studies of the deliquescence behavior of sea-salts (by SNL, NRC, and others), which show a stepwise increase in absorbed water mass (or conductivity, or impedance, depending on the method used) at the deliquescence point of magnesium chloride. However, Turnbull indicated that in experimentation he has conducted, this was not observed. While thermodynamic predictions suggest that the brine should evolve towards a moderately acidic, Mg-rich brine, experiment in the NPL labs and corroborated by results at the Swedish Institute for Metals Research (SIMR), have found that when evaporatively concentrating seawater (natural or ASTM artificial ocean water) the sodium content remains high, and the brine pH remains close to neutral. To explore this further, they started with a $MgCl_2$ brine then attempted to increase the Na concentration via titration with NaCl – in that case, the brine remained a $MgCl_2$ brine, consistent with thermodynamic predictions. The results suggest that there may be interactions between the various components within the brine that are not accurately captured in the existing thermodynamic databases, possibly due to disequilibria that occur during rapid evaporation of seawater. The implication is that a low pH, Mg rich brine may not be what is formed as seawater is evaporatively concentrated. (Turnbull et al., Corrosion Vol. 64, No. 4 (2008), pp. 325-333.) This would have significant implications as to the anticipated corrosiveness of the deliquesced brine.

Some concerns were also expressed with respect to the solid phases which form upon the evaporation of seawater. Andy Duncan indicated that he had evaporated seawater and identified a species not predicted by the thermodynamic analyses – tachyhydrite (dimagnesium calcium chloride, 12 hydrate). This material is highly deliquescent, and would yield a deliquescence relative humidity below that of magnesium chloride. Charles Bryan indicated that the precipitation of ternary and quaternary salt species occurs during evaporation of seawater, the actual species being a function of the temperature at which evaporation took place, however, the predicted species form at intermediate concentration values, and with the exception of carnallite, redissolve with further evaporation.

In addition to the species present on the surface as solid salts (which may deliquesce to form a liquid brine), Rob Kelly pointed out that there are a variety of gaseous constituents of environments which can have a profound impact on the corrosivity of the environment, as well as the resulting phases/corrosion products which can form. As an example, in performing

standard ASTM B117 salt fog testing of silver very little corrosion product is formed, and what does form is predominantly sulfides with little or no AgCl. However, when gaseous oxidizing atmospheric contaminants (such as ozone, oxides of nitrogen, etc.) are added to the salt fog environment much more significant attack is observed, with copious amounts of AgCl being formed. W. Abbott at Battelle laboratories has made an effort to characterize the aggressiveness of atmospheres located around the country (predominantly at military installations), and that information could be leveraged in evaluating the susceptibility of stainless steel to localized corrosion and stress corrosion cracking at different spent fuel storage locations.

3.3 Localized Corrosion

Rob Kelly began the discussion of localized corrosion of austenitic stainless steels under atmospheric conditions, with a discussion of an ongoing program he has led at the University of Virginia aimed at developing a model to predict the maximum pit size that might form on the surface as a function of the environmental conditions. In modeling pit depth with time, most models in the literature are power laws (i.e., $d=At^m$, where d is the size, t is time, and both A and m are empirically derived parameters associated with the material and exposure condition), with the pit size increasing as an exponential function of time (note that the exponent, m, is less than 1, resulting in a slowing of the growth rate over time). While these expressions can be accurate over short times, they do not capture the long term behavior that has been observed. Part of the problem is the inability to obtain the required accuracy in the parameters used for these models (i.e., A and m), where small uncertainties can yield substantial differences in the predicted pit size with time. In the field, localized corrosion sites appear to have a limiting size that they reach – as such, the maximum pit size on a structure appears to increase with time, and then plateau at this maximum depth. While the number of pits may increase with time, none appear to grow larger in size than the observed plateau, or maximum pit depth. This depth is a function of the exposure conditions and the alloy being considered, and the time to reach the plateau size can take years, or in some cases can be more rapid. In building a power law model, the measured pit size as a function of time is fit to the expression described above. The accuracy of that measurement then, in terms of the ability to capture the maximum pit size that could form as a function of time, will thus define the ability of the model to predict a maximum pit size.

The source of this observed upper limit to the pit size is believed to be due to the limited ability of the surface surrounding the pit to supply the cathodic current needed to support propagation. In order for a pit to grow, the oxidation (anodic) reactions taking place within the pit (i.e., the corrosion of the metal) must be equal in magnitude to reduction (cathodic) reactions taking place outside of the pit (e.g., oxygen reduction). In the model developed by Kelly and his colleagues, the cathodic capacity of the surface is modeled as a function of the salt loading of the surface, the relative humidity of the gas phase, the electrochemical kinetics of the relevant cathodic reaction(s), and the exposure temperature. The limiting pit size is determined by combining the maximum cathodic current available from the surface with the Galvele pit stability product. The advantage of this model is that the critical parameters can all be determined experimentally or calculated via thermodynamics. As with all models, a number of assumptions are made in implementing this one as well. First, it is assumed that the pit will be hemispherical in shape. Other geometries can be described by this model, but the expressions presented are for a hemispherical pit (which is often observed for austenitic stainless steels). In addition, Kelly mentioned that his group had recently received a series of specimens which had undergone long term exposure in Hawaii. The nature of the localized corrosion on those sites, including pit

geometry, must be extensively characterized to validate the assertions on typical pit geometry. Second, it is assumed that the active pits will be sparse enough that the maximum size pit being modeled will be positioned such that no neighboring pits will be close enough to impact the ability of the surface to supply cathodic current to it. Because the ability of the surface outside of the pit to support cathodic activity is limited, if two or more pits are pulling cathodic current from the same location, the total current density required from a point on the surface to support all of the nearby active pits must be less than or equal to the maximum cathodic current density that the surface can deliver. Under these competitive conditions, the observed pits will not approach the calculated theoretical maximum pit size.

Once a localized corrosion site reaches to the point where its required cathodic current is greater than what the surrounding surface can provide, the site will begin to repassivate as it will not be possible to maintain the critical chemistry within the site. Thus while an actively propagating pit has two key features – an acute geometry that acts as a stress concentrator coupled with a highly aggressive critical pit chemistry – a pit which has repassivated will only have the former. It was noted by John Scully that the repassivation of a pit is not an abrupt event. As the repassivation process progresses, regions of the pit will remain active until the chemistry within the pit becomes sufficiently dilute to allow the protective oxide along the pit walls to reform (i.e., the surface becomes passive) and the rapid electrochemical dissolution within the pit to stifle. During this process, the chemistry within the pit becomes increasingly dilute, and the pH gradually increases. This gradual repassivation process has been demonstrated experimentally by Scully's group for crevice geometries using multi-electrode arrays. The likelihood of re-initiation of a localized corrosion site was discussed – specifically, once a localized corrosion site has repassivated due to exceeding the ability of the surrounding cathodic region to support it, will it reactivate once conditions are again favorable for localized corrosion to take place? For example, if the humidity decreases, resulting in a thinner brine layer and reduced cathodic capacity of the exposed surface, and as a result an actively propagating pit is forced to repassivate, will that pit reinitiate once the humidity increases again? Scully and Kelly responded that once a pit has repassivated, the process of getting it to reactivate is complex, requiring rehydration of the oxides and hydroxides within the passivated pit, followed by the development of an aggressive environment within the pit – as a result, repassivated pits do not typically reinitiate.

Repassivated pits behave differently than other regions of the surface (i.e., the regions of the surface surrounding the once active pit). Scully described research in his group using multi-electrode arrays which has indicated that repassivated pits can act as stronger cathodic sites compare to the unpitted surrounding surfaces, presumably due to the reduction of species within the repassivated pit. (i.e., the repassivated pit will contain numerous oxides, hydroxides, and other species which could offer cathodic reactions in addition to the oxygen reduction reaction (which would be prevalent on the unattacked regions of the surface around the once active pit). That being said, Scully also indicated that cyclic wet/dry experiments have indicated that in some situations, using NaCl/MgCl salt assemblages, that reinitiation may have been observed.

The discussion moved to a more general review of the conditions that would lead to pit initiation. Turnbull expressed that understanding the window of conditions under which pitting might initiate was critical in assessing the response of a system. Generally, pitting takes place when the salts/solution is drying out on the surface of interest, consistent with the environment presentation given earlier. As the solution concentrates, it becomes increasingly aggressive, and

can result in local depassivation of the stainless steel. Scully reminded everyone that the chloride concentration, in and of itself, does not necessarily dictate the aggressiveness of the environment. As an example, he cited work on 2205 (a duplex stainless steel) where pitting and cracking is observed in magnesium rich brines, but not in sodium rich brines of the same chloride level.

The question was then raised about the number and location of localized corrosion nucleation sites on an austenitic stainless steel surface, considering its microstructure and the impact of the construction process (i.e., grinding). For engineering alloys, microstructurally, there are a variety of features that have been observed to serve as preferential nucleation sites. These include grain boundaries, second phase constituents (e.g., MnS inclusions), and other high energy structures. Similarly, the forming process also generates preferential initiation sites, such as highly deformed regions on the surface and the deposition of second phase materials (e.g., iron from the tooling used to form the structure). In some cases, the deformation associated with the formation process – be it mechanical deformation or deformation due to the welding process – can result in the formation of strain-induced martensite. However, Peter Andresen indicated that he had not seen appreciable martensite formation associated with welded stainless steel pipe. Presumably the heat input from the welding process prevents such a transformation. The question was posed as to whether there are a limited number of these preferential initiation sites, such that they might be consumed early in the life of the container, or if there were so many that nucleation could be assumed to be a continuous process, to the extent that there would always be sufficient nucleation sites once the environment was established. The panel argued that it would be a given that there will be numerous corrosion nucleation sites. The panel agreed that while there are some sites, such as MnS inclusions, that are perhaps easier to nucleate pitting, that there would be plenty of easy nucleation sites – the supply would not be exhausted.

While discussion the model developed by Kelly and coworkers to capture the impact of the surface environment on localized corrosion (in terms of the ability to supply the necessary cathodic current for the localized corrosion site), Turnbull suggested that this model could also be used to evaluate SCC cracks that grow from the surface. This approach could be particularly effective at assessing the CRIEPI data from 4-point bend tests. The change in crack growth rates with time observed in that work has been suggested to be the result of a cathodic limitation. The use of the model to assess the CRIEPI data would help provide a sound technical basis for such statements, or demonstrate that the notion is incorrect.

3.4 The Pit to Crack Transition

Localized corrosion is believed to play a critical role in the initiation of stress corrosion cracking. A localized corrosion site, such as a pit, has physical features that provide an acute geometry which will act as a stress amplifier, locally magnifying the stress, along with a concentrated, low pH and chloride rich solution within the pit. The question was posed whether the combination of the above two factors was necessary for crack initiation, or if only one, such as the stress amplification, were sufficient to result in crack initiation. Scully, Kelly and Turnbull all agreed that the environment within the pit was necessary for crack initiation, and that crack initiation would occur from an actively propagating pit, rather than a repassivated one. Turnbull indicated that the requirement for localized corrosion appeared to hold true for most steels. However, for duplex stainless steels there have been instances where a dealloyed layer was found under a corrosion product deposit, and that brittle dealloyed layer had served as the initiation site. Some

discussion followed about the discussion by R. Newman in the recent Faraday Discussions ("Localized Corrosion: General Discussion", Faraday Discuss., 2015, Vol. 180, pp. 381-414) on the dealloyed layer model of Newman and Sieradzki. Andresen offered a counter point, indicating that it was not at all uncommon to find SCC crack nucleation from features other than a localized corrosion site in high purity, high temperature water environments (i.e., primary side of pressurized water reactors). Turnbull countered that the mechanisms through which such cracks initiated in high purity water would be difficult to envision for an atmospherically exposed stainless steel container. Andresen reiterated that while aggressive environments would indeed initiate cracks more readily, the possibility of crack initiation cannot be dismissed under conditions where pitting was not occurring actively. In other words, it is difficult to support the assertion that an SCC crack will never initiate from sites other than pits (active or repassivated) on the surface of the container. Peter showed crack growth rate data at constant K (no cycling) that was quite high in pure, deaerated water at ~100 °C. Key issues include the experimental technique and crack monitoring resolution.

As with localized corrosion, there often appear to be threshold environmental conditions which must be met or exceeded before crack initiation will take place. Scully pointed out that austenitic stainless steels tend to exhibit a critical temperature below which they will not undergo stress corrosion cracking (though other crack mechanisms, such as hydrogen induced cracking, can be operative). Experimentally, this temperature is found to be a function of the environment (i.e., chemistry). As the temperature is reduced, there is a transition in mode – suggesting that hydrogen effects are more important or controlling at lower temperatures. To more thoroughly assess this, it would be necessary to evaluate the impact of the species present on the hydrogen uptake behavior of the materials. Andresen countered the idea of a threshold temperature, indicating that these types of thresholds don't exist with more sophisticated experiments and high crack length resolution. In high purity water, stress corrosion cracking below 50°C (the historic "threshold" temperature) has been observed. There are effects such as cold work that can have a large effect. Scully asked if delta ferrite could be present, or perhaps deformation induced martensite. Andresen indicated that modern materials, often are less homogeneous than expected. In the field, he has seen material that should be solution annealed (based upon the material certification) show up with an as-cast microstructure – in other words, there appears to be significant variability in material quality, when based upon the nominal specifications or historical experience, there should not be. Addressing Scully's question, while the presence of undesirable phases would be unlikely for solution annealed plate, in his experience you can't guarantee that you get what you are expecting – as such, phases such as delta ferrite could be present in some cases.

Assuming that a stable SCC crack will have to initiate from a localized corrosion site, it is likely that it does not immediately form a stable crack. Turnbull pointed out that crack initiation needs to be thought of in terms of an incubation time or process. Initially, a crack embryo (something smaller than what is required to form a stable crack) will form, then progress with time into a critical flaw size. Research has indicated that the initial growth processes working towards forming such an embryo can be very slow. Turnbull went on to explain that once a pit has reached a combination of critical size, chemistry, and internal geometry, microcracks are often formed. Microcracks are seen at pit sizes as small as 50 microns in diameter, and tend to follow slip planes in the parent metal. In many cases, these microcracks run out of mechanical driving force, or are overcome by the advancing corrosion front, before they can become a stable crack. The specific location at which the microcracks initiate is a complex function of a number of

factors, including the local environment at a point within the pit, as well as the surface topography along the walls of the pit. Turnbull pointed out that the most aggressive region may not be at the base of the pit, and instead could be closer to the surface. Other factors which may reduce the threshold for crack initiation include grinding/surface deformation which can, in addition to lowering the resistance to pit nucleation, also enhance microcrack formation.

Peter Andresen offered some general comments on crack initiation, specifically highlighting the difficulties associated with quantifying initiation. While evidence presented to date supports the assertion that SCC initiation for welded austenitic stainless steel storage containers will take place at a pitting site, the data is far from comprehensive/conclusive. Looking more broadly, there are a number of phenomena that have been observed to result in SCC crack initiation, including pitting, intergranular corrosion, grain boundary oxidation during thermal processing, surface cold work (deformation due to processing, such as grinding, bending, etc.), mechanical cracking, fatigue, etc. While it may be tempting to exclude such diverse sources of crack initiation, some of them may be influential, if not completely responsible, for crack initiation under some relevant (but perhaps as yet unexplored) conditions. A comprehensive treatment of crack initiation would need to encompass all of the potential degradation mechanisms through which cracking could initiate. Microstructurally, initiation relies on an understanding of a thin surface layer of material, on the order of 100 microns in thickness or less, the characteristics of which can be highly variable.

Overall, the panel agreed that the critical environmental conditions under which SCC can take place on the surface of an interim storage container – or more specifically, the threshold conditions beyond which cracking is possible – are poorly defined. Andresen inquired if there were other sources of information that could be leveraged to predict the behavior of interim storage containers – both in terms of conditions where cracking can take place, as well as when it does not. There are a wide variety of atmospherically exposed, austenitic stainless steel structures and piping under broadly similar conditions at both nuclear and other industrial sites – could these installations be evaluated in terms of whether localized corrosion has been observed under such conditions? There could potentially be a large volume of information available that could be tapped upon to inform on the anticipated behavior of the storage containers. Darrell Dunn agreed with Andresen – that data from industrially exposed components of similar materials is needed. Pit depths, pit distributions, crack geometries (if present) and how/what is depositing on the surface of the containers. While the fielded installations are from differing environmental conditions, they could be used to inform on how interim storage containers might be have.

3.5 Crack Growth Measurement

The discussion of SCC crack growth measurement was prefaced by a review of the pertinent literature data. While the surveyed studies all explore SCC of austenitic stainless steels under atmospheric conditions, the methods through which each researcher approached the problem differed substantially, ranging from optical measurements made after the fact to efforts to implement more traditional crack measurement techniques, such as direct current, potential drop (DCPD). The surveyed studies utilized a variety of metal treatments including as-fabricated, solution annealed, welded, and sensitized material. Furthermore, different surface treatments (polished vs ground) were also used. In addition, most of these studies were accomplished using

techniques that are not generally accepted for high-fidelity crack growth rate measurements, and in cases where more traditional approaches were taken, these methodologies may not be applicable to the atmospheric conditions of interest here. The wide variety of methods and materials results in the observed large scatter in measured crack growth rates (CGRs).

Peter Andresen offered a general summary of the limitations of SCC measurements. SCC processes, much like other materials-degradation related processes, are complex, and as a result, the experimental studies aimed at evaluating them are, more often than not, flawed. Compilations of SCC growth rate data generally show vast amounts of scatter, often the result of the methods through which the data was acquired. This significant scatter hinders the ability to see inter-dependencies or to accurately predict trends in the data, softens trends such as the impact which temperature has on crack growth rates. Furthermore, it is not possible to overcome bad experiments, or more specifically, experiments that are flawed in their approach to evaluating the problem, through statistics – the experimental program must be fundamentally sound, and executed with an appropriate level of precision. Part of the issue appears to be the prevalence of the concept of immunity to stress corrosion cracking being presented as an achievable goal (particularly in industrial codes), which encourages the use of simplistic experiments, and undermines the ability to generate comprehensive test programs that improve our ability to understand. There is also an inclination to see specific material/environment combinations as separate systems and evaluating them empirically, rather than seeking out the connections/similarities between things and developing mechanistic models that could then be applied to multiple systems.

Kelly discussed the definition of the environment space over which experiments were to be performed. Due to the large number of variables, and the extended duration over which SCC and localized corrosion tests take place, it would be difficult to employ something like a traditional design of experiments. The desire would then be to explore the extremes of the environment. In doing so, Kelly impressed that it is critical that plausible extremes be explored. The conditions should be selected such that they bracket the anticipated field conditions, but not by too much as there is a danger that other degradation modes could be introduced. Andresen expanded on this, adding that in designing experiments, it is important not to get too greedy in terms of changing too many variables in each test, or in terms of trying to simulate the complexities of the waste canister and its environment in a few tests. In other words, limit the degree to which multiple variables are changed from test to test. Andresen also added that given our limited understanding of the phenomenon, there is a need to perform proof of principle tests in addition to performing tests that will provide data to feed a model.

There was significant discussion as to the difficulties of conducting atmospheric SCC testing. The ability to tune variables that directly impact the chemistry within the crack and the crack growth rate is limited. Andresen offered that the use of inundated experiments, which are simpler to run and less prone to ambiguity, can be leveraged to understand *qualitatively* the impact of key variables, such as oxygen availability, chloride chemistry, or even surface characteristics of the sample (i.e., cold work, etc.) on the crack growth rate. Insights into effects such as external cathode limitation could be gained from inundated conditions by selectively masking portions of the surface. Effects such as surface stress/strain distributions could also readily be pursued via inundated experiments. Such experiments could then guide the establishment of appropriate variables to explore during atmospheric testing. Other difficulties with performing atmospheric SCC work that Andresen called attention to were issues associated

with initiation testing. We presently have a poor understanding of the stresses, strains, and microstructural heterogeneities associated with the near surface region of structures such as an interim storage container.

The atmospheric SCC work that has been performed on austenitic stainless steels in marine environments to date has utilized a variety of sample geometries, though the dominant implementations have been U-bend samples and 4-point bend bars. As implemented, neither are able to yield high fidelity assessments of crack growth rate. The topic of how to perform relevant atmospheric SCC growth rate tests was discussed. This brought about a discussion of the need to understand the accuracy of the measurement (i.e., what can you see, and what is beyond the capability of the measurement). Selection of an appropriate geometry/test method needs to consider what level of fidelity is needed. Other things to consider are what test specimen geometries do we think have worked thus far, and what data do we need to get? Once those questions can be answered, we will be in a place to evaluate the existing test methodologies, and determine if they are sufficient.

Turnbull suggested beginning with a flat specimen (of which there are a variety of potential forms, including dog-bone samples, etc.) specimens that could be appropriately loaded with contaminants, then exposed to relevant environmental conditions (i.e., T, RH) such that a pit could be nucleated and grown. The sample could then be fatigued in air such that a fatigue precrack was grown from the pit. The sample could then be exposed to a monotonic load and the growth rate measured as a function of time using high accuracy methods such as DCPD. One concern with this geometry that was voiced was the fact that SCC cracks under these conditions tend to be heavily branched. As a result, while this geometry would be a more ideal geometry for capturing what happens in the field, measurement of crack growth rates could be complicated if the crack branches. Turnbull pointed out that there are stress intensity (K) solutions for branched cracks, and that the effective crack "length" is measured as the depth of the deepest crack. Bluntly notched samples were also discussed, though as with planar surface samples, crack initiation would be slow until the crack had reached 50-100 microns in length, at which point it would accelerate to standard growth rates. Andresen stressed that for any non-standard geometry, he would strongly encourage enlisting the assistance of a structural mechanics modeler to predict the true applied stress intensity as a function of crack length. The manner in which the stress intensity changes with time (obviously more of a concern for fixed load or displacement experiments, than an instrumented specimen in a load frame) can have a profound impact on the crack growth rate. While slightly declining K experiments do not strongly impact the growth rate of an actively growing crack, rising K experiments can result in substantial increases in crack propagation rates.

Andresen indicated that while other sample geometries may look more like the surface of the system we are simulating, they are limited in their ability to deliver highly accurate crack growth rates. While fracture mechanics specimens, such as a compact tension (CT) sample force the plane in which crack propagation proceeds, and thus significantly limit crack branching, they allow precise control over the experiment. Other fracture mechanics geometries can also be considered, though their impact on the stress intensity as a function of crack length (i.e., do they yield a rising or falling K experiment) should be considered.

3.6 Summary (from Panel)

Environment: There is no consistent view on what constitutes the water chemistry at the surface with atmospheric exposure in marine environment; we "believe" that simple $MgCl_2$/NaCl models that make up bulk of laboratory testing are not representative and recognize that water chemistry associated with evaporated seawater and atmospheric exposure is complex and may not be as aggressive as simple salts (see also very recent work from Prosek in support of this). It is also not clear in relation to dynamic atmospheric conditions how the metal-solution interface is changing with time; for example, droplets, thin liquid layer, drying out combinations, and temperature variation, all of which will impact on pit and crack development. In that context, the definition of a suitable laboratory simulation and its relationship to service is required.

There is also the issue of the distribution of environments across the different sites AND across a single cask. It would be expected that there exist occluded regions at the bottom of the casks (either vertical or horizontal) that could act as preferred sites for pitting/SCC. Their location leads to some sheltering from deposition relative to the top surface, but over time they could become more of a problem than the top, and they are certainly less inspectable to the point of impossibility. The dynamics of the environment are important, including the likely change in wettability with cycles/time. Some of the organics that are deposited are surfactants. Their deposition will lead to increased wettability of the surface, creating a more uniform film. Understanding this in terms of time and temperature will be important in capturing the critical factors.

Finally, the importance of the oxidizing ability of the environment must be captured in all laboratory tests as it is well known that localized corrosion and SCC initiation and propagation are strong functions of potential. Some data in this regard is available from Abbott's self-published book on atmospheric corrosion testing as the facilities of interest may well be near to sites Abbott has tested. In addition, some simple exposures at some of the actual sites would be very illuminating. Even simply putting Ag and stressed and unstressed SS samples at/near the inlets would provide data in the short-term that would be invaluable. Getting as much information as possible from the SCC failures of atmospherically exposed SS within the facilities would be important as well. Some/much/all may be anecdotal, but on the off-chance that some failed pipe is available, it would be a treasure trove.

One approach would be to define the bounds of plausible extremes of environments (and metallurgy and mechanics). What constitutes "extreme" would necessarily be based on experience and the literature. Determining the localized corrosion/SCC behavior at these plausible extremes should effectively bound the susceptibility/possible damage rates. In parallel, an assessment of the likelihood of these plausible extreme of the environments needs to be developed as a function of geolocation. This approach would also allow an assessment of the likely effectiveness of mitigation strategies (e.g., peening).

Localized corrosion: initiation sites for pits can be MnS inclusions, physical defects with the latter often more significant for ground surfaces in our experience. There is a need to consider whether crevice/crack-like defects may exist and pre-empt the need for pitting (as indicated by Andresen). The Chen and Kelly model is educational in highlighting the cathodic limitations to

growth, but there is a need to consider droplets, wetting and drying, physical deposits. Is there too much uncertainty in relation to pit propagation and the complex and dynamic nature of environment to allow confidence in any quantitative prediction. Use models to understand effect of variables.

Models can be also be used to assess what parts of the parameter space of the plausible extremes represent the greatest risks to allow a focusing of the research efforts to those areas. The maximum pit size model would need to be extended to consider the effects of droplets vs. thin film, wetting and drying and physical deposits. All of these aspects could be included, with the wetting and drying effect being the most challenging. Do we have evidence that during service in the temperature range of importance that there is wetting and drying?

Pit-to-crack transition: Combination of factors that affect transition including stress concentration associated with micro-topography (Burns, etc.) and macro-topography (FE analysis of Turnbull), local environment, pit growth rate (strain rate effect) and Kondo criterion. Very hard to predict pit distribution and what constitutes initiation without actual exposure data as a baseline (our own pit and crack model has been used in service but had access to lot of service data). One approach would be to the idea of ignore the impact of precursor development and focus on measuring growth from a prepared defect - could be a specially grown pit of controlled size or physical notch. Input is needed from structural mechanics analysts to determine the size of a damage site that is important for cracking, to at least bounded the defect sizes which must be considered.

Crack-growth measurement:
Both full immersion and atmospheric exposures are need, with full immersion being used to explore variables to focus the more challenging atmospheric exposure tests. Question of what constitutes a meaningful environment that is just conservative but not extreme. We cannot answer that until we actively monitor marine atmosphere conditions (Humidity, temperature, etc.) over sufficient representative period. Such data may be around already.

We do need to measure crack growth. Simple specimen geometry, high resolution DCPD, small pre-crack from pit or alternative approach if these are branched. Long cracks testing may be useful to see to what extent there is electrochemical driving force for crack growth.

4. PANEL RECOMMENDATIONS

1. As the ultimate goal of this work is to establish a means to predict the nature/risk of SCC for various ISFSI sites, need to consider what the model needs to tell you (i.e., what data, level of fidelity, etc. are needed), as that will drive how the model is designed, and the quality of the data that it needs. (Turnbull)
2. The effective application of a localized corrosion model, such as the model developed by Kelly and coworkers, requires accurate kinetic data that must be acquired under representative environmental conditions. (Kelly)
3. In order to develop an understanding of the phenomenon, there will be a need to perform proof of principle tests in addition to performing tests that provide data to feed a model. (Andresen)
4. Given the low state of understanding of the atmospheric SCC process, care should be taken when defining any test matrix such that multiple variables are not changed at the same time – one at a time. (Andresen)
5. A structural mechanics analysis should be performed on any non-standard (i.e., not a CT specimen) sample geometry to enable the accurate prediction of K as a function of crack length. (Andresen)
6. Formation of a series of small working groups should be considered, with the different groups focusing on different aspects of the process. Focus groups can then evaluate data as the project moves along. (Andresen)

APPENDIX A: PANEL MEMBER BIOGRAPHIES

Dr. Peter L. Andresen

Principal Scientist, GE Global Research Center

Schenectady, New York

EDUCATION

Ph.D. in Materials Science, 1978 Rensselaer Polytechnic Institute.

M.S. in Materials Science, 1974, Rensselaer Polytechnic Institute.

B.S. in Materials Engineering (Cum Laude), 1972, Rensselaer Polytechnic Institute.

EXPERIENCE

Dr. Andresen's expertise is in the area of corrosion and environmental effects on mechanical properties and integrity of materials. His research has focused on corrosion and environmental fracture of iron- and nickel-base alloys under conditions of interest to the energy industries.

Dr. Andresen is the author of over 450 publications, holds twenty six patents, has given hundreds of invited talks and written numerous chapters for books. He is a member of the National Academy of Engineering, and is a Fellow of the American Society for Metals and the National Association of Corrosion Engineers. He has received two Whitney Gallery of Achievers Awards and two Dushman Awards from GE, the Speller Award from NACE, the U.R. Evans Award from the British Institute of Corrosion, and was selected as one of "50 Stars to Watch" by Industry Week in 1996. He was recognized with the Lee Xun Award in 2011 from the Institute for Metals Research in Shenyang, China, and was awarded the U.R. Evans Award by the British Institute of Corrosion in 2014.

Dr. Andresen has built the largest and most sophisticated laboratory in the world for studying environmental effects in nuclear systems, especially related to stress corrosion cracking (SCC) and corrosion fatigue. This involves over 60 high temperature water systems, including 42 systems complete with individual water chemistry, autoclave, computer controlled loading, DC potential drop crack monitoring and related instrumentation – systems that have been copied in a number of universities and national laboratories throughout the world, including University of Michigan, Pacific NW National Lab, Idaho National Lab, MIT, Tohoku University, Institute for Metals Research and Shanghai JiaoTong University. He has studied a full spectrum of structural materials in both boiling and pressurized water reactor environments, and been a primary force behind viewing these different examples of environmentally assisted cracking in a unified fashion, understanding and quantifying the roughly dozen most influential parameters, and demonstrating that true thresholds and immunity are generally an artifact of poor experiments and/or crack length resolution.

He is a co-inventor of NobleChem™, and electrocatalytic technology that was implemented in all U.S. boiling water reactors by 2013. This process creates a uniform distribution of 1 – 5 nm Pt particles on all wetted surfaces in a simple process that can be done during full power operation. He has been highly involved in evaluating the effects of dissolved H_2 and Zn on SCC in pressurized water designed to mitigate SCC.

He has served in many capacities in professional societies, including currently on the Board of Directors of NACE; Board of Editors for Corrosion Journal; Chairman of the NACE Research

Committee; Chair of the NACE Awards Committee and the Advisory Panel for the Halden Test Reactor in Norway and the Idaho National Lab Science User Facility. He has worked with dozens of laboratories throughout the world to help establish and/or improve their capabilities.

He has served on many expert panels for the nuclear industry related to degradation by corrosion and stress corrosion cracking of stainless steels and other structural materials, and is unique in having served on all four major international efforts on Proactive Materials Degradation. He has served on more than twenty expert panels convened by EPRI to address disposition curves for different materials, and screen and evaluate stainless steels, irradiated stainless steel and various nickel alloys and weld metal. He is a key driver and contributor to the Alloy 690 International Collaboration group that is addressing the stress corrosion cracking vulnerabilities of Alloy 690 and its weld metals. He regularly gives invited tutorials to a spectrum of industrial and academic forums throughout the world.

He serves on the organizing committee and as technical chair of the International Cooperative Group on Environmentally Assisted Cracking and the International Conference on Environmental Degradation in Nuclear Power Systems – Water Reactors. He is a consultant / advisor to several national labs and universities, and has been on several DOE review panels, including a long term role on the highest level Consulting Board for Yucca Mountain Waste Disposal Project.

Dr. Robert G. Kelly

AT&T Professor of Engineering, Department of Materials Science and Engineering
Co-chair, Center for Electrochemical Science and Engineering
University of Virginia, Charlottesville, VA

EDUCATION

Ph.D. The Johns Hopkins University, January, 1989
M.S.E. The Johns Hopkins University, May, 1986
B.E.S. The Johns Hopkins University, May, 1984

RESEARCH EXPERTISE and CAPABILITIES

Robert G. Kelly has been conducting research on the corrosion of metals for the past 30 years. After completing his Ph.D. studies at Johns Hopkins University (1989), he spent two years at the Corrosion and Protection Centre at the University of Manchester (UK) as a Fulbright Scholar and as an NSF/NATO Post-doctoral Fellow. He joined the faculty of the University of Virginia in 1990. His past work has included work on the corrosion of metals and alloys in marine environments, non-aqueous and mixed solvents as well as stress-corrosion cracking and other forms of localized corrosion. His present work includes studies of the electrochemical and chemical conditions inside localized corrosion sites in various alloy systems, corrosion in aging aircraft, development of embeddable corrosion microinstruments, microfabrication methods to probe the fundamentals of localized corrosion, and multi-scale modeling of corrosion processes.

He has co-authored over one hundred papers, presented fifty invited talks and is the Co-Director of the Center for Electrochemical Science and Engineering at UVa. He was selected as the recipient of the 1997 A. B. Campbell Award for the best paper by an author 35 years old or younger and the 1999 H. H. Uhlig Award for young corrosion educators from the National Association of Corrosion Engineers. He is also a Fellow of NACE International. He has won several teaching awards while at UVa, including an All University Teaching Award in 2004. He was the 2001 recipient of the Robert T. Foley Award from the National Capital Section of the Electrochemical Society. He has rendered technical assistance to the NRC and DOE concerning the Yucca Mountain Project, the USAF Aging Aircraft Program, the NASA Safety and Engineering Center, and the 9/11 Pentagon Memorial design team. He has supervised 20 Ph.D. students to completion as well as 18 M.S. students.

SELECTED RECENT PUBLICATIONS

1. M. T. Woldemedhin, M. E. Shedd, R. G. Kelly, “Evaluation of the Maximum Pit Size Model on Stainless Steel under Atmospheric Conditions,” J Electrochem. Soc., 161 (8) E1-E9 (2014). http://dx.doi.org/10.1149/2.023408jes
2. E. Schindelholz, B. E. Risteen, R. G. Kelly, "Effect of relative humidity on corrosion of steel under sea salt aerosol proxies I: NaCl," J. Electrochem Soc., 161 (10) C450-C459 (2014). http://dx.doi.org/10.1149/2.0221410jes
3. E. Schindelholz, B.E. Risteen, R. G. Kelly, "Effect of relative humidity on corrosion of steel under sea salt aerosol proxies II: MgCl2, Seawater," J. Electrochem Soc., 161 (10) C460-C470 (2014). http://dx.doi.org/10.1149/2.0231410jes

4. B. E. Risteen, E. Schindelholz, R. G. Kelly, “Marine Aerosol Drop Size Effects on the Corrosion Behavior of Low Carbon Steel and High Purity Iron,” J. Electrochem. Soc., 161 (14) C580-C586 (2014)
5. J. Srinivasan, R. G. Kelly, “Experimental and Modeling Studies on Mass Transport and Electrochemical Factors Influencing Stainless Steel Pitting and Repassivation,” Corrosion J., Vol. 70, No. 12, pp. 1172-1174. (2014). http://dx.doi.org/10.5006/1422
6. P. Khullar, J. V. Badilla, R. G. Kelly, "The Use of a Sintered Ag/AgCl Electrode as Both Reference and Counter Electrode for Electrochemical Measurements in Thin Film Electrolytes", ECS Electrochemistry Letters, 4 (10) C1-C3 (2015). http://dx.doi.org/10.1149/2.0051510eel
7. J. Srinivasan, M. J. McGrath, R. G. Kelly, “A High-Throughput Artificial Pit Technique to Measure Kinetic Parameters for Pitting Stability,” Journal of The Electrochemical Society, 162 (14) C725-C731 (2015). doi: 10.1149/2.0281514jes
8. M. L. C. Lim, J. R. Scully, R. G. Kelly, “Overview of Intergranular Corrosion Mechanisms, Phenomenological Observations, and Modeling,” Corr. J, 72(2), 198-220 (2016). http://dx.doi.org/10.5006/1818
9. C. B. Crane, R. G. Kelly, R. P. Gangloff, "Crack Chemistry Control of Intergranular SCC in Sensitized Al-Mg," Corr. J, 72(2), 242-263 (2016). http://dx.doi.org/10.5006/1852
10. M. L. C. Lim, R. Matthews, M. Oja, R. Tryon, R. G. Kelly, J. R. Scully, “Model to Predict Intergranular Corrosion Propagation in Three Dimensions in AA5083-H131,” Materials and Design, 96, 131-142 (2016).

Dr. John R. Scully

Charles Henderson Chaired Professor of Materials Science and Engineering
Co-director Center for Electrochemical Science and Engineering
University of Virginia, Charlottesville, VA

Education

Ph.D., Materials Science and Engineering, The Johns Hopkins University, May 1987.
M.E.S., Materials Science and Engineering, The Johns Hopkins University, May 1983.
B.E.S., Materials Science and Engineering, The Johns Hopkins University, May 1980.

Dr. John Scully is the Charles Henderson Chaired Professor of Materials Science and Engineering and the Co-Director of the Center for Electrochemical Science and Engineering at the University of Virginia. Previous to this, he was a senior member of the technical staff at Sandia National Laboratories and a materials engineer at the David Taylor Naval Ship Research and Development Center. He received his Ph.D. in Materials Science and Engineering from The Johns Hopkins University and was a visiting scientist at A.T. & T. Bell Laboratories. Dr. Scully is a technical fellow of NACE International, the Electrochemical Society, and the American Society for Metals.

Dr. Scully is the current Technical Editor for the NACE Corrosion Journal, and has also served on the editorial boards of several other journals. He has actively taken part in several national studies aimed at identifying the current corrosion research and education priorities of the U.S., including the National Academy studies on *Corrosion Education* and *Research Opportunities in Corrosion,* as well as the Office of the Undersecretary of Defense sponsored *Corrosion Control* and *Airborne Refueling Task Forces*. In addition, he has reviewed various aspects of the spent nuclear fuel repository corrosion programs for the United States, Canada, the United Kingdom as well as Sweden and has conducted a U.S. Department of Energy workshop on this topic. Dr. Scully has also been a member of numerous national and international panels on key corrosion issues, including eight dealing specifically with spent nuclear fuel disposition and nuclear reactor safety.

Throughout his career, John has focused on research, engineering, and education in corrosion science. John is the recipient of the Henry B. Linford Award for Teaching Excellence, The Electrochemical Society, (2016)., the U.R. Evans Award, "*for Corrosion Science*," U.K. Institute of Corrosion, (2013). The Lee Hsun Lecture Award, Institute of Materials Research (IMR), Chinese National Academy of Science (2012)., the W.R. Whitney Award (from NACE) for recognition of career achievements based on scientific advances in corrosion science and engineering (Awarded 2012), the H.H. Uhlig Award (from ECS) for recognition of career achievements based on scientific advances in corrosion science from the Electrochemical Society (Awarded 2009)

Professional Interests

Technological advancements that improve the standards of living, safety, and the quality of life of the citizens of the commonwealth and nation place ever-increasing demands on engineers to provide materials with improved properties that enable these advancements. As materials engineers, our goal is to design materials with suitable properties to meet these demands. Unfortunately, most materials suffer from "time dependent" degradation phenomena that tend to

alter their properties over time. This can cause safety and reliability concerns. One example of time-dependent degradation phenomena is the corrosion of metallic materials. This phenomenon costs the US over $270 billion dollars annually. My specialty within the Materials Science and Engineering field is to understand the scientific mechanisms of corrosion, the prevention and protection against corrosion phenomena, discovery of novel corrosion protection mechanisms, as well as the lifetime prediction of time-dependent corrosion degradation phenomena. Lifetime prediction enables the determination of safe-life, fail-safe, retirement-for-cause material conditions as well as inspection intervals.

More specifically, my primary research interest is to understand the relationships between a material's structure and composition and properties related to environmental degradation. The properties of focused interest and activity are those associated with hydrogen embrittlement, stress corrosion cracking, localized corrosion, and passivity of materials. My historical current focus is on advanced aluminum, magnesium, titanium, ferrous and nickel-based alloys, as well as stainless steels and aluminum-based intermetallic compounds. A secondary engineering objective is development of methodologies for lifetime prediction engineering materials in corrosive environments. A recent focus has been on nano-engineered materials including multifunctional metallic glasses that deliver novel barrier, sacrificial anode, and chemical inhibition properties. All funded research projects and research gifts or donations fall into one of these two areas. Funding in each of these areas is provided through a mixture of Federal Government (NSF, ONR, NASA, AFOSR, DOE), specific Federal Laboratories (Sandia National Labs), and industrial sources (Alcoa, DuPont, Reynolds, GE, Newport News Shipbuilding, Copper Development Assoc.). Occasionally, funding from state agencies is also achieved (VDOT).

Dr. Alan Turnbull, OBE, FRS, FREng, FIMMM, FNACE, FICORR

Electrochemistry and Corrosion Group
National Physical Laboratory
Teddington, Middlesex

Education

1966-1970 University of Strathclyde (Chemistry) BSc 1st Class
1970-1973 University of Bristol (Chemistry Department)
PhD for "Neutron Scattering Studies of Molecular Crystals"

Alan Turnbull is a Fellow of the Royal Society, the Royal Academy of Engineering, NACE International, the Institute of Materials, Minerals and Mining, and the Institute of Corrosion. Since joining NPL in 1973, Alan has produced over 250 publications on environment induced cracking of metals and of thermoplastics, on localized corrosion, and on modelling of corrosion processes, and has been the principal author of ten international standards. He is a recipient of the T P Hoar Prize (twice) from the Institute of Corrosion; the Bengough Prize and Medal from the Institute of Materials; a Technical Achievement Award from NACE International; the Cavallaro Medal from the European Federation of Corrosion; the U R Evans Award from the Institute of Corrosion, the Whitney Award from NACE International, and the Alex Hough-Grassby Award from the Institute of Measurement and Control. He was elected Fellow of the Royal Academy of Engineering in 2011 and Fellow of the Royal Society in 2013. In 2016, he was awarded the Order of the British Empire (OBE) for services to science and engineering.

Publications

- Author of 123 peer-reviewed research papers, 84 conference papers, plus over 70 NPL technical reports (mostly C-in-C); principally on corrosion but also on polymer degradation; in addition, numerous failure analysis reports unlisted.
- Principal author of ten international standards and significant contributor to many other ISO and NACE standards.
- Chapter/sections in five books
- Editor of two international conference proceedings.

Primary scientific achievements

- Initiated major advance in scientific understanding and prediction of stress corrosion cracking and corrosion fatigue crack growth rates by developing robust fundamentally-based models and in-situ measurement techniques to quantify the local chemistry and electrochemistry at a reacting crack tip.
- Established the critical foundations for prediction of hydrogen assisted cracking through comprehensive, integrated models for hydrogen generation, diffusion, and trapping in metals.
- Novel X-ray tomographic measurement and modelling of the pit-to-crack transition showing for the first time how stress corrosion cracks actually develop from corrosion pits and providing a radical mechanistic explanation for the process.

- Developing innovative techniques to characterize the electrochemistry and stress corrosion cracking resistance of corrosion resistant alloys for oil and gas applications.

Major consultancies

- Lead scientist investigating $6bn catastrophic failure of Great Man-Made River pipeline, Libya, 2000.
- Expert on international 5-man panel to assess the BP Inherently Reliable Facilities Flagship program, 2009 (continued as advisor to BP)
- Evaluation of risk of hydrogen embrittlement of nuclear waste containment for NAGRA, Switzerland, 2009.
- Independent expert investigating fracture of a pipeline in the power industry that led to serious injury to 3 workers, 2007.
- Expert advisor on disparate corrosion and cracking studies in nuclear waste reprocessing including highly active storage containers and the Thorpe weld cracking failure.

Research history

- An undergraduate project on self-diffusion in naphthalene was followed by a PhD study of molecular reorientation in plastic crystals using the neutron scattering technique with supportive modelling to unravel the rotational hopping mechanism.
- Joining the Corrosion Group at NPL in 1973, my responsibility was to develop a new research program on corrosion fatigue of offshore structures. Somewhat controversially for the time, I focused on the local chemistry and electrochemistry at crack tips using my evolving expertise in modelling transport processes combined with insight into chemical kinetics. This research evolved into the general theme of "Corrosion Chemistry within Pits, Crevice and Cracks" for which I became acknowledged as the world leader with an invitation to MIT to aid the development of their modelling.
- Recognizing the potential importance of hydrogen assisted cracking, especially in the oil and gas industry, I set out in a new direction in 1986 to advance the measurement and modelling of hydrogen transport in metals and to link that with different methods of testing resistance to hydrogen assisted cracking (compatible with NPL's metrology remit). This led to new models of hydrogen permeation and international standards for measurement such that NPL became the world leader in the field.
- In parallel with this work, a new focus on polymer degradation was initiated in1993, with the first application of nanoindentation and new insights into weathering of polymers.
- Corrosion pitting and the transition to cracking is an issue of major engineering concern and innovative modelling and novel X-ray tomography measurements established NPL at the forefront of ideas and their translation to engineering practice.
- Anticipating the demand for supportive research on energy generation, new projects on fuel cells (modelling and in-situ measurement) and 3rd generation solar photovoltaic systems were initiated with scanning electrochemical microscopy (SECM), SECM-AFM, photoconducting AFM all being explored as supportive tools.

APPENDIX B: SUMMARY OF AVAILABLE CRACK GROWTH RATE DATA

Summary of available data for estimating chloride-induced SCC crack growth rates for 304/316 stainless steel

Charles Bryan and David Enos

B.1 Introduction

The majority of existing dry storage systems used for spent nuclear fuel (SNF) consist of a welded 304 stainless steel container placed within a passively-ventilated concrete or steel overpack. More recently fielded systems are constructed with dual certified 304/304L and in some cases, 316 or 316L. In service, atmospheric salts, a portion of which will be chloride bearing, will be deposited on the surface of these containers. Initially, the stainless steel canister surface temperatures will be high (exceeding the boiling point of water in many cases) due to decay heat from the SNF. As the SNF cools over time, the container surface will also cool, and deposited salts will deliquesce to form potentially corrosive chloride-rich brines. Because austenitic stainless steels are prone to chloride-induced stress corrosion cracking (CISCC), the concern has been raised that SCC may significantly impact long-term canister performance. While the susceptibility of austenitic stainless steels to CISCC in the general sense is well known, the behavior of SCC cracks (i.e., initiation and propagation behavior) under the aforementioned atmospheric conditions is poorly understood.

A literature survey has been performed to identify SCC crack growth rate (CGR) studies conducted utilizing conditions that may be relevant to existing SNF interim storage canisters, the results of which are presented in this document. The data presented here have been restricted to those representing atmospheric corrosion of stainless steels due to deliquescence of marine salts, or marine salt components, on the metal surface. A suite of experimental studies representing both long-term field tests and accelerated laboratory tests has been identified. Potentially relevant data are summarized in Figures 1-1 (304 SS) and Figure 1-2 (316 SS). In the Figures, when a particular reference utilized a series of samples, the range is shown as a bar, and the average value shown with a symbol. A summary of the test methods, sample geometry, and environmental conditions for each study is given in Table 1-1.

While the surveyed studies all explore SCC of austenitic stainless steels under atmospheric conditions, the methods through which each researcher approached the problem do differ, as illustrated in Table 1-1. The surveyed studies utilized a variety of metal treatments including as-fabricated, solution annealed, welded, and sensitized material. Furthermore, different surface treatments (polished vs ground) were also used. In addition, most of these studies were accomplished using techniques that are not generally accepted for high-fidelity crack growth rate measurements, and in cases where more traditional approaches were taken, these methodologies may not be applicable to the atmospheric conditions of interest here. The wide variety of methods and materials results in the observed large scatter in measured CGRs. Each of the data sets in Figures 1-1 and 1-2 is described in more detail in the following sections. A short summary of crack growth rates based on operational experience is also presented.

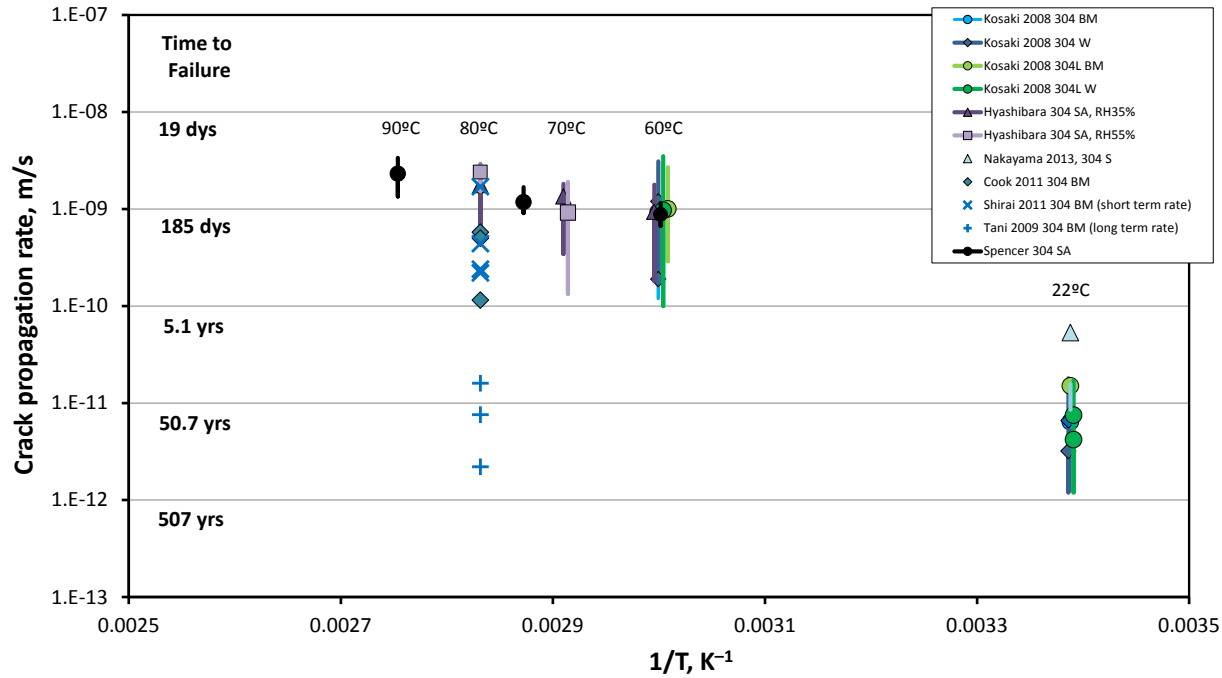

Figure 1-1. SCC propagation rates for atmospheric corrosion of 304SS. BM –base metal; W–weld sample; SA–solution annealed; S–sensitized. Bars represent reported ranges (if more than one), while symbols represent average values. "Times to failure" are for a 5/8" thickness, assuming continuous crack propagation over time.

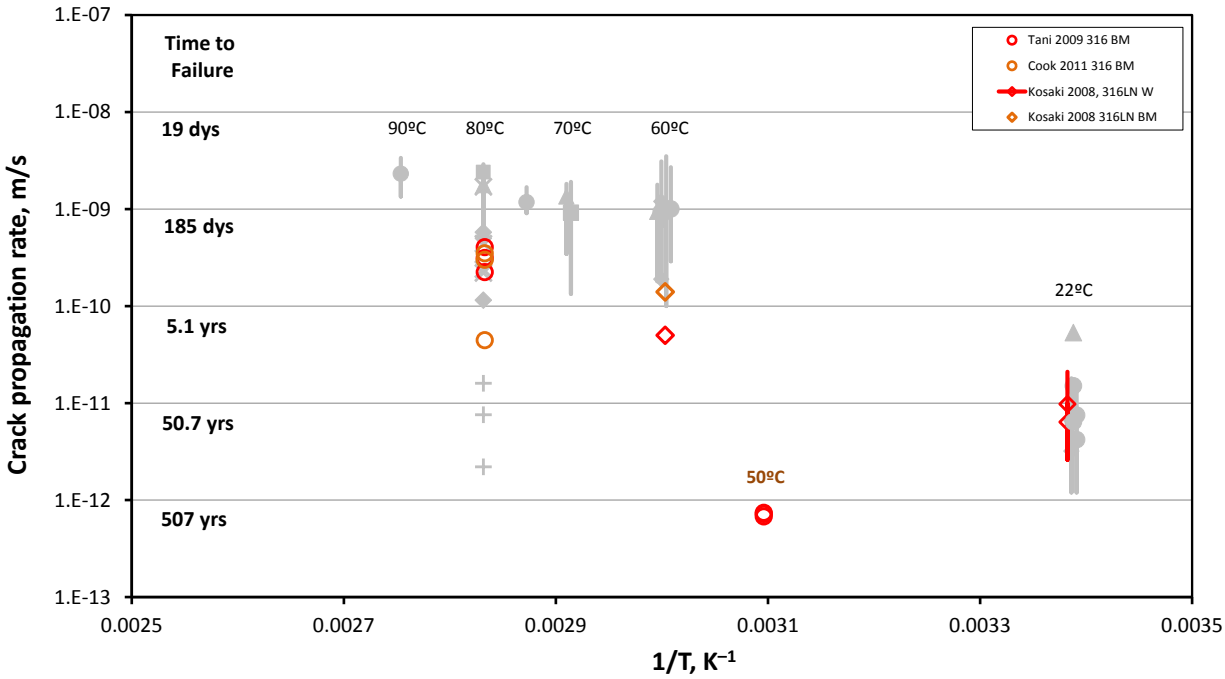

Figure 1-2. SCC propagation rates for atmospheric corrosion of 316SS. "Times to failure" are for a 5/8" thickness, assuming continuous crack propagation over time.

Table 1: Summary of SCC Crack Growth Rate Studies

Researcher		Materials	Salt Loading Method	Environments	Sample Geometry	Crack Geometry	CGR Measurement method
Kosaki	2008	304, 304L, 316LNG	1. Natural exposure 2. Salt fog (saturated NaCl)	1. Ambient 2. 60C/95% RH	Initiation: 4 point bent Propagation: 3 point bend	Fatigue precrack described as through crack and half-elliptical surface crack	Optical - max depth/time
Hayashibara	2008	304 (solution annealed)	10 uL droplet of seawater placed on samples	35-75% RH, 60-90C	Dogbone, spring loaded	no precrack, nucleation from localized corrosion sites Final geometry not described	Length measured in SEM, depth optically
Nakayama	2013	304, 304H	natural exposure	ambient	U-bend	no precrack, nucleation from localized corrosion sites	Optical - surface length measured, depth calculated
Cook	2011	304L, 316L	coated with sea salt or $MgCl_2$ applied as a mist then dried	32% RH, 80C	U-bend	no precrack, nucleation from localized corrosion sites	Optical - surface length measured, depth calculated
Spencer	2014	304L, cold worked	$MgCl_2$ applied via air brush with an EtOH carrier. Deposit weight not measured	60-90C, 10-70% RH	Bend bar	no precrack, nucleation from localized corrosion sites Crack length on surface measured	Optical - surface length measured. Rate = length/time
Tani	2009	316L, 312	synthetic seawater droplet injected into notch	80C, 35% RH	CT specimen	Crack geometry not presented upon completion of test	DCPD
Shirai Tani	2011 2010	304L	$MgCl_2$ droplet or possibly spray	80C, 35% RH	4 point bend bar	no precrack - nucleation from localized corrosion site	DCPD

B.2 Available Data on Atmospheric SCC Crack Growth Rates

B.2.1 Kosaki [2008]

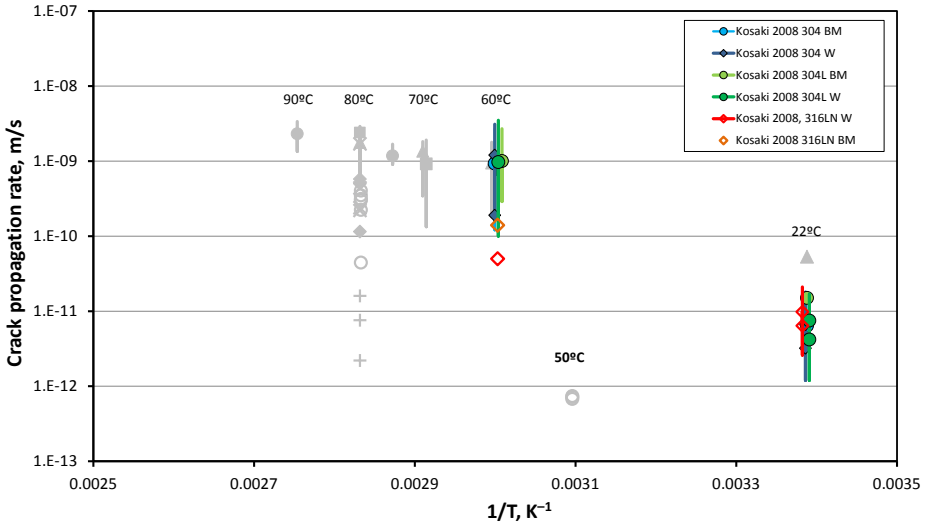

Figure 2.1-1. Data from *Kosaki* [2008].

Kosaki [2008] evaluated performance of stainless steels, including 304, 304L, 316LN, and both base-metal and welded specimens were used. Corrosion rates were measured in long-term natural exposure tests in a near-marine setting (Miyakojima Island south of Okinawa; tropical rainforest to humid subtropical climate); both exposed samples and under-glass samples (to avoid rain washing) were used. An accelerated test was also run (60ºC, 95% RH, NaCl "steam"). Both crack initiation and crack growth experiments were run.

The crack initiation experiments were run using 4-point bend specimens at tensile stresses of 0.5 and 1.0 σ_y. At ambient conditions, exposed and under glass, SCC crack initiation was observed only of the 304 weld specimens, over the ~2.5 year duration of the test. Under accelerated conditions, SCC cracking was observed within 30 days for all samples.

Crack growth experiments were done with 3-point bend specimens, with applied outer fiber stresses of 0.4 and 0.8 σ_y. Pre-cracks were induced by fatiguing (thermal?) and are described as "*…through crack and half-elliptical surface crack…*" It is not clear what "*through crack*" means, but the diagram in the paper (see Figure 2.1-2), seems to show a vertical crack penetrating the sample (with crack propagation rates measured as lateral growth?). SCC crack growth rates were measured by fully fracturing the samples and performing post-mortem visual analysis (reported CGRs were calculated ignoring incubation time, and are hence minimum values). While SCC

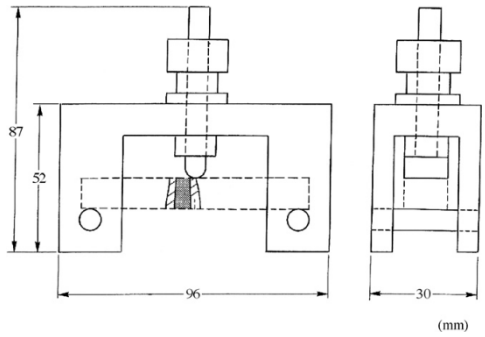

Figure 2.1-2. 3-point bending specimen for SCC propagation test [*Kosaki* 2008, Figure 5].

initiation was rarely observed in the initiation experiment, SCC crack growth was measured in most of the pre-cracked CGR test samples. Results are summarized in Table 2.1-1 [*Kosaki* 2008, Table 2]. There was little difference between weld and base metal samples for 304 and 304L, and little difference in measured rates for those two materials. The 316LN performed better, with no observed SCC in the unwelded samples at ambient conditions, and slightly slower corrosion rates in the accelerated test. Perhaps surprisingly, the under-glass specimens performed significantly better than the exposed specimens.

Table 2.1-1. Propagation rates of SCC in test materials [*Kosaki* 2008, Table 2]

	SCC propagation rate, natural exposure (m/s)		SCC propagation rate, accelerated test (m/s)
Material	**Direct exposure A1**	**Under glass exposure A2**	
Type 304			
Base metal	6.4E−12	(no SCC)	9.3E−10 (1.2E−10 to 2.7E−9)
Weld	6.6E−12 (2.1E−12 to 1.8E−11)	3.2E−12 (1.2E−12 to 6.4E−12)	1.2E−09 (1.9E−10 to 3.1E−9)
Type 304L			
Base metal	1.5E−11	(no SCC)	1.0E−09 (2.9E−10 to 2.7E−9)
Weld	7.5E−12 (1.2E−12 to 1.7E−11)	4.2E−12 (4.1E−12, 4.3E−12)	9.7E−10 (1.0E−10 to 3.5E−9)
Type 316LN			
Base metal	(no SCC)	(no SCC)	1.4E−10
Weld	9.8E−12 (2.6E−12 to 2.1E−11)	6.4E−12	5.0E−11

Note: Propagation rates of SCC show average values and values in ( ) show scattering range of data.

Raw data are shown in Figure 2.1-3 [*Kosaki* 2008, Figures 5 and 6]. The authors report no CGR dependence on stress intensity factor (K_I) over a range of 0.5 to 30 MPa. However, for the stated experimental design—three-point bend specimens with a fixed load and with pre-cracks of different geometries---it seems impossible to actually calculate an accurate K_I value, or to achieve the range described. For instance, for an elliptical crack, at the cited applied stresses, the CGR would have to be measured at a depth of 10 microns to obtain a rate at $K_I = 0.5$ MPa $m^{½}$. Conversely, actually achieving a measurable or calculable K_I of 30 MPa $m^{½}$ would be very difficult in a sample of the cited dimensions (90 mm long × 15 mm wide × 10 mm thick). For either of the proposed pre-crack geometries, it is not clear how K_I values could have been accurately estimated at any point along the crack front.

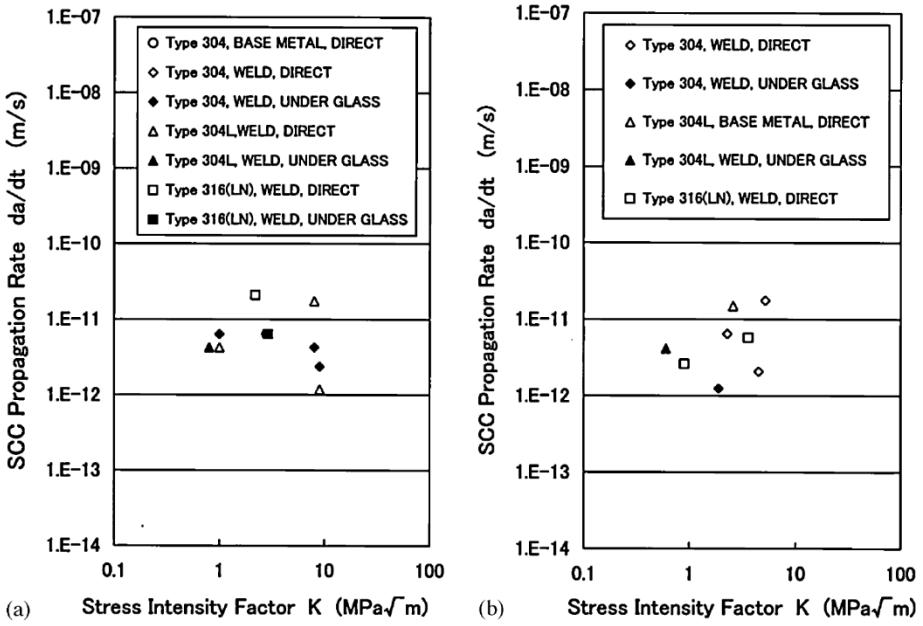

Fig. 6. SCC propagation rate of Type 304 (natural exposure test). (a) Penetrate pre-crack; (b) half elliptical surface pre-crack.

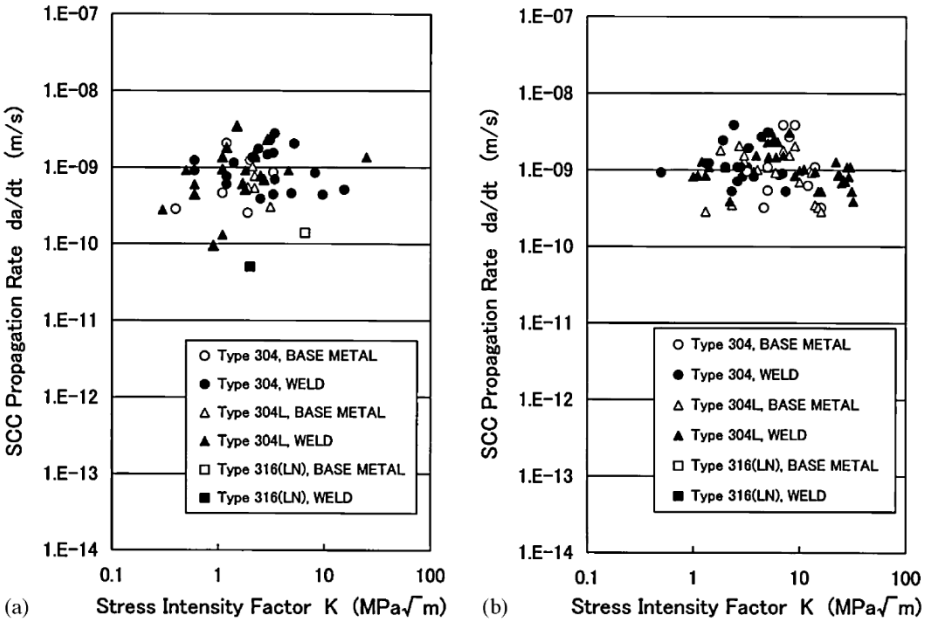

Fig. 7. SCC propagation rate of Type 304 (accelerated test). (a) Penetrate pre-crack; (b) half elliptical surface pre-crack.

Figure 2.1-3. CGR data as a function of K_I from *Kosaki* [2008, Figures 6 and 7].

B.2.2 Hayashibara et al. [2008]

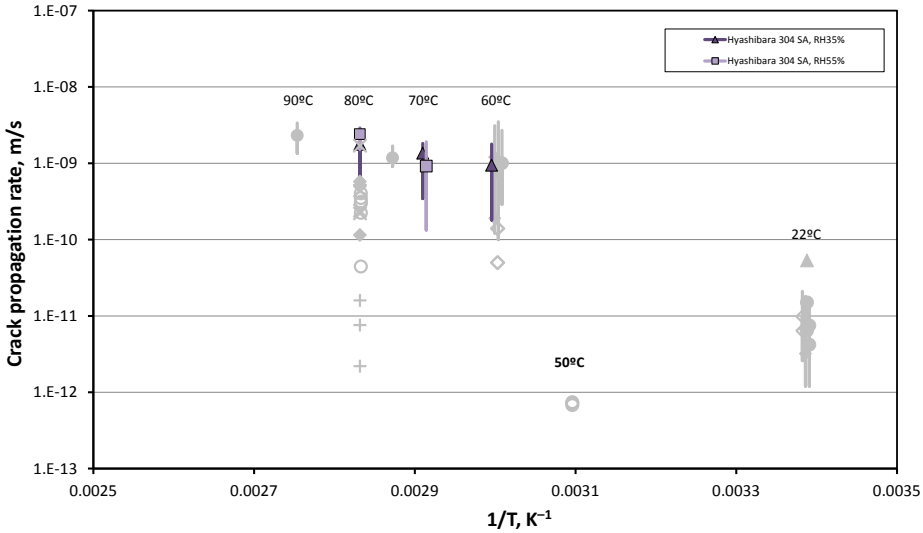

Figure 2.2-1. Data from *Hayashibara et al.* [2008]

This laboratory study was carried out using solution-annealed 304 stainless steel under constant load uniaxial tensile stresses of 0.5 to 1.25 $\sigma_{0.2}$ (reported to be 313 MPa at room temperature). Specimens were dogbone-type specimens, 100 mm long and 26 mm wide with an 8 mm gauge section, and 2 mm thick. Specimens were held at temperatures of 80ºC, 70ºC, and 60ºC, at RH values of 35%, 55%, and 75% for 120 to 1075 hours. Samples were loaded with salt by applying 10µL droplets of synthetic seawater onto three points of the metal surface within the gauge section. Crack lengths were measured optically after conclusion of the experiment (reported CGRs were calculated ignoring any incubation time, and are hence minimum values). CGRs as a function of applied tensile stress from *Hayashibara et al.* [2008] are shown in Figure 2.2-2 and Figure 2.2-3. At 80ºC, the maximum growth rate did not depend on applied stress, but at 70ºC and 60ºC, the crack growth rate increased with increasing tensile stress. SCC initiation strongly depended on RH at all temperatures. At 55% RH, SCC initiated at all chloride spots, while at 35% RH, SCC initiated at all applied stresses, but a much higher fraction of chloride spots initiated at tensile stresses equal to $\sigma_{0.2}$ or higher. Measured crack growth rates were highly scattered, and the range of possible activation energies was estimated to be 23–105 kJ mol^{-1}. The authors suggested that the scatter was due to differences in crack incubation time with temperature, and proposed that the lower end of this range, from 23 to 39 kJ mol^{-1} (based on the highest crack rates, which were likely the first to initiate and hence the most likely to not include a significant incubation time) were preferred.

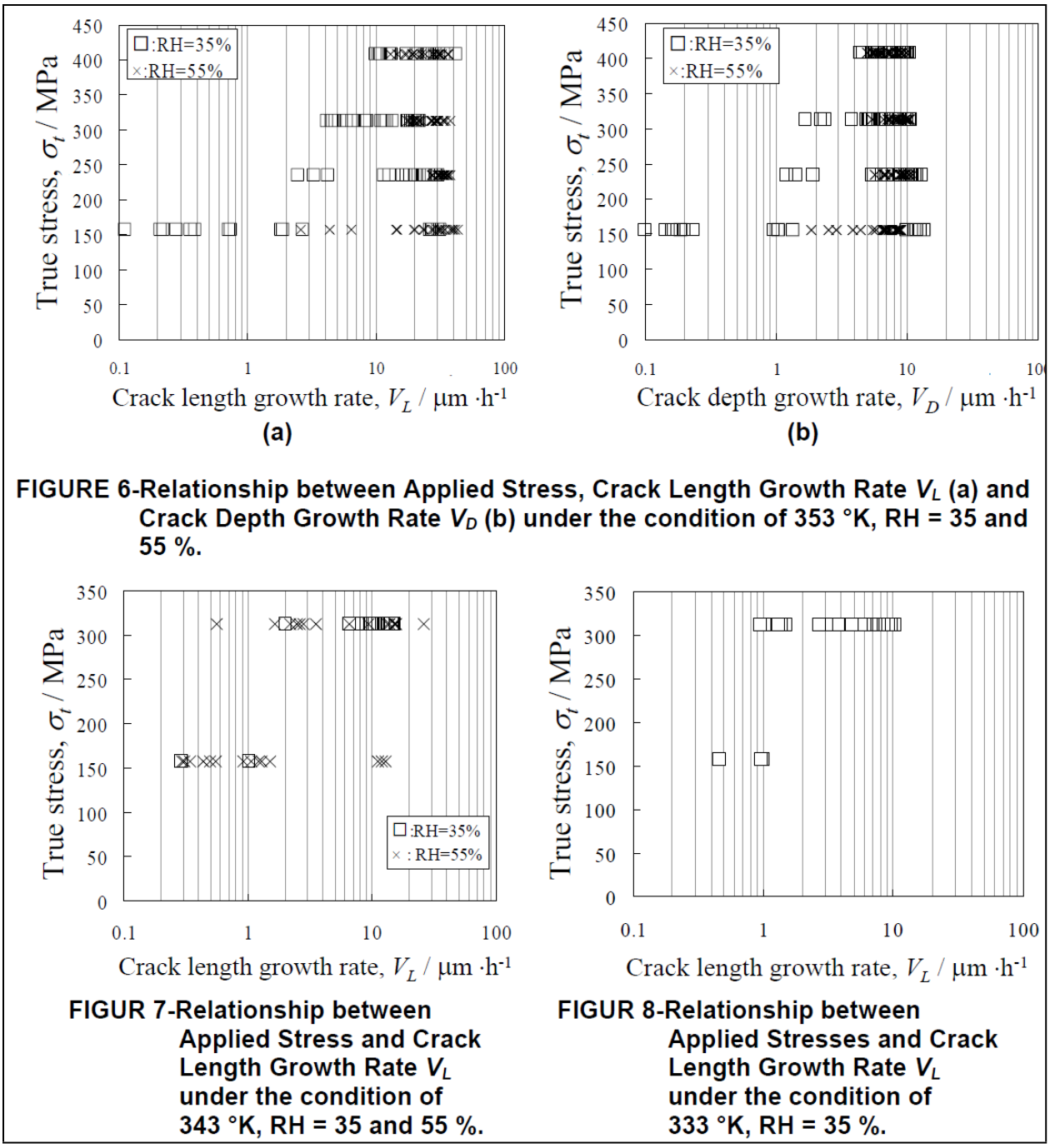

FIGURE 6-Relationship between Applied Stress, Crack Length Growth Rate V_L (a) and Crack Depth Growth Rate V_D (b) under the condition of 353 °K, RH = 35 and 55 %.

FIGUR 7-Relationship between Applied Stress and Crack Length Growth Rate V_L under the condition of 343 °K, RH = 35 and 55 %.

FIGUR 8-Relationship between Applied Stresses and Crack Length Growth Rate V_L under the condition of 333 °K, RH = 35 %.

Figure 2.2-2. CGR data for both crack length and crack depth, as a function of applied tensile stress. Data from *Hayashibara et al.* [2008; Figures 6-8].

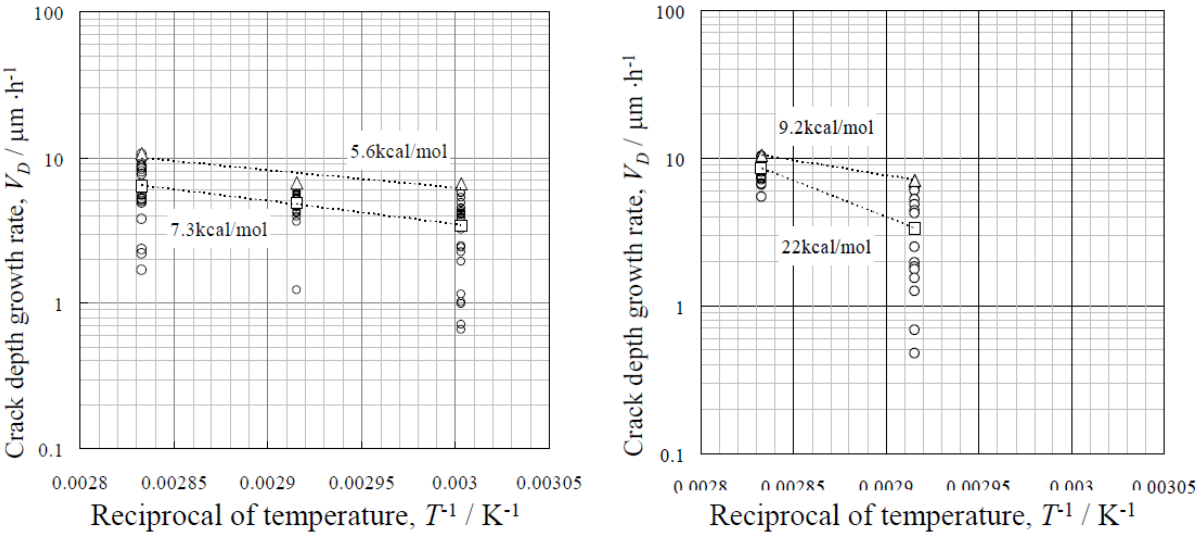

FIGURE 10-Arrhenius Plot of Crack Depth Growth Rate V_D under the condition of RH = 35 % (a) and 55 % (b). Δ and □ mean the maximum value and average values, respectively.

Figure 2.2-3. Arrhenius plots for crack depth CGR data from *Hayashibara et al.* [2008; Figure 10].

B.2.3 Nakayama and Sakakibara [2013]

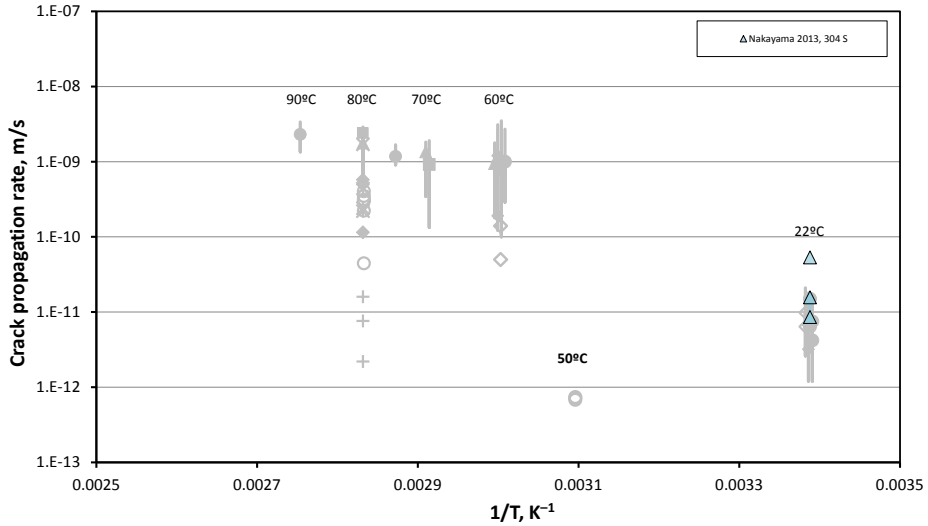

Figure 2.3-1. Data from *Nakayama and Sakakibara* [2013].

This article summarized test data collected in Japan that is published in several Japanese-language reports. The authors used the data to build a time-to-failure model for repair-welded joints, for 304 SS canisters with wall thicknesses of 20 mm. The authors describe two in-service failures of 304 stainless steel (containing a notably high carbon content of 0.079), one 16.5 mm thick, and one 14 mm thick, in 7 and 35 years, respectively. These correspond to penetration rates of 2.3 mm yr^{-1} and 0.4 mm yr^{-1}. The failures occurred at weld repairs.

The testing work used 304 stainless steel U-bend specimens sensitized to R_a values of 2% to 20%, and demonstrated that SCC initiation and propagation rates, over the interval of the test, were strongly a function of R_a. One set of samples was exposed to marine salts at a shipyard (both without a roof and under a roof), while a second set was placed at an inland site. The exposed near-marine samples cracked within half a year, with crack length growth rates of 0.54 – 3.36 mm yr^{-1}; the under-roof near-marine samples initiated SCC more slowly, but once initiated (0.8 yrs), grew quickly at 0.99 mm yr^{-1}. The crack depth data in Figure 8 were calculated by assuming a crack depth-to-half-surface-length ratio of 0.5—the range of 0.3 to 0.5 is typical for austenitic materials (Lu et al., 2005). The authors present other data showing strong crack growth rate dependencies on R_a, $[Cl^-]$, m_{Cl} on the surface, and applied stress, and present a SCC initiation and growth models incorporating all of these.

B.2.4 Cook et al. [2011]

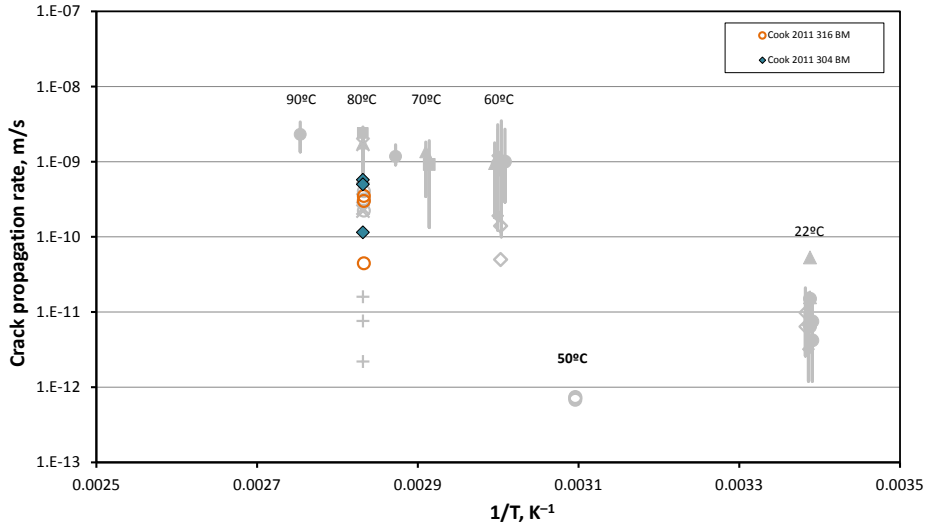

Figure 2.4-1. Data from *Cook et al.* [2011].

Cook et al. [2011] evaluated SCC of both 304L SS and 316L SS U-bend samples (applied stresses not provided) coated with sea-salts and with magnesium chloride in laboratory tests at a temperature of 80ºC and a RH of 30% (conditions not possible on a canister surface). Corrosion was measured after 42 days of exposure. SCC crack lengths were measured and reported in the reference; the crack depth data in Figure 2.4-1 were calculated from those data by assuming a crack depth-to-half-surface-length ratio of 0.5—the range of 0.3 to 0.5 is typical for austenitic materials [*Lu et al.*, 2005]. CGRs were calculated from the total exposure time (no incubation time) and hence are minimums.

B.2.5 Spencer et al. (2014)

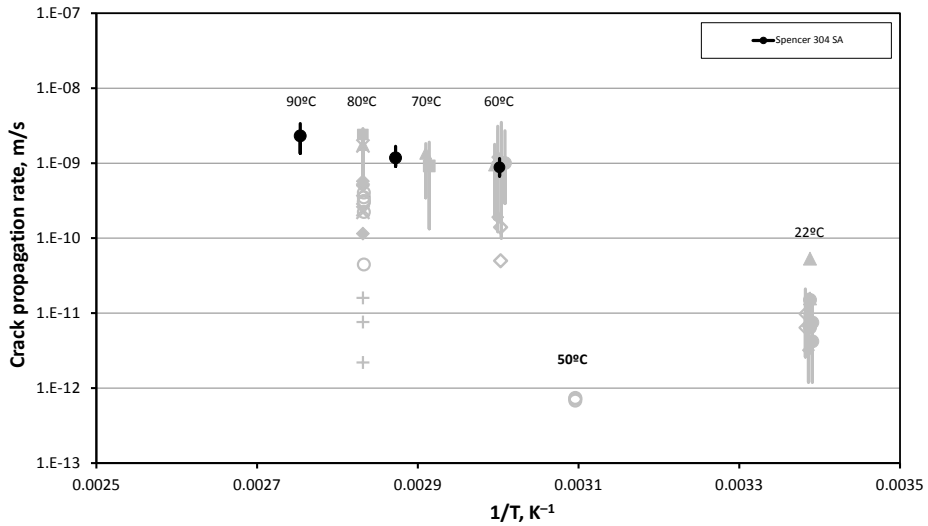

Figure 2.5-1. Data from *Spencer et al.* [2014].

Spencer et al. [2014] performed laboratory tests evaluating SCC crack growth rates in annealed 304L ($\sigma_{0.2}$ was 210 MPa after annealing), and to which a uniaxial plastic strain had been applied (the authors were evaluating, in part, the importance of prior plastic strain on SCC initiation and growth). A spring-loaded bend geometry was used for the CGR tests (Figure 2.5-2). Samples were loaded with a visible coating magnesium chloride, applied as a methanol spray and allowed to dry. Surface loading was not measured.

Tests were run at 60º, 75º, and 90ºC, and saturated salt solutions were used to maintain constant relative humidities in the test chambers, at values varying from 10% to 70%. Plastic strains varied from 0 -40%, and tensile stresses (outer fiber) up to 180 MPa. Test results showed a strong dependence on the degree of prior plastic strain, with maximum CGR at values of less than 10% strain; at higher strains, cracking did not occur (Figure 2.5-3). Although here appeared to be a threshold tensile stress of about 10 MPa, crack parameters (maximum and average growth rate, and crack density) rose quickly with increasing stress and plateaued rapidly. Cracking was not observed at 10 % RH, the lowest value tested, but was observed at 30% RH and above, for tensile stresses of both 60 MPa and 120 MPa. CGRs showed a general increase with RH, but the overall response to variation in RH varied with tensile

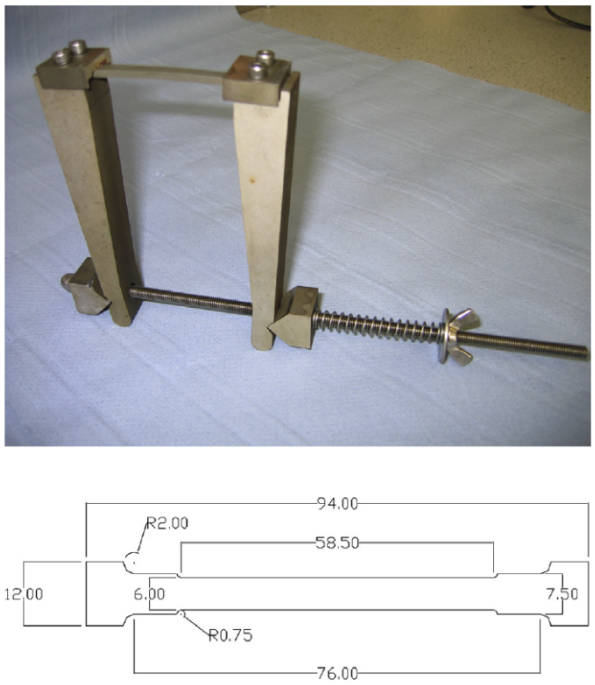

Figure 2.5-2. Bend test assembly used in *Spencer et al.* [2014, Figure 1].

stress and degree of prior strain (Figure 2.5-4).

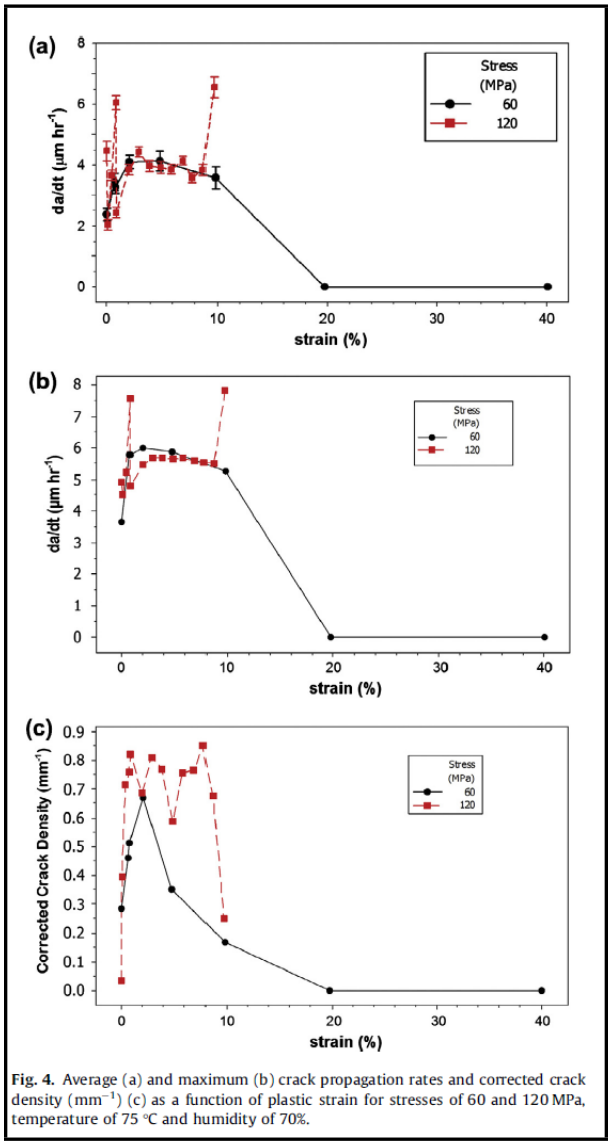

Fig. 4. Average (a) and maximum (b) crack propagation rates and corrected crack density (mm^{-1}) (c) as a function of plastic strain for stresses of 60 and 120 MPa, temperature of 75 °C and humidity of 70%.

Figure 2.5-3. Measured crack parameters as a function of degree of prior plastic strain. Data from *Spencer et al.* [2014; Figure 4].

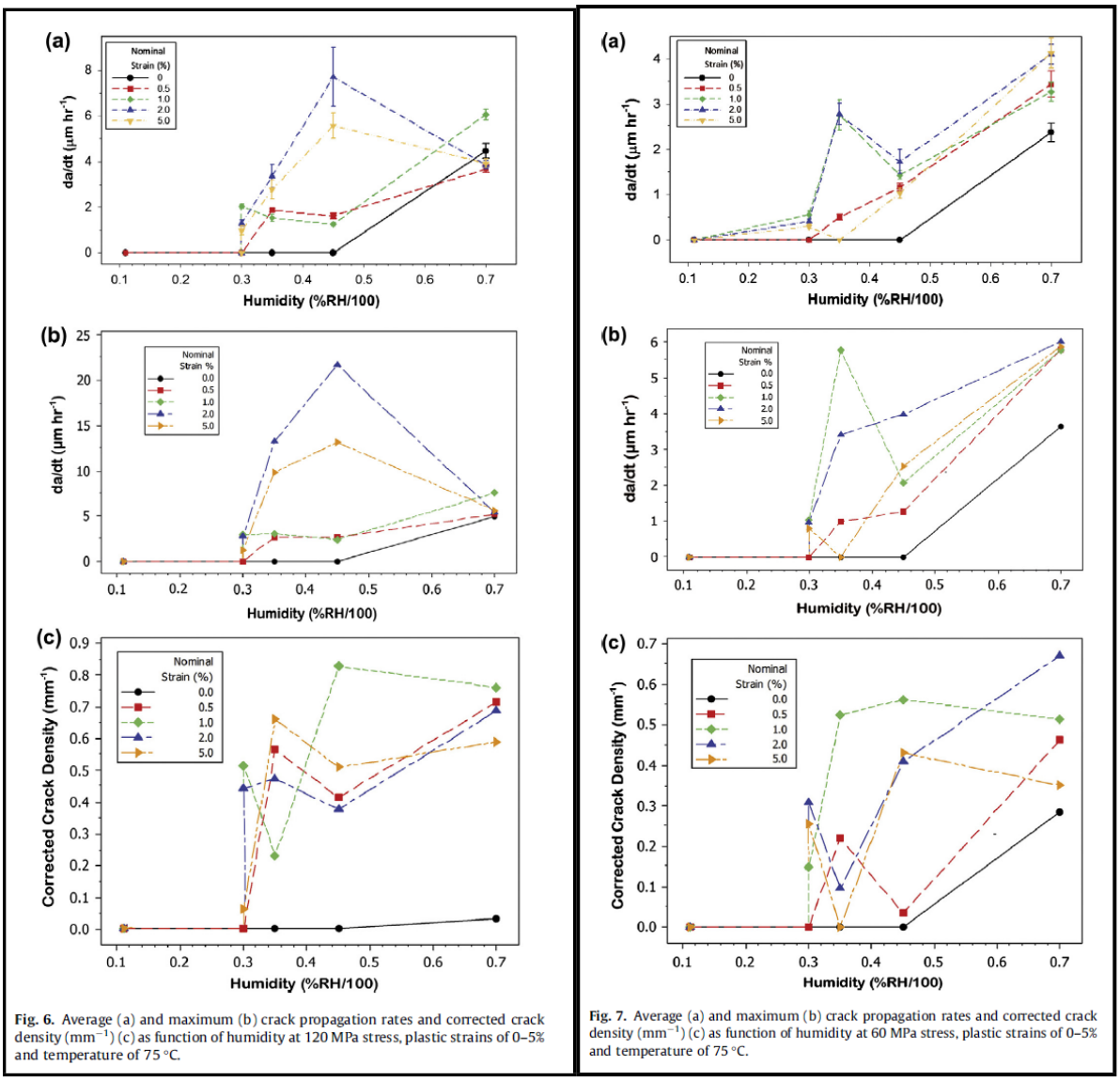

Fig. 6. Average (a) and maximum (b) crack propagation rates and corrected crack density (mm^{-1}) (c) as function of humidity at 120 MPa stress, plastic strains of 0–5% and temperature of 75 °C.

Fig. 7. Average (a) and maximum (b) crack propagation rates and corrected crack density (mm^{-1}) (c) as function of humidity at 60 MPa stress, plastic strains of 0–5% and temperature of 75 °C.

Figure 2.5-4. *Spencer et al.* [2014; Figures 6 and 7]; measured crack parameters as a function of relative humidity, for tensile stresses of (left) 120 MPs, and (right) 60 MPa.

Measured CRGs reported by *Spencer et al.* [2014], for samples with 2-5% plastic strain at 70% RH, were 8.9±3 μm/hr (2.5E-9 m/s) at 90ºC; 4.2±0.956 (1.2E-9 m/s) at 75ºC; and 3.2±0.64 μm/hr (8.9E-10 m/s) at 60ºC. Spencer used these samples to estimate an apparent activation energy of 33.7 kJ mol^{-1}.

B.2.6 Data from CRIEPI

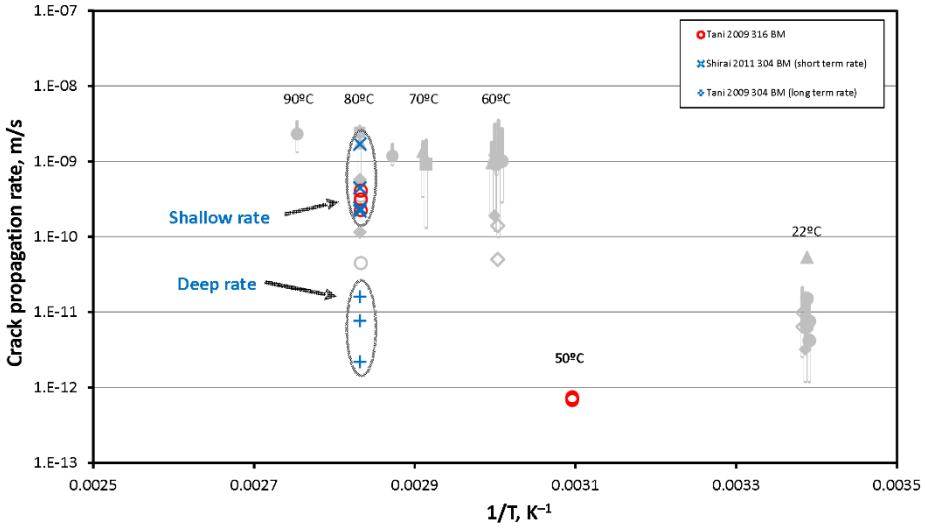

Figure 2.6-1. Data from CRIEPI.

The Central Research Institute of Electric Power Industry (CRIEPI), a research institute of the Japanese nuclear industry, ran two types of experiments evaluating CGR under atmospheric conditions. In the first [*Tani et al.*, 2009], compact tension tests were run with 316 SS, loaded to achieve K values of 5–30 MPa $m^{0.5}$. Samples were loaded with salt by applying 20µL droplets of synthetic seawater directly to the CT notch. Tests were run at 50ºC and 80ºC, at a constant RH of 35% for the duration of the test. Crack depths were determined by DCPD. At stress intensity factors of 10 MPa $m^{0.5}$ and above, there was no variation in crack growth rate with applied stress; the single 80ºC test at 5 MPa $m^{0.5}$ was about 60 times lower than the 80ºC tests at higher K values (note that this point is not shown above, as it was apparently not a "plateau" value, and is not directly relatable to the other data.

The second type of experiment that CRIEPI ran were four-point bend tests [*Shirai et al.*, 2011a; *Shirai et al.*, 2011b; *Shirai et al.*, 2011c; *Tani et al.*, 2010]. The beams used for these tests were 20 mm wide, 10 mm thick, and 220 mm long. These tests were run using 304SS, at 80ºC and 35% RH (conditions corresponding to an absolute humidity too high to be achieved on a canister surface), with an applied outer fiber tensile stress of 270 MPa. The specimens used are quite thick, so that crack growth rates at depths greater than a few mm could be measured. Four tests were run, three with synthetic seawater and one with saturated magnesium chloride brine. As shown in Figure 2.6-2 [*Shirai et al*. 2011, Figure 3-2], the seawater and magnesium chloride brine were applied as a single 20µL droplet in the center of the beam. (*It should be noted that in several conference publications, and in Figure 3-6 of the same CRIEPI project report, the salt was described as being applied as a spray, with a loading of 10 g/cm² Cl. This is inconsistent with the earlier Figure 3-2, and with the text in the report. Given the*

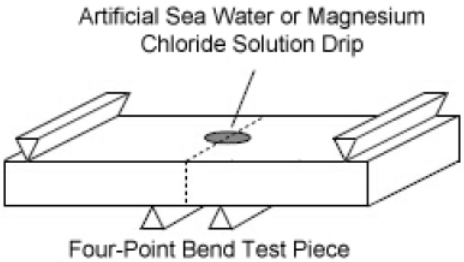

Figure 2.6-2. CRIEPI 4-point bend tests [*Shirai et al.* 2011; Figure 3-2].

droplet loading scheme, and the fact that saturated magnesium chloride brine contains 15 times as much Cl as seawater, it seems clear that the actual salt loadings used for the bend tests varied, and are poorly defined). Crack areas were measured by DCPD, and depths were estimated by assuming a half-elliptical crack observed crack aspect ratio at the end of the experiment was typical of the entire experiment—that is, that the crack aspect ratio was constant. The observed a/c (crack depth to half length) ratios were between 0.5 and 1.

Observed crack depths over time are given in Figure 2.6-3 [*Shirai et al*. 2011a, Figure 3.6]. For each of the three samples loaded with synthetic seawater, the crack growth curves seem to show two segments. These is an initial fast growth, which transitions into a much slower, steady rate at a depth of about 2-3 mm. The early crack growth rate data that were measured ($\sim 4 \times 10^{-10}$ m s^{-1}) are consistent with the other studies presented here; but the long-term rate is much slower ($\sim 2 \times 10^{-11}$ m s^{-1} to 8×10^{-12} m s^{-1}). For the sample loaded with saturated magnesium chloride brine, there was no slowing of CGR with depth. The initial interpretation of the slowing in crack growth was that it was due to the changing stress state in the bend sample with depth (*Shirai et al*. 2011a); if so, then the slower rate would not be applicable to SNF storage canisters, which have been shown to have through-going tensile stresses. However, several other papers by CRIEPI make use of the slower rate data when assessing possible canister penetration rates without comment (e.g., *Tani et al.* 2010; *Shirai et al.* 2011b). *EPRI* [2014] makes use of the bimodal crack growth data and attributes the slower rate at depth to cathodic limitations related to the thin and discontinuous brine film and the presence of undissolved salt particulates; in the case of magnesium chloride, all salts would have deliquesced, so cathodic limitation would not occur.

It is important to note that the long-term CRIEPI rate does not represent the "plateau rate" that is commonly seen with increasing K_I, because the rate actually drops to a constant low value, rather than increasing to a constant maximum value.

Because of the potential importance of the CRIEPI observations, we discuss the experiments here in detail. There are many issues with interpreting or applying the CRIEPI data:

Use of DCPD to estimate elliptical crack depth requires assuming a constant crack aspect ratio.

CRIEPI utilized reversing DCPD to measure crack length as a function of time – little information is provided on the current used or the positioning of the voltage sense leads relative to the crack being measured. As demonstrated by CRIEPI, DCPD data only provided a voltage proportional to the area of the crack, not the crack geometry or instantaneous depth of the crack. Crack depths were estimated assuming a half-elliptical crack with a constant c/a ratio. The reported crack depths were calculated assuming a constant crack aspect ratio, although the ratio was not specified for each test. This assumption is most likely incorrect. *Newman and Raju* [1981] have shown that for fatigue crack growth under bending, no matter the starting a/c, the a/c will quickly follow the line where $a/c = 1 - (a/t)$, where t is sample thickness. This is because of variations in K_I along the perimeter of the crack, and the dependence of the CGR on K_I. It is not clear that this relationship is applicable to SCC, which also faces constraints related to reactant transport and possibly cathode area (see below), but if it is applicable to these bending tests, the a/c would start at 1 and decrease to 0.7 at 3 mm depth. Hence, calculated crack depths, which assume a constant aspect ratio, would be incorrect.

Application of salts as a droplet instead of as a uniform coating.

In the 4-point bend tests, salts were applied to the beam by placing a 20 µL droplet of either synthetic seawater or saturated $MgCl_2$ solution on the center of the beam. If deposited as a hemispherical droplet, this would correspond to a spot 4.2 mm in diameter; however, the droplet may have spread out to be larger. Because the salt was deposited as a droplet, the limited size of the salt-covered area may have artificially limited the external surface area of the sample that could act as a cathode. This would especially be true once the length of the crack extended beyond the edge of the droplet, and further growth would require diffusion along the crack to the crack tip outside of the salt covered area. For a

crack aspect ratio of $c/a = 1$, this would occur when the crack length exceeded 4-6 mm (corresponding to a crack depth of 2.0-3.0 mm) exactly where the slow-down in growth occurred in the CRIEPI experiments. For a surface evenly coated with salts, the cathode would be adjacent to and surrounding the crack tip, where it intersects the surface. Why would the magnesium chloride specimen see no slowing of crack growth? Because at the temperature and RH used, the entire salt droplet would be deliquesced, and may have spread to cover a much larger fraction of the surface (or completely wetted the growing crack).

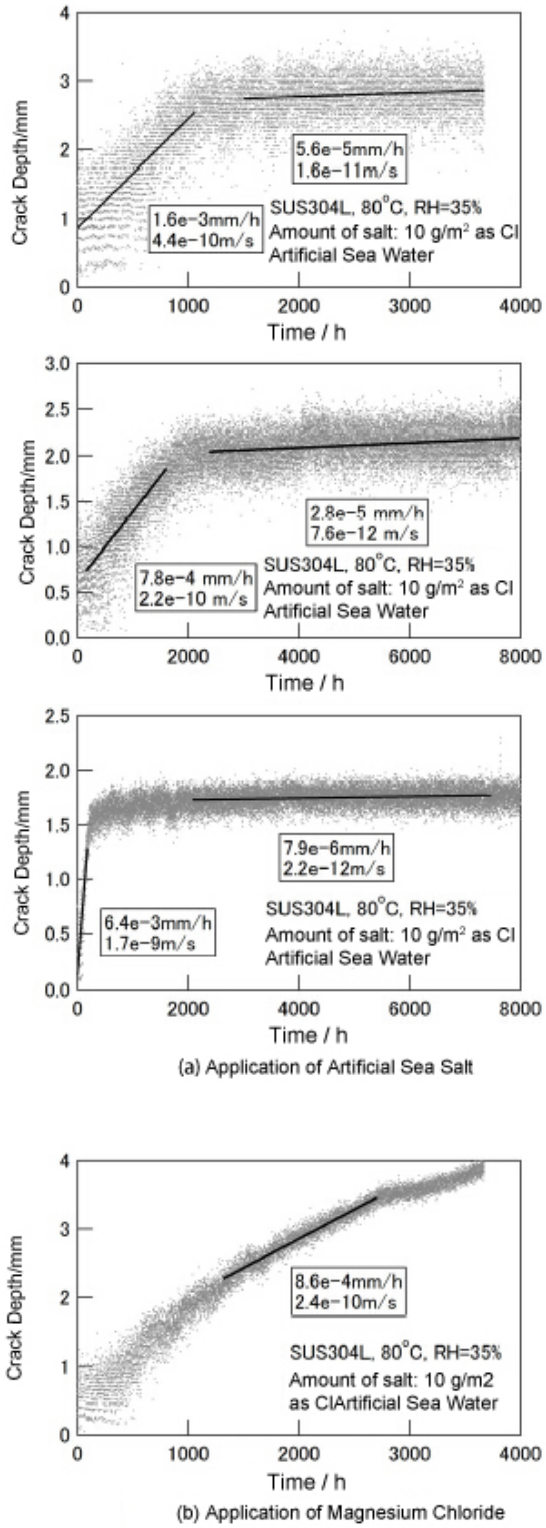

Figure 2.6-3. Crack growth data collected by *Shirai et al.* [2011a].

Use of a bend specimen introduces a changing stress field with depth.

Four-point bend specimens are commonly used to assess susceptibility to stress corrosion cracking, and there is an ISO method for this: ISO/FDIS 16540 *Corrosion of metals and alloys — Methodology for*

determining the resistance of metals to stress corrosion cracking using the four-point bend method. However, this method is for assessing SCC susceptibility, not for measuring crack growth rates. The reason for this is given in the ISO method:

> *The four-point bend test is a constant displacement test that is performed by supporting a beam specimen on two loading rollers (bearing cylinders) and applying a load through two other loading rollers so that one face of the specimen is in tension (and uniformly stressed between the inner rollers) and the other is in compression. The stress at mid-thickness is zero and there will be significant gradients in stress through the thickness, this being most marked for thin specimens. As a consequence, cracks may initiate, but then arrest or their growth rate decrease.*

In the four-point bend specimens used by CRIEPI, the initial bending moment produced a 270 MPa outer fiber tensile stress; which decreased to 0 at a neutral plane in the center of the sample. With further increases in depth, the stress state becomes increasingly compressive, finally reaching a value of 270 MPa compressive stress at the inner fiber of the sample. As a crack propagates though the sample, the change in stress condition is reflected in the crack tip stress intensity factor (K_I). Values of K_I as a function of crack depth at crack tip locations corresponding to the bottom of the crack (90º) and the crack tip at the surface (0º) been recalculated here (Figure 2.6-4) using the methods of *Newman and Raju* [1979]. Also shown is the predicted change in K_I for an infinite plate under the same bending moment, and the results are also shown for a crack in a sample under a uniform tension of 270 MPa, instead of under a bending moment. Uniform tension is a good representation for a storage canister, because even a through-penetrating SCC crack will be very small relative to the area of the outside of a storage canister (5 m long and about 5.3 m in circumference). All calculations were done using a crack depth to half-length ratio (a/c) of 1. That is, the crack is assumed to be semicircular (although CRIEPI reported a/c values of 0.5 to 1).

In the case of the infinite plate, if $a/c = 1$, then K_I at the bottom of the crack (90º) initially increases with depth, and then, after reaching a depth of a 1-2 millimeters, begins to decrease, passing though zero at a depth of 5 mm, or half the plate thickness. This is because, in an infinite plate, lateral constraints maintain the original stress profile in the sample. For a sample the dimensions of the CRIEPI beam, some constraint is lost as the crack grows and the crack length becomes a significant fraction of the beam width. This result is a downward shifting of the neutral plane below the crack, and the neutral plane is forced down to about 7.4 mm. At the 0ºC position, on the surface of the sample, K_I continues to increase as the crack grows. Thus, K_I varies greatly around with location on the crack tip, from the surface to the bottom. It is unlikely that this actually occurs—instead, the crack aspect ratio probably changes as the crack grows, maintaining a more or less constant K_I along the perimeter of the crack. For instance, for a longer, shallower crack ($a/c = 0.5$), K_I is nearly constant along the entire crack perimeter.

Conversely, in a sample under uniform tension (i.e., constant load), K_I continues to increase as the crack depth increases until penetration occurs. Moreover, the value of K_I varies only slightly with location on the crack tip, from where it intersects the surface to the bottom of the crack. Hence, the crack aspect ratio may remain more or less constant as the crack grows.

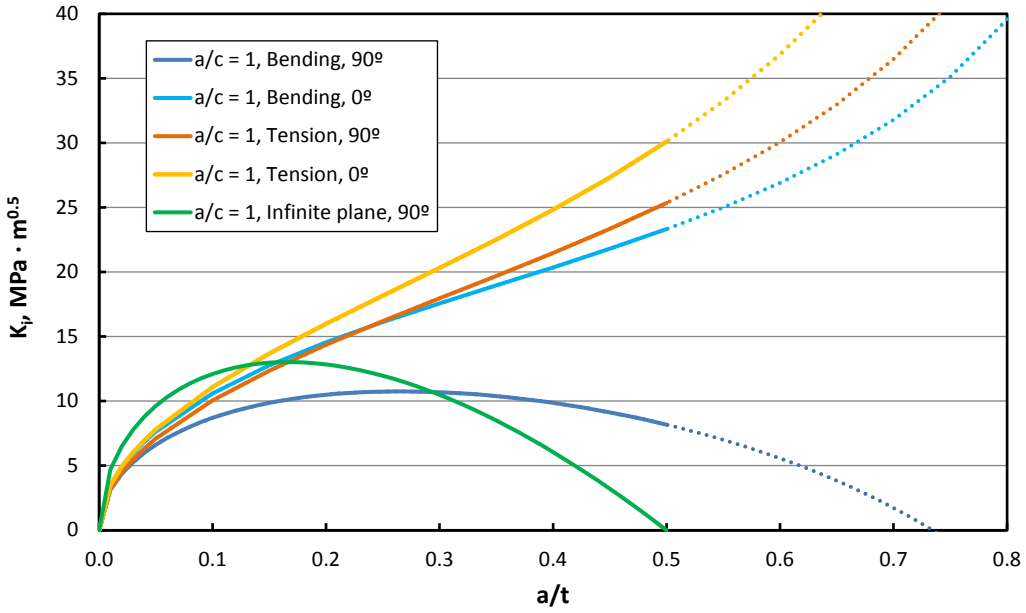

Figure 2.6-4. Stress distribution in the CRIEPI four-point bend specimens, calculated using the methods of *Newman and Raju* [1979]. Dotted lines are outside of the range of the model used to calculate K_I values.

One important aspect of this is that, in a bend specimen, the K_I varies strongly as a function of crack aspect ratio and of location along the advancing crack front, and that relationship changes with increasing crack depth. If we assume that crack growth tends to preserve a constant K_I along the crack tip, then the crack aspect ratio will change as the crack grows, just as it does for fatigue cracks. On the other hand, for a sample under uniform and constant tension, the difference in K_I along the crack front is much smaller, suggesting that the crack should be more semicircular ($a/c = 1$). This behavior has been observed experimentally and modeled theoretically for fatigue cracks by *Newman and Raju* [1981], and may apply to SCC cracks as well.

Again, why was the magnesium chloride specimen not affected? Possibly because the deliquesced droplet was larger, supporting more lateral crack growth—as the crack grows longer, the predicted stress distribution changes, and K_I no longer rolls over as in Figure 2.6-4, but instead continues to increase with depth.

Application of the CRIEPI model.

Even should the EPRI interpretation of cathodic limitation in the case of sea-salts be correct, it is important to note that the actual fraction of the salts in sea-salt that deliquesces is a function of RH. For a given salt load, at a higher RH, the brine volume increases dramatically. Crack growth rates may be more strongly controlled by deliquesced brine volume than by amount of salt present, the temperature, or the crack depth. An important part of any experimental study will be to isolate and evaluate each of these parameters individually.

B.2.7 Crack growth rates based on operational experience.

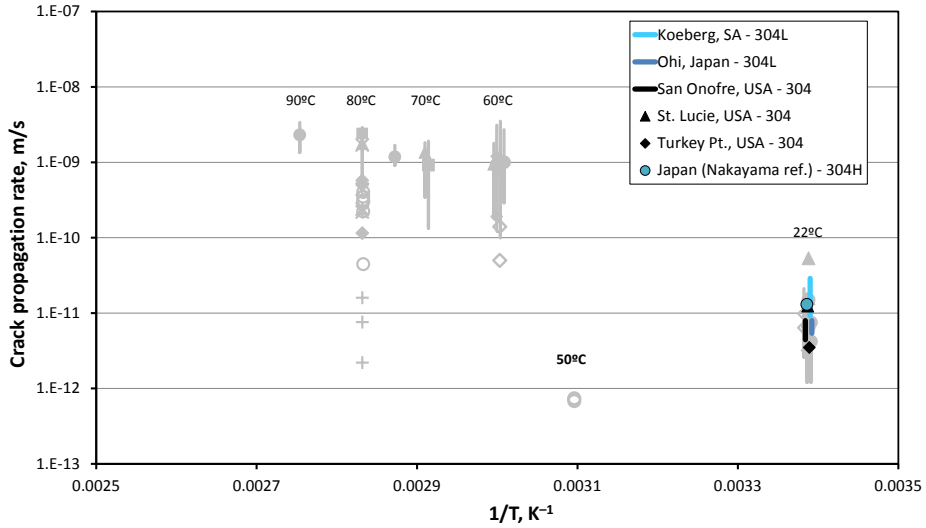

Figure 2.7-1. Data from nuclear plant operational experience.

While near-marine nuclear plants have frequently reported SCC of 304 SS, details are scarce. Estimates for crack growth rates from operating experience were recently summarized by the NRC [*Dunn*, 2015]. The data are all ambient temperature data, and are mostly for thinner components than SNF interim storage canisters. The available data shown in Table 2.7-1 [Dunn, 2015].

Table 2.7-1. Summary of reactor operating experience with atmospheric CISCC in welded stainless steel components [from *Dunn*, 2015]

Plant	Distance to salt water, m	Material and Component	Thickness, or crack depth, mm	Time in Service, years	Average crack growth rate, mm/yr
Koeberg (South Africa)	100	304L refueling water storage tank	5.0 to 15.5(?)[a]	17[b]	0.29 to 0.91(?)[a]
Ohi (Japan)	200	304L refueling water storage tank	1.5 to 7.5	30	0.17 to 0.25
St Lucie (FL, USA)	800	304 refueling water storage tank pipe	6.2	16	0.39
Turkey Point (FL, USA)	400	304 pipe	3.7	33	0.11
San Onofre (CA, USA)	150	304 pipe	3.4 to 6.2	25	0.14 to 0.25

[a]Cracks were observed in the thickest components, but it is not clear if penetration occurred.
[b]Some thin-walled components apparently failed within as little as 11 years, but details are unavailable.

The most extensive and perhaps best documented examples of atmospheric SCC due to marine salts are from the Koeberg Nuclear Power Station in South Africa. At this facility, several different 304L components of a borated water storage tank system and associated piping were degraded by externally-induced atmospheric stress corrosion cracking. On the storage tanks, SCC was most commonly observed in areas where attachment fillet welds and butt plate welds created high residual stresses. In the piping, SCC occurred due to high stresses imparted during pipe and elbow fabrication [*Alexander et al.*, 2010]. The water tanks in question are 16-17 meters high, and consist of 5 cylinders welded together, the lowermost being 15.5 mm thick and the uppermost, 5 mm thick. The tank roof is also 5 mm thick. All thicknesses exhibited SCC. The tanks are not pressurized, and the system was ambient temperature.

The plant began operation in 1984. The water storage tanks were originally constructed in the open, but were enclosed in specially-built rooms in 1990; although this reduced the rate of salt deposition by an estimated 2 orders of magnitude and the tanks were periodically washed, it has been speculated that enclosing the tanks exacerbated the SCC problem by eliminating rain-washing of salts from the surface of the tanks and piping [*Alexander et al.*, 2010; *Basson and Wicker*, 2002]. A few pinhole leaks near welds were identified as early as 1990, but were attributed to weld flaws. Several more leaks of thinner walled 304 SS components occurred between 1995 and 2001, when an extensive inspection program was initiated, and the extent of the problem was realized. Inspection of the piping and the tank indicated that the metal was extensively pitted, and that the pitted areas served as initiation points for SCC cracks. In a number of instances, while pitting was observed, no cracks were detected via dye penetrant – however, ultrasonic evaluation yielded indications. By grinding off 50-100 μm of metal from the surface, cracks were revealed and detected via dye penetrant examination. Cracks tended to initiate from the base of pits, and did not necessarily breach the metal surface, hindering detection without material removal via grinding. SCC cracks were present both as both linear cracks and networks. About 10% of all pipe spool pieces associated with one reactor were cracked, while a smaller number were cracked for the second reactor. Similarly, for one of the two water storage tanks examined, SCC cracks were associated with nearly all of the welds; the second tank was cracked to a lesser degree [*Basson and Wicker*, 2002].

CGR were not explicitly calculated, but have been estimated, based on installation and crack detection dates to be 0.29-0.91 mm/yr. These would be minimum crack growth rates, as no incubation time was assumed.

Nakayama and Sakakibara [2013] describe an additional example of atmospheric SCC of a large diameter 304 (0.079% C) pipe at a Japanese nuclear plant. The crack initiated externally and occurred where there had been a weld repair on the internal surface of the pipe, further sensitizing the material in the weld heat affected zone. The pipe was exposed to the atmosphere, and was found to typically have a NaCl surface load of 0.1 g/m^2; occasional rains washed the surface and prevented heavy buildup. The crack was confirmed to have penetrated about 14 mm in 35 years, or 0.4 mm/yr (1.3E-11 m/s). This is a minimum penetration rate, as the timing of crack initiation is not known, nor was it known exactly when penetration occurred.

B.2.8 Crack growth rate data collected under immersed conditions, for high chloride brines

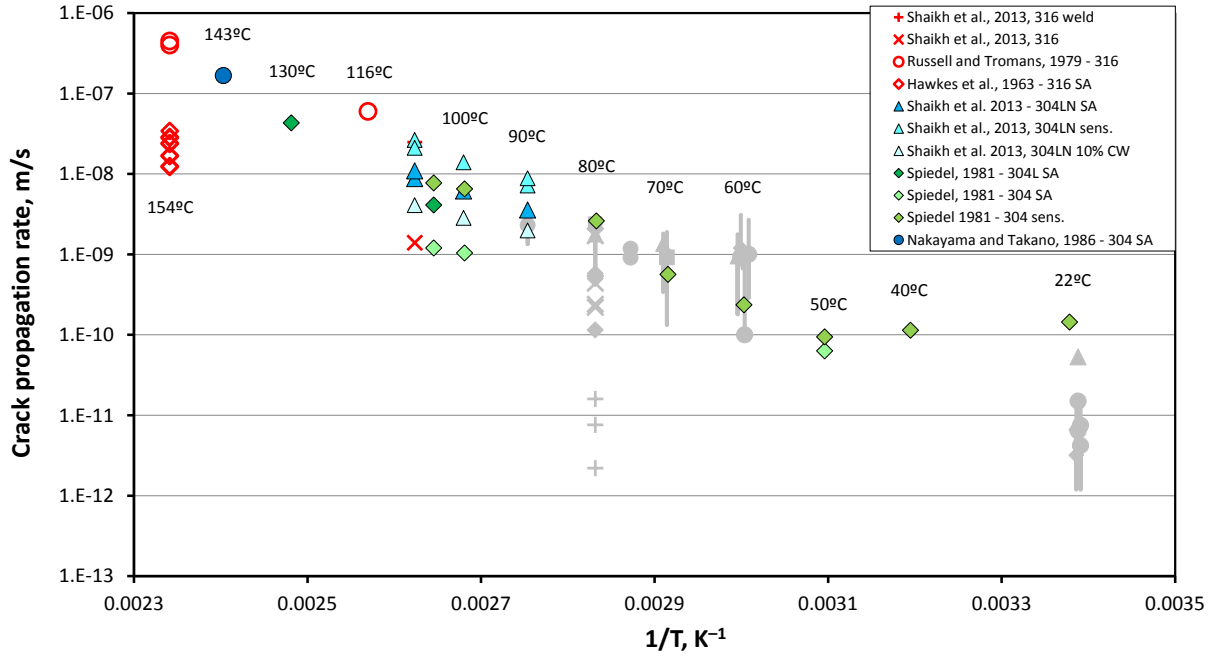

Figure 2.8-1. Data from chloride-rich brine immersed experiments.

Data for SCC crack growth rates under immersed conditions in chloride-rich brines have been compiled and are provided here as a potential talking point. The data extend to higher temperatures than data collected for atmospheric SCC. An aqueous brine cannot be present at temperatures higher than 60-70ºC, based on the possible range of absolute humidities in air circulating through a SNF interim storage system; however, these data may provide insights into the mechanism of the corrosion process.

The following data sets have been identified:

- *Spiedel* [1981] — Solution annealed 304L, in 42% $MgCl_2$ (130ºC), and in 22% NaCl (105ºC). Also, solution annealed and sensitized 304 samples, in 22% NaCl, over a range of temperatures from 23ºC to 105ºC.
- *Shaikh et al.,* [2013] — 316LN base and weld metal samples, in 5M NaCl + 0.15 M Na_2SO_4 + 2.5 ml/L HCl. Also, solution annealed, sensitized, or 10% cold worked 304LN samples, at 90ºC, 100ºC, and 108ºC, in the same solution.
- *Russell and Tromans*, [1979] — Cold worked (25 and 50%) 316 SS in 44.7% $MgCl_2$, at 116 and 154ºC.
- *Hawkes et al.*, [1963]. — Solution annealed 316 SS in 42% $MgCl_2$, at 154ºC.
- *Nakayama and Takano*, [1986]. — Solution annealed 304 SS, in 42% $MgCl_2$, at 143ºC.

B.3 Summary

Available SCC crack growth rate data from corrosion testing under atmospheric conditions is highly scattered, in part due to wide variety of testing methods used to collect the data. Other contributing factors are study-to-study variations in potentially important parameters such as salt load and RH. Moreover, operational experience from operating reactors does little to fill the knowledge gaps, as it is restricted to ambient conditions. While ambient testing and operational experience yield relatively similar SCC crack growth rates, the potential effects of temperature are poorly understood. Corrosion is a thermally activated process, and under immersed conditions, CGR increases with temperature. However, under atmospheric conditions, elevated temperatures correspond to lower relative humidity (RH) values, which in turn result in (1) more concentrated, potentially more corrosive brines, and (2) smaller brine volumes (thinner brine films for a given salt load) which may limit the size of the cathode area on the metal surface, or limit transport between the anode and cathode. Sufficient data do not appear to be available to currently predict what the effects of elevated surface temperatures on SCC crack initiation or growth under a deliquesced brine film.

B.4 References

Alexander, D., P. Doubell, and C. Wicker (2010), Degradation of Safety Injection System and Containment Spray Piping and Tank Fracture Toughness Analysis, FONTEVRAUD 7, Contribution of Materials Investigations to Improve the Safety and Performance of LWRs, 26-30.

Basson, J., and C. Wicker (2002), Environmentally induced transgranular stress corrosion cracking of 304L stainless steel components at Koeberg, Proc. Fontevraud, 5.

Cook, A., N. Stevens, J. Duff, A. Mishelia, T. S. Leung, S. Lyon, J. Marrow, W. Ganther, and I. Cole (2011), Atmospheric-induced stress corrosion cracking of austenitic stainless steels under limited chloride supply, Proc. 18th Int. Corros. Cong., Perth, Australia.

Dunn, D. S. (2015), NRC Perspective on Information Needs for CISCC of Spent Fuel Dry Storage Systems, in DOE UFD Stress Corrosion Cracking Workshop, 22 Sept. 2015, edited, Las Vegas, NV.

EPRI (2014), Flaw Growth and Flaw Tolerance Assessment for Dry Cask Storage CanistersRep. 3002002785, 84 pp, Electric Power Research Institute, Palo Alto, CA.

Hawkes, H., F. Beck, and M. Fontana (1963), Effect of Applied Stress and Cold Work On Stress Corrosion Cracking of Austenitic Stainless Steel By Boiling 42 Percent Magnesium Chloride, Corrosion, 19(7), 247t-253t.

Hayashibara, H., M. Mayuzumi, and Y. Mizutani (2008), Effects of temperature and humidity on atmospheric stress corrosion cracking of 304 stainless steel, CORROSION 2008.

Kosaki, A. (2008), Evaluation method of corrosion lifetime of conventional stainless steel canister under oceanic air environment, Nuclear Engineering and Design, 238(5), 1233-1240.

Lu, B., Z. Chen, J. Luo, B. Patchett, and Z. Xu (2005), Pitting and stress corrosion cracking behavior in welded austenitic stainless steel, Electrochimica Acta, 50(6), 1391-1403.

Nakayama, G., and Y. Sakakibara (2013), Prediction Model for Atmospheric Stress Corrosion Cracking of Stainless Steel, ECS Transactions, 50(31), 303-311.

Nakayama, T., and M. Takano (1986), Application of a slip dissolution-repassivation model for stress corrosion cracking of AISI 304 stainless steel in a boiling 42% MgCl2 solution, Corrosion, 42(1), 10-15.

Newman, J., and I. Raju (1981), An empirical stress-intensity factor equation for the surface crack, Engineering Fracture Mechanics, 15(1), 185-192.

Newman, J. C., and I. S. Raju (1979), Analysis of Surface Cracks in Finite Plates Under Tension or Bending LoadsRep., NASA, Hampton, VA.

Russell, A. J., and D. Tromans (1979), A fracture mechanics study of stress corrosion cracking of type-316 austenitic steel, Metallurgical Transactions A, 10(9), 1229-1238.

Shaikh, H., H. Khatak, and P. Rodriguez (2013), Stress corrosion crack growth behaviour of austenitic stainless steels in hot concentrated chloride solution, paper presented at ICF10, Honolulu (USA) 2001.

Shirai, K., J. Tani, and T. Saegusa (2011a), Study on Interim Storage of Spent Nuclear Fuel by Concrete Cask for Practical Use -- Feasiblity Study on Prevention of Chloride Induced Stress Corrosion Cracking for Type 304 Stainless Steel Canister (English translation) Rep.

Shirai, K., J. Tani, M. Wataru, T. Saegusa, and C. Ito (2011b), Long-term containment performance of test metal cask. 10-14 April, in International High-Level Radioactive Waste Managment Conference (IHLRWMC), edited, pp. 816-823, American Nuclear Society, Albuquerque, NM.

Shirai, K., J. Tani, T. Arai, M. Wataru, H. Takeda, and T. Saegusa (2011c), SCC evaluation test of a multi-purpose canister. 10-14 April, paper presented at 13th International High-Level Radioactive Waste Management Conference (IHLRWMC), American Nuclear Society, Albuquerque, NM.

Speidel, M. O. (1981), Stress corrosion cracking of stainless steels in NaCl solutions, Metallurgical Transactions A, 12(5), 779-789.

Spencer, D., M. Edwards, M. Wenman, C. Tsitsios, G. Scatigno, and P. Chard-Tuckey (2014), The initiation and propagation of chloride-induced transgranular stress-corrosion cracking (TGSCC) of 304L austenitic stainless steel under atmospheric conditions, Corrosion Science, 88, 76-88.

Tani, J. I., M. Mayuzurmi, and N. Hara (2009), Initiation and propagation of stress corrosion cracking of stainless steel canister for concrete cask storage of spent nuclear fuel, Corrosion, 65(3), 187-194.

Tani, J. I., K. Shirai, M. Wataru, and T. Saegusa (2010), Stress Corrosion Cracking of Stainless Steel Canister of Concrete Cask, paper presented at International Seminar on Interim Storage of Spent Fuel (ISSF) 2010.

APPENDIX C: INTRODUCTORY PRESENTATION

Exceptional service in the national interest

Sandia National Laboratories

UFD Expert Panel on Chloride Induced Stress Corrosion Cracking of Interim Storage Containers for Spent Nuclear Fuel

Sandia National Laboratories
Albuquerque, NM

March 24th and 25th, 2016

ENERGY NNSA

Degradation Mechanism of Concern: Stress Corrosion Cracking (SCC)

Susceptible Material?
Well established for 304/304L in Cl^-

Stress?
Mockup container and other literature indicate stress field strongly tensile

Aggressive Environment?
Maybe…

Why are we here?

- Atmospheric stress corrosion cracking has been identified as a significant potential degradation mode for fielded interim storage containers
- Current understanding of what governs this cracking process under atmospheric conditions is lacking…
  - Induction period
  - Localized corrosion initiation and growth
  - Pit to crack transition
  - Growth rate of stable cracks
- Critical need to understand each aspect of the process as well as how to characterize it
  - What needs to be done experimentally to address the existing data gaps?

3

The Panel

- Expert panel has been assembled to work through this degradation process and help establish a viable path forward
- Dr. Peter Andresen
  GE Corporate Research and Development
- Dr. Robert Kelly
  University of Virginia
- Dr. John Scully
  University of Virginia
- Dr. Alan Turnbull
  National Physical Laboratory

4

Schedule – Day 1

- Times are just rough estimates

7:30		Meet at badge office, then travel to CGSC
8:00	8:30	Introduction, Goals, and ground rules
8:30	9:30	Surface environment on the containers (C. Bryan)
9:30	10:30	UVA Localized corrosion model (R. Kelly)
10:30	10:45	Break
10:45	12:00	Localized corrosion
		Initiation
		propagation
		Impact of RH, T, etc.
12:00	1:00	Lunch
1:00	3:00	Crack intiation
		Pit to crack transition
		Early crack growth
		Measurement Methodologies - how do we quantify crack nucleation?
3:00	3:15	Break
3:15	5:00	Crack initiation (continued)
5	5:30	Return to hotel
6:00		Dinner

5

Schedule – Day 2

7:00		Meet at CGSC
7:00	7:30	Recap of day 1 (review conclusions, action items)
7:30	9:30	Crack propagation
		Impact of microstructure
		Crack branching
		Measurement methodologies - how do we effectively measure crack growth?
9:30	9:45	Break
9:45	11	Crack propagation (continued)
11	11:30	Recap of day 2 (review conclusions) and plan path forward for documentation
11:30		Meeting can continue if there is time/interest - facility is available all day.

6

Topic 1: Localized Corrosion

SCC in atmospherically exposed stainless steels has typically been observed to initiate from localized corrosion sites.

- What are the key processes that govern localized corrosion under atmospheric conditions in terms of:
  - the induction period prior to pit nucleation
  - the sites from which meaningful/stable pits nucleate.
    - How important is the underlying microstructure?
      MnS stringer and other precipitates, chromium depleted zones, deformation induced martensite, local plastic deformation, etc.
  - the growth of stable pits?
- Are there data gaps that need to be addressed?

7

Topic 2: Crack Initiation

SCC crack initiation on austenitic stainless steels under atmospheric conditions is believed to take place from localized corrosion sites

- What are the key factors that determine when crack nucleation is likely in terms of:
  - Is a localized corrosion site necessary?
  - Is there a critical combination of factors that governs when crack nucleation is likely from a localized corrosion site?
  - Is there a critical size or geometry?
  - Is the pit internal chemistry necessary for crack nucleation?
  - Is there a necessary underlying microstructure and stress field?
- How can the crack nucleation process be effectively monitored?
- Are there data gaps that need to be addressed?

8

Topic 3: Crack Propagation

Many different views have been expressed in terms of the required surface chemistry, salt load or brine layer characteristics, location of the cathode supporting crack propagation, and underlying microstructural features of importance.

- In your opinion, what are the critical conditions and processes that govern atmospheric SCC crack propagation?
- Given the documented difficulties in determining accurate crack growth rate measurements for atmospheric SCC cracks, how might this issue be attacked experimentally?
- Chloride driven SCC cracks in austenitic stainless steels observed in the field tend to be highly branched in nature – how should this be addressed experimentally?
- What are the key data gaps that must be addressed?

9

Recap – Day 1

- Surface Environment
  - C. Bryan – presentation of limitations of existing data, and predictions of likely surface conditions
  - Some studies suggest other phases may be present, differing from thermodynamic predictions
  - Assessment of oxidative strength via Abbott work, etc.
- Localized Corrosion
  - R. Kelly – presentation and discussion on maximum pit depth model
  - Nucleation site discussion
  - Impact of passivated pits
  - Data needs for the model – cathodic kinetics, validation data
- Crack Nucleation
  - Very difficult area to tackle experimentally
  - Necessity of a pit – generally agreement that needed for this system, but not universally so. While pits appear to be needed, doesn't mean absence of a pit will translate to immunity to nucleation
  - Limited understanding of surface stress state – lots of factors to consider

10

Recap – Day 1 (continued)

- Crack Propagation
  - Increased scrutiny of existing data from other structures
  - Evaluation by structural mechanics folks on varying stress state with crack propagation
  - Experimental approach
    - Evaluation of plausible extremes
    - Explore variables in a controlled manner
    - Inundated experiments to evaluate impact of variables (qualitative)
    - Atmospheric experiments – options with limitations
      - Elliptical crack from surface
      - Traditional fracture mechanics specimens
  - Presentation of CT and ESE(T) sample work from SWRI

11

APPENDIX D: ENVIRONMENT PRESENTATION

Used Fuel Disposition Campaign

Stress Corrosion Cracking of SNF Interim Storage Canisters:
Canister Surface Environment

Charles Bryan and David Enos

Sandia National Laboratories is a multi program laboratory managed and operated by Sandia Corporation, a wholly owned subsidiary of Lockheed Martin Corporation, for the U.S. Department of Energy's National Nuclear Security Administration under contract DE-AC04-94AL85000. SAND2015-XXXXX.

Used Fuel Disposition

Overview

- **Background**
- **Types of Interim Storage Systems**
- **Describing the environment on the surface of in-service storage canisters. Required Information:**
  - ***Salt Compositions***
    - *ISFSI locations*
    - *Anticipated Dust/Salt Compositions*
    - *EPRI Dust Sampling Program and Results*
  - ***Determining Relative Humidity***
    - *Calculated from Canister Surface Temperature and Ambient Humidity of Inflowing Air*
  - ***Determining Initial Temperature and Temperature Evolution over Time***
    - *Modeled and Measured Data*
  - ***Salt surface load (?)***

2

Used Fuel Disposition

Background

- The United States currently does not have a disposal pathway for SNF. Dry storage canisters currently in use may be required to perform their function for decades beyond their original design criteria. Localized corrosion, especially stress corrosion cracking (SCC), of welded stainless steel (304/304LSS) canisters is considered the most important potential failure mechanism.
- Canisters are stored in passively ventilated overpacks and accumulate dust on the surface over time. SCC of stainless steel due to deliquescence of chloride-rich salts on metal surfaces is a well-known phenomenon, especially in near-marine environments. Operational experience with stainless steel SCC at CA and FL nuclear sites.
- Directly inspecting in-service canisters for corrosion, or for dust composition, is difficult due to high radiation fields at the canister surfaces and limited access through vents in the storage overpacks.
  - *EPRI sampling program collected and analyzed surface dusts from in-service storage canisters at three near-marine ISFSI locations, and established that chloride-rich salts can be present.*
  - *Attempts to deterministically or probabilistically predict canister penetration rates have been hampered by limited and highly scattered experimental data at relevant environmental conditions. However, data collected during development of those models helps define the anticipated physical and chemical environment on the canister surfaces.*
  - *Work is progressing to develop in situ SCC inspection technologies for canisters within their overpacks*

3

Used Fuel Disposition

Criteria for Stress Corrosion Cracking

What is the canister surface environment, and how does it affect SCC crack initiation and growth?

Dust on canister surface at Calvert Cliffs (EPRI 2014)

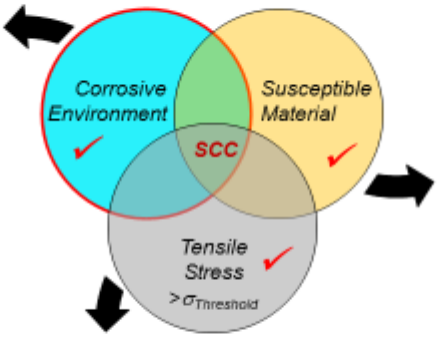

Weld zone, Ranor 304 SS plate

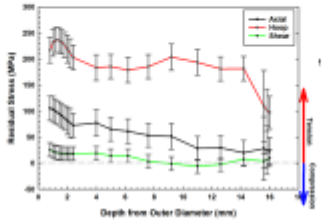

Measured Stresses, Circumferential weld HAZ, Sandia Canister Mockup

4

Used Fuel Disposition

Canister Surface Environment

- ***Environmental Requirements for SCC are:***
  - *Presence of an aqueous solution*
    - *Immersed conditions unlikely — casks are protected from weather by overpacks*
    - *Deliquescence of salts in dust — passive ventilation draws large volumes of outside air through the overpacks, and dust and aerosols are deposited on the cask surfaces.*
  - *Chemically aggressive environment (e.g., chloride-rich)*
- ***Salt deliquescence and brine composition are dependent on:***
  - *Composition/amount of deposited salts*
  - *Temperature at the container surface*
  - *Relative humidity at the container surface*

Characterizing the canister surface environment means understanding how these evolve with time in storage.

5

Used Fuel Disposition

ISFSI Locations

Different environments

- **Varying salt assemblages**
  - *Coastal (marine salt aerosols)*
  - *Inland (ammonium, sulfate, and nitrate-rich aerosols; possible road salts, cooling tower emissions)*
  - *Salt assemblages control DRH and RH_L*
- **Range of weather conditions**
  - *Dewpoints (AH)*
  - *Ambient temperatures*
- **Temperature range of interest (when deliquescence can occur)**
  - *Determined by RH_L and AH*

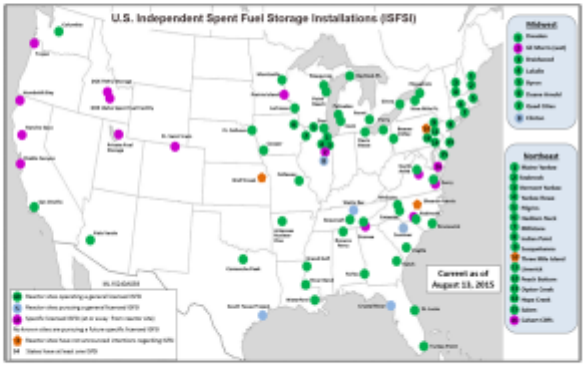

Used
Fuel
Disposition

General Storage System Designs

7

Used
Fuel
Disposition

Interim Storage Systems for SNF

- **Stainless steel (generally 304/304L) welded canisters are stored in concrete/steel overpacks.**
- **Canisters are 1/2" to 5/8" thick, single shell. Formed and sealed using multi-pass welds. Canister closure welds at one end are double-shell.**
- **Passively ventilated for cooling. Unfiltered air enters lower vents in the overpack, passes up and around the canister, and exits upper vents.**
- **Two major storage types**
  - Vertical systems. Canisters are stored vertically, in cylindrical steel/concrete overpacks.
  - Horizontal systems. Canisters are emplaced on steel rails into rectangular concrete overpacks.

8

Used Fuel Disposition

Dry Storage Systems: Horizontal

- For example, Areva/TN NUHOMS storage systems
- ~38% of current dry storage

- Passive airflow through the overpack cools the package
- Relatively air high flow rates (m³/min) bring in dust; deposited on the canister surface

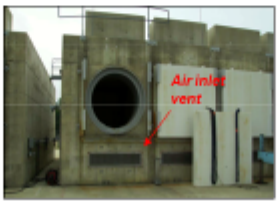

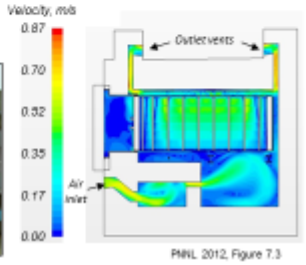

PNNL 2012, Figure 7.3

9

Used Fuel Disposition

Dry Storage Systems: Vertical

- Several different vertical storage system designs, with different vent and internal geometries. For example, Holtec HI-STORM 100 system.
- Air enters slit-like vents at the base, moves up through a narrow 2"- 4" annulus between the overpack and the canister, and exits vents at the top of the overpack.

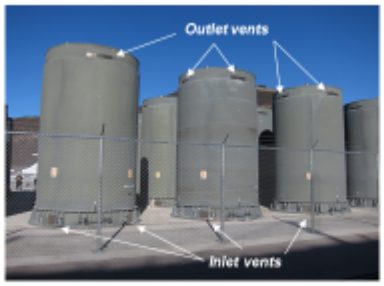

HI-STORM 100 storage systems at Diablo Canyon

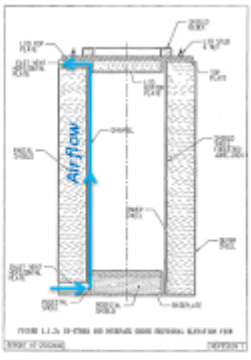

10

Used
Fuel
Disposition

Storage Canister Surface Environment

11

Used
Fuel
Disposition

Chemical Composition of Salts Deposited on Canister Surfaces:

Sampling of Dust on In-Service Storage Canisters

12

Used Fuel Disposition

Sampling of Dust on In-Service Interim Storage Canisters

EPRI sampling program: Assess the composition of dust on the surface of in-service stainless steel SNF storage canisters, with emphasis on the deliquescent salts.

- *Emphasis on near-marine sites, as sea-salts are known to cause SCC of stainless steels.*
- *Sampling difficult and expensive*
  - *Limited access to canister surface within overpacks*
  - *High canister surface radiation levels (1000-10,000 Rad/Hr).*
- *ISFSI locations sampled:*
  - *Calvert Cliffs: Transnuclear NUHOMS system, horizontal storage canister (June, 2012)*
  - *Hope Creek: Holtec HI-STORM system, vertical canister (Dec, 2013)*
  - *Diablo Canyon: Holtec HI-STORM system (Jan 2014)*
- *Samples delivered to Sandia National Laboratories for analysis*

Removing the Gamma Shield

Sampling with the remote sampling tool

Sampling a HI-STORM 100 canister at the Diablo Canyon ISFSI

13

Used Fuel Disposition

EPRI Dust Sampling:

Calvert Cliffs Site

ISFSI is ~0.5 miles from Chesapeake Bay

- *Sheltered bay*
- *Brackish water*

Eastern U.S.

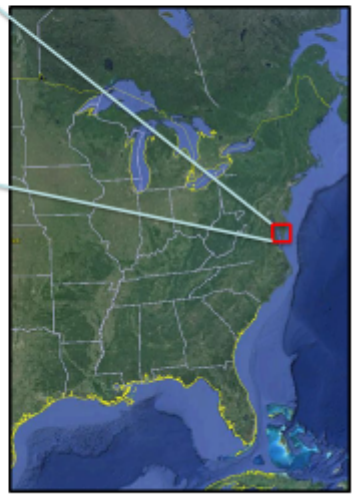

14

Used Fuel Disposition

EPRI Dust Sampling:
Hope Creek Site

Eastern U.S.

ISFSI is ~0.25 miles from the Delaware River, 15 miles upstream from Delaware Bay

- *Brackish water*
- *Sheltered from open ocean*

15

Used Fuel Disposition

EPRI Dust Sampling:
Diablo Canyon Site

Western U.S.

ISFSI is ~1/3 mile from the shoreline, on a hill above the plant.

- *Elevated (~400 feet) above sea level*
- *Rocky shore, breaking waves*
- *Open ocean*

16

Used Fuel Disposition

EPRI Dust Sampling:
Types of Samples Collected

- **Entry**
  - NUHOMS horizontal storage systems—entered through door, annulus around shield plug (~2.5 cm)
  - HI-STORM systems—entered through upper ventilation opening
- **Wet sampling**
  - Salt-Smart® sensors
  - Used to characterize soluble salts (quantify amount per unit area)
  - After use, sensor was split and captured salts were rinsed out for analysis
- **Dry dust samples**
  - Scotch-Brite™ pads
  - Used to characterize salt components (chemistry, mineralogy, texture); cannot quantify amount per unit area

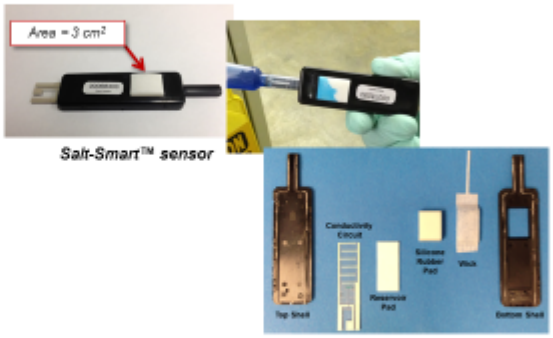

Salt-Smart™ sensor

Scotch-Brite™ pad

17

Used Fuel Disposition

EPRI Dust Sampling:
Results: Calvert Cliffs

- *The canister upper surface was more heavily coated with dust and salts due to gravitational settling. Samples from upper surface contained abundant pollen.*
- *The soluble salts are Ca- and SO_4-rich. Gypsum is the dominant salt phase present.*
- *Chlorides comprise a small fraction of the total salt load, and are dominantly NaCl.*
- ***Despite the proximity to the coast and prevailing winds from the east, the dusts sampled from in-service containers at Calvert Cliffs do not appear to have a large sea salt component. Chesapeake Bay is brackish, and may be sheltered sufficiently to limit wave-generated sea-salt aerosols.***

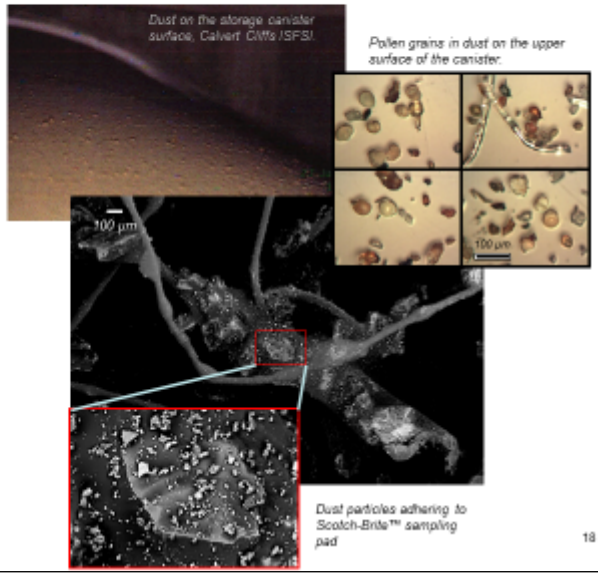

Dust particles adhering to Scotch-Brite™ sampling pad

18

Used Fuel Disposition

EPRI Dust Sampling:

Results: Hope Creek

- *Flat canister top much more heavily coated than vertical sides.*
- *Dust dominated by insoluble minerals (quartz, clays, aluminosilicates). Soluble salts minor; dominantly gypsum, carbonates. Sparse chlorides, mostly isolated grains of NaCl.*

Despite the proximity to the coast, the dusts sampled from in-service containers at Hope Creek do not have a large sea salt component. Delaware River is brackish, and may be sheltered sufficiently to limit wave-generated sea-salt aerosols.

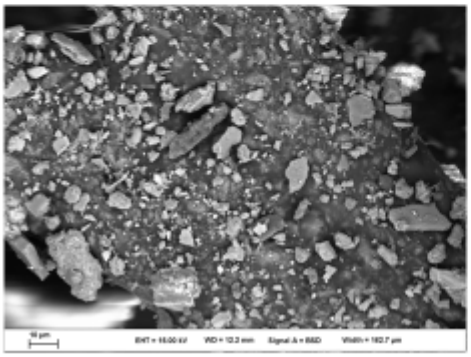

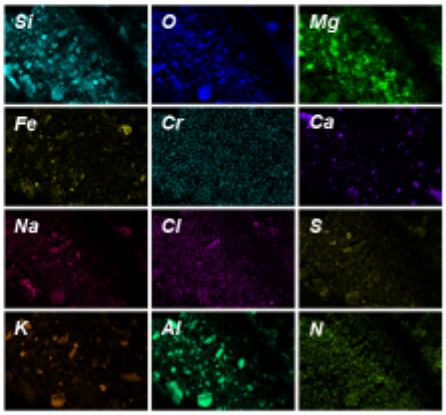

19

Used Fuel Disposition

EPRI Dust Sampling:

Results: Hope Creek Salt-Smarts®

Sample #	Loc.	Depth, ft	Temp., °F	Amount present, µg/sample										SUM
				Na	K	Ca	Mg	NH_4^+	F^-	Cl^-	NO_3^-	PO_4^{3-}	SO_4^{2-}	
144-008	Side	13.0	93.2	*0.1*	*0.8*	3.4	0.6	2.7	nd	0.9	2.7	nd	4.1	15.4
144-009	Side	7.5	116.5	*0.1*	1.7	4.5	0.5	2.7	nd	0.9	6.4	*1.1*	6.5	24.3
144-010	Side	1.0	133.9	*0.4*	1.4	4.2	0.4	2.4	nd	1.2	5	nd	4.4	19.4
144-013	Top	0.0	138	42	18	102	33	2.8	0.4	4.2	19	4.8	91	317
144-014	Top	0.0	141.2	13	6.4	29	8	2.7	0.4	18	7.3	1.3	55	142
144-003	G.S.	—	—	nd	*0.6*	2.2	0.4	1.4	nd	*0.5*	3.3	1.2	2.1	11.6
144-004	G.S.	—	—	nd	*0.3*	3.2	0.6	2.9	nd	0.8	1.8	*0.5*	1.7	11.8
145-006#	Side	13.0	70.6	*0.5*	2.2	4.4	0.6	2.3	nd	2.2	8.1	nd	4.7	25.1
145-007	Side	7.5	100.8	*0.7*	1	2.4	0.6	2.9	nd	2.1	2.2	*0.7*	5.3	17.9
145-014	Side	1.0	130.3	*0.6*	*0.9*	3.2	0.8	3.2	nd	1.2	2.5	nd	9.1	21.5
145-013**	Top	0.0	174.1	32	15	91	30	2.8	nd	2.2	15	3.5	82	273
145-011*	Blank	—	—	nd	*0.2*	2.3	0.3	3	nd	*0.7*	1.3	nd	1.7	9.6
145-002	G.S.	—	—	nd	1.2	4.8	0.5	2.7	nd	*0.7*	5.9	*0.8*	2	18.5
SS-BI-8 min-1	—	—	—	nd	nd	1.3	0.2	1.1	nd	*0.4*	1.6	nd	*0.5*	5.1
SS-BI-8 min-2	—	—	—	nd	nd	1.2	0.2	1.5	nd	*0.7*	*0.9*	*0.5*	*0.2*	5.2
SS-BI-15 min	—	—	—	nd	nd	1.5	0.5	5.7	0.2	*0.7*	1.1	1.6	1.7	12.9

Blanks

Notes: Italicized values in gray were above blank values, but too low to quantify accurately. nd = not detected. G.S. = gamma shield

* Reservoir pad only damp

** Reservoir pad only partially saturated

\# SaltSmart™ wick appears to have only partially contacted the canister surface (~1/3 of the pad).

20

Used Fuel Disposition

EPRI Dust Sampling:
Results: Diablo Canyon

- *Canister sides lightly coated, tops more heavily coated.*
- *Dust dominated by insoluble minerals (quartz, clays, aluminosilicates), but chloride-rich soluble salts are abundant, present as sea-salt aggregates.*

Canister Top (EPRI 2018)

Heavy wave action at the Diablo Canyon site generates abundant sea-salt aerosols. Although 400 feet above sea level, Diablo Canyon canisters have a significant amount of sea-salts on the canister surfaces.

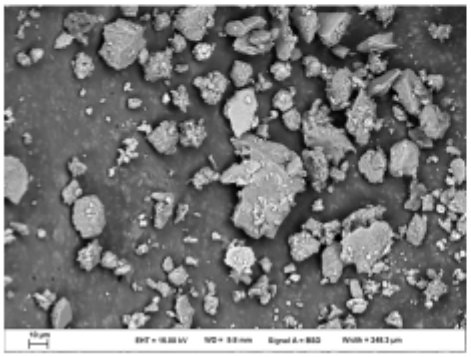

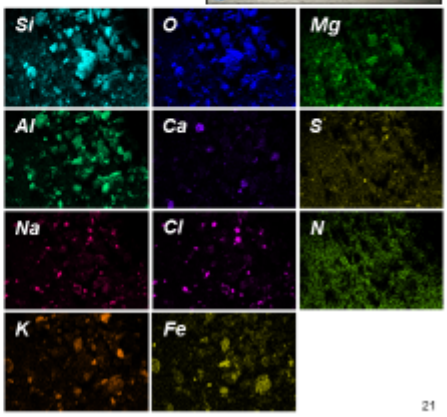

21

Used Fuel Disposition

EPRI Dust Sampling:
Results: Diablo Canyon

Sea salt aggregate, comprised largely of NaCl and Mg-SO_4 (the two most abundant minerals that form when seawater evaporates. Smaller amounts of K and Ca minerals. A Mg-Cl_2 phase, if present, is not distinguishable.

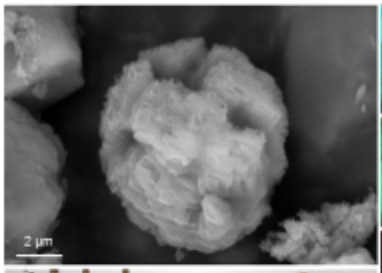

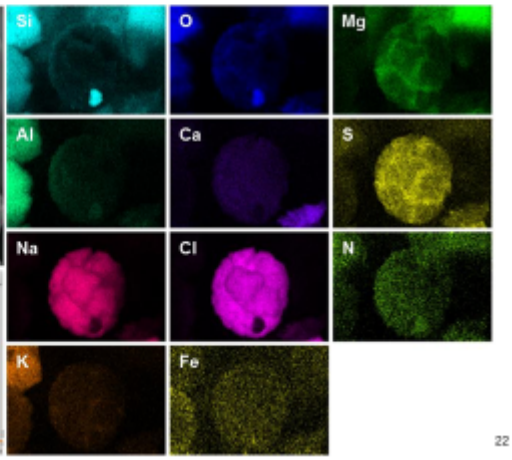

22

Used Fuel Disposition

EPRI Dust Sampling:
Results: Diablo Canyon

Examples of Sea-salt aerosols

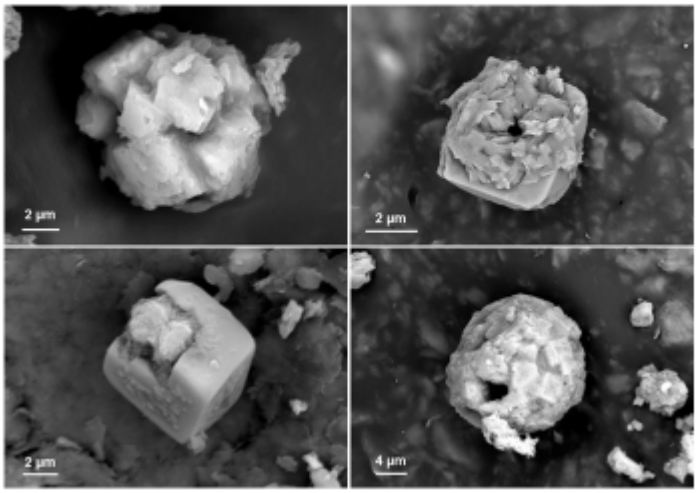

23

Used Fuel Disposition

EPRI Dust Sampling:
Results: Diablo Canyon Salt-Smarts®

High canister surface temperatures limited the canister surface that could be sampled, and where samples were collected, data are suspect—it is not clear that surface salts were quantitatively recovered.

Sample #	Loc.	Depth, ft	Temp., °F	Amount present, µg/sample										SUM, µg
				Na	K	Ca	Mg	NH_4^+	F^-	Cl^-	NO_3^-	PO_4^{3-}	SO_4^{2-}	
123-003	Side	14	119.7	0.3	0.76	2.9	0.73	2.5	0.4	1.4	1.8	*0.51*	5.1	16.4
123-004	Side	11.5	173.4	0.29	1.4	3.2	0.46	1.9	*0.17*	1.1	4.5	*0.15*	2.6	15.8
123-005*	Side	10.5	187	nd	0.33	4.5	0.3	1.7	0.35	0.59	0.7	*0.58*	1.7	10.7
123-002	G.S.	—	—	17.7	1.1	7.4	1.1	2.4	1.2	17.4	13.9	nd	12.8	75.0
123-010	Blank	—	—	4	2.3	2.7	0.59	2.8	1.2	7.5	1.6	1.03	2	26.0
170-007*	Side	10.5	177.5	1.2	0.43	2.5	0.31	1.4	0.32	1.3	2.4	nd	1.7	11.6
170-008*	Side	9.5	182.8	0.23	0.62	2.9	0.26	1.8	0.4	0.87	2.8	0.77	0.7	11.4
170-009*	Side	9	188.2	0.33	2.8	4	0.25	1.3	0.3	0.76	11.5	0.72	1.1	23.0
170-002	G.S.	—	—	9	1.6	7.3	1.6	2.6	*0.27*	4	26	0.98	7.6	61.0
Blank-6	—	—	—	0.88	1.2	2.2	0.23	1.4	*0.1*	1.3	3.9	0.87	0.45	12.5
Blank-8(1)	—	—	—	nd	0.23	1.2	0.15	1.4	0.53	0.42	*0.29*	*0.34*	*0.26*	4.8
Blank-10	—	—	—	*0.01*	0.35	1.5	0.21	1.1	0.38	0.68	2.3	0.97	0.35	7.8
Blank-12	—	—	—	0.33	1	1.3	0.19	1.2	*0.26*	1.2	2.2	0.91	0.33	8.9
Blank-14	—	—	—	nd	*0.14*	1.1	0.16	1.2	0.32	0.44	0.92	1.29	*0.23*	5.8
Blank-8(2)	—	—	—	nd	0.26	1.4	0.27	1	0.38	0.39	1.3	nd	0.52	5.5

Notes: No SaltSmart® samples were collected from canister tops, as the temperatures were too high--outside of the operational range of the Saltsmart®. Italicized values in gray were above analysis blank values, but too low to quantify accurately. nd = not detected. G.S. = gamma shield

*Canister surface temperatures too high. Wick adhered to the silicone pressure pad, and reservoir pad only partially saturated; surface salts may not have been quantitatively recovered.

24

Used Fuel Disposition

Summary of EPRI In-Service Canister Sampling

- Dusts on Calvert Cliffs and Hope Creek canisters are largely insoluble minerals; salts are limited, and are salts are largely Ca-sulfate and nitrate-rich. NaCl was observed as rare isolated grains.
- Dusts on Diablo Canyon canisters are sea-salt rich. Sea-salts are present are present in both the fine (<2.5μm) and coarse (10-20μm fraction). Larger grains are spherical aggregates or euhedral crystals of halite, with associated Mg-sulfate, and lesser amounts of Ca and K.
- Dust loads generally much heavier on canister upper surfaces than on vertical surfaces.

Observations of heavy canister dust loads at some sites (e.g., Calvert Cliffs) and of sea-salt-rich canister surface dusts at different sites (Diablo Canyon) indicate that at some near-marine sites, heavy chloride-rich dust loads could eventually be deposited. Once deliquescence occurs, SCC may be possible.

25

Used Fuel Disposition

Modeling Brine Compositions that Form by Deliquescence, and Conditions of Deliquescence

26

Used Fuel Disposition

Deliquescence:

Deliquescence is controlled by RH:
RH = *f*(salt composition, AH, temperature)

- Salt assemblages have a minimum RH at which they deliquesce (RH_d)
- $RH = P_{water\ vapor}/P_{sat}$
- $P_{water\ vapor} = f(AH_{outside\ air})$
- $P_{sat} = f(T_{WP\ surface})$
- During cooling, *T* decreases and $RH_{WP\ surface}$ increases until RH_d is reached, and deliquescence occurs.
- The limiting RH for corrosion, RH_L, is somewhat below RH_d (adsorbed water films).

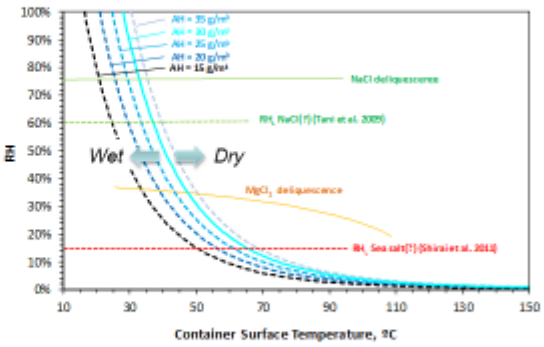

27

Used Fuel Disposition

Salt Composition and RH_d:

Marine aerosols—observed

Sea salt/spray — generally simulated with synthetic ocean water (ASTM D1141-98)

Species	Conc., mg/L ASTM D1141-98	McCaffrey et al. (1987)
Na^+	11031	11731
K^+	398	436
Mg^{2+}	1328	1323
Ca^{2+}	419	405
Cl^-	19835	21176
Br^-	68	74
F^-	1	—
SO_4^{2-}	2766	2942
BO_3^{3-}	26	—
HCO_3^-	146	—
pH	8.2	8.2

Sea-salt aggregate on Diablo Canyon ISFSI storage canister

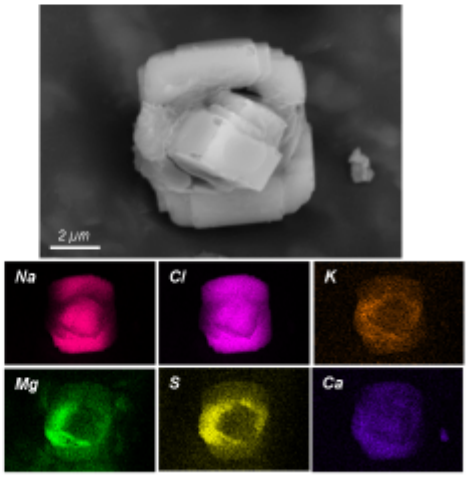

28

Used Fuel Disposition

Salt Compositions and RH_d: Geochemical modeling of seawater evaporation

Brine composition:

- Upon evaporation, salts precipitate and redissolve. Removed salts dictate the composition of remaining brine
- Seawater evolves towards concentrated Mg-Cl brine as NaCl precipitates
- Br and B conserved (but Pitzer database used for these calculations is not qualified for B, and may not be accurate)
- Ca, K, S are mostly removed by minerals, and are very low in the remaining brine.
- *Deliquescence is the reverse of evaporation.*

Precipitated salts:

- *Upon evaporation, several salts precipitate and re-dissolve.*

Final assemblage determines deliquescence RH (RH_d)

- *NaCl (halite)*
- *$MgCl_2{\cdot}6H_2O$ (bischofite)*
- *$MgSO_4{\cdot}2H_2O$ (kieserite)*
- *$KMgCl_3{\cdot}6H_2O$ (carnallite)*
- *$CaSO_4$ (anhydrite)*

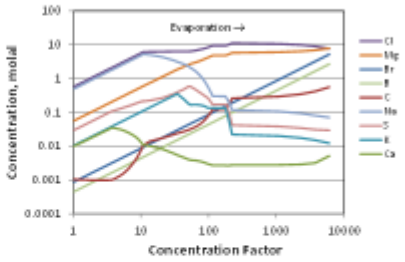

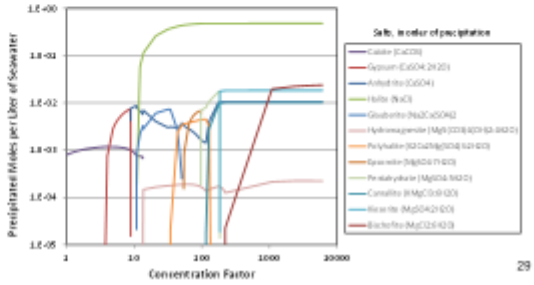

29

Used Fuel Disposition

Predicted Deliquescence of Individual Sea-Salt Minerals and of Assemblage

Deliquescence points:

- **Ca-SO_4 (gypsum or anhydrite): DRH >99%**
- **Mg-SO_4 (four different hydrates): DRH = 93-84%**
- **NaCl: DRH = ~77% at all temperatures**
- **$KMgCl_3{\cdot}6H_2O$ (±sylvite): DRH = 55-49%**
- **$MgCl_2{\cdot}6H_2O$: DRH = 36-29%**
- **$MgCl_2{\cdot}6H_2O$ plus any or all other salts: DRH = ~Same as $MgCl_2{\cdot}6H_2O$**

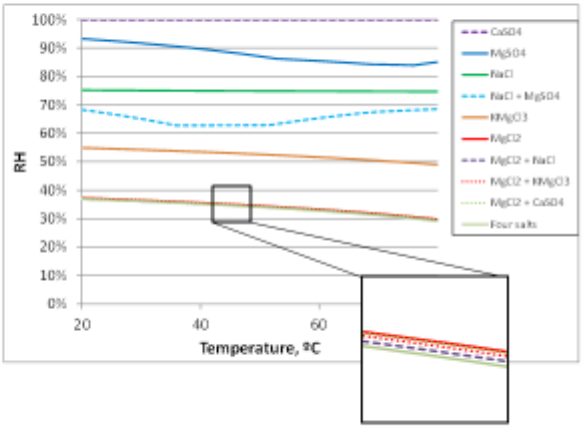

But is deliquescence RH = RH_L? Experimental data indicate that corrosion occurs at lower RH values...

30

Used Fuel Disposition

RH_d vs RH_L (RH Threshold for Corrosion)

Corrosion Below the Deliquescence RH

- *NaCl (DRH 77%)*
  - *Schindelholz et al. (2014b) summarizes several studies--corrosion of mild steel at RH values of 50-58% RH. Their own study showed corrosion as low as 33% RH.*
  - *Once corrosion starts, it can persist to lower RH (at least 27% RH) due to highly deliquescent iron chloride salts.*
- *$MgCl_2$ (DRH ~33%) (Schindelholz et al. 2014c)*
  - *Observed corrosion (mild steel) as low as 11% RH (21ºC), at a loading of 8 µg/cm².*
- *Sea-salts (Schindelholz et al. 2014c)*
  - *Corrosion (mild steel) observed as low as 33% RH (21ºC), at a loading of 16 µg/cm².*
  - *Corrosion observed as low as 23% RH (21ºC), at a loading of 160 mg/m².*
  - *Inferred that at higher sea-salts loadings, results would match $MgCl_2$*
- *Observations of SCC*
  - *NRC (2014)—SCC (304SS) observed as between 20% and 30% RH (variable temperatures), using sea-salts.*
  - *Shirai et al. (2011)—SCC (304SS) observed at 15% RH and 80ºC, using sea-salts.*
  - *Fairweather et al. (2008)—SCC (304SS) observed at 15% RH and 45ºC and 60ºC, using $MgCl_2$.*

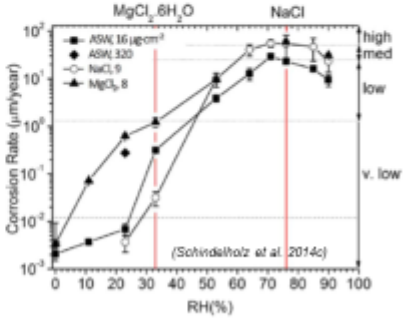

Sea-salt RH_L for SCC of 304 SS poorly constrained, and may be a function of salt load. Could be as low at 15%.

31

Used Fuel Disposition

Absolute Humidity

Possible Range of AH Evaluated for 65 ISFSI Sites by using Data from Nearby Weather Stations

At any given site, AH (here represented as dewpoint) varies both daily and seasonally.

Does corrosion stop if daily fluctuations in RH cross the RH_L? Quite possibly not (Schindleholz et al., 2014); but it may stop if seasonal variations are large enough.

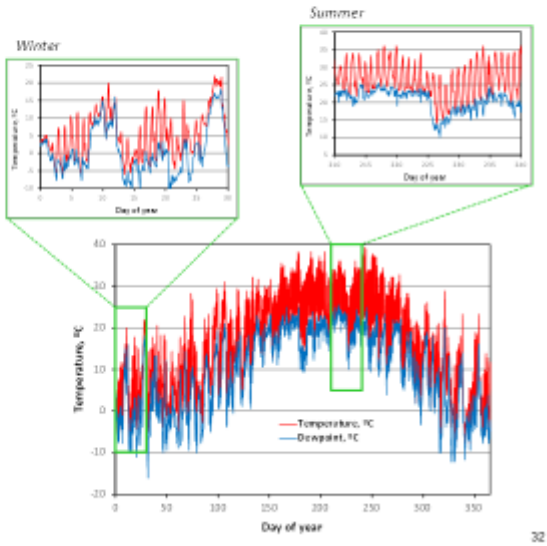

32

Used Fuel Disposition

What about AH?

Possible Range of AH Evaluated for 65 ISFSI Sites by using Data from Nearby Weather Stations

NRC/CNWRA (2014) suggested 30 g/m^3 was an upper limit for AH, based on meteorological monitoring data.

Weather data from 65 ISFSI sites, collected for the SNL probabilistic SCC model, confirm this is true.

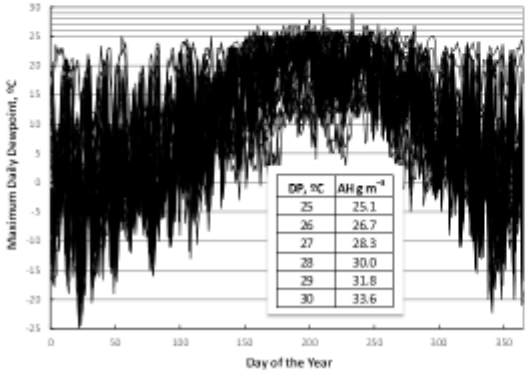

DP, °C	AH g m^{-3}
25	25.1
26	26.7
27	28.3
28	30.0
29	31.8
30	33.6

Average yearly dewpoint may be a better indicator of time of wetness. Dominant control on average dewpoint? Latitude (~ average yearly temperature).

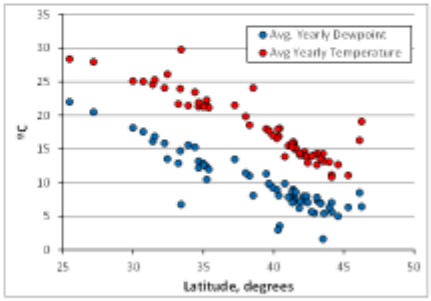

30 g/m^3 is a reasonable upper limit for AH

33

Used Fuel Disposition

Given AH and RH_L, what is the temperature range at which corrosion can occur?

The actual RH_L has a big effect on the potential maximum temperature for corrosion. Max. T. in turn affects:

- Timing of corrosion initiation as the canister cools (lower RH_L equals earlier corrosion)
- Total time-of-wetness – earlier initiation, and less chance of dryout during daily/seasonal variations in AH
- Corrosion rate (pitting and crack growth rates), if thermally activated. Decreasing initial T from 63ºC to 54ºC changes initial CGR by about a factor of 2.

Considering uncertainty in RH_L, the maximum temperature for atmospheric chloride-induced SCC is poorly defined, but is likely to be in the range of 55º to 65ºC(?). No operational experience??

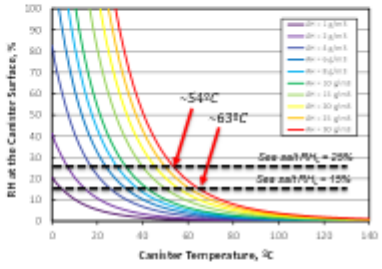

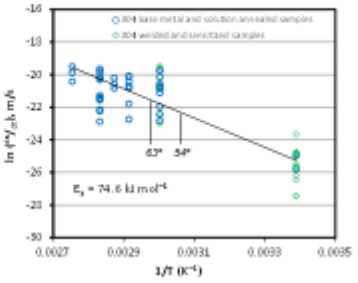

34

Used
Fuel
Disposition

Evolution of Waste Package Surface Temperatures

35

Used
Fuel
Disposition

Waste Package Surface Temperatures: Evolution and Variation with Surface Location

Horizontal Storage System Thermal Model (PNNL 2012)

- Calvert Cliffs NUHOMS HSM-15 (24 PWR) storage module
- CFD model provides temperature map of canister surface, internals; map of ventilation velocities through overpack; thermal response times
- Results:
  - *Huge temperature range (>90°C) on the surface*
  - *High advective flow rates through the overpack are very effective at cooling the canister*
  - *Seasonal temperature fluctuations correspond to similar-magnitude container surface temperature fluctuations*

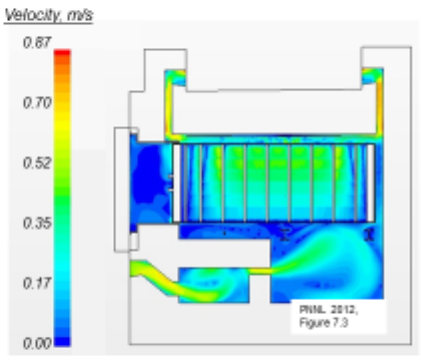

Modeled airflow through the overpack

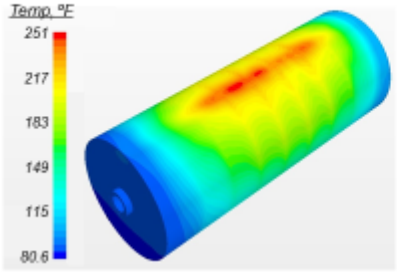

Modeled canister surface temperatures, after ~19 years in dry storage (~7.61 kW)

36

Used Fuel Disposition

Evolution of Surface Temperatures:
Thermal Model, Horizontal Canister

Horizontal canister model. 24 kW initial heat load *(actual canisters are generally loaded with a much lower heat load)*

- Evaluate temperature evolution at 35 points on the canister surface
- Heat load decays rapidly, and advective cooling is effective. Some canister surface locations are below 50°C immediately, and a significant fraction of the canister surface is below 50°C within 10-20 years after emplacement.

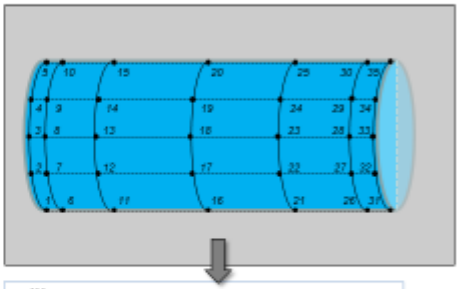

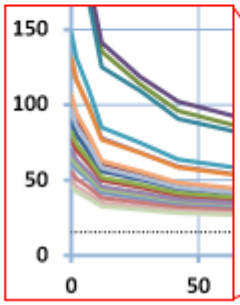

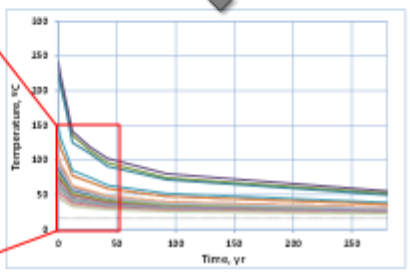

…and most packages are loaded well below the maximum heat load.

37

Used Fuel Disposition

Evolution of Surface Temperatures:
Thermal Model, Horizontal Canister

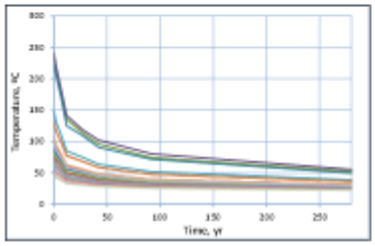

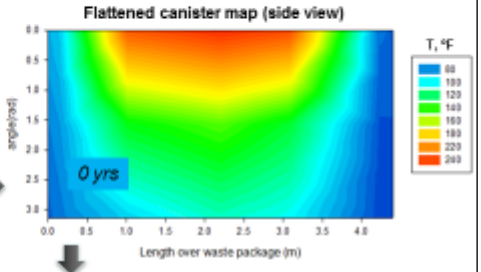

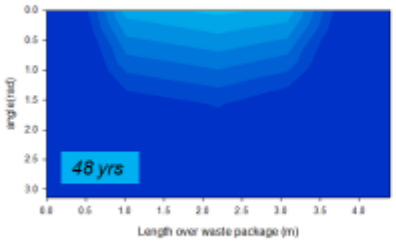

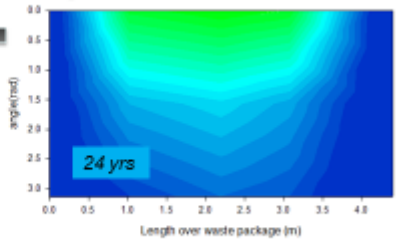

38

Used Fuel Disposition

Evolution of Surface Temperature:
Thermal Model, Horizontal Canister

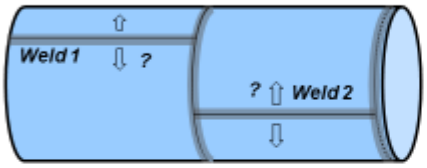

Weld Locations: we anticipate SCC will occur at welds due to high weld residual stresses

Welds:

- Longitudinal welds: 2, location uncertain
- Circumferential center weld
- End-plate weld *(on vertical canisters only)*

Canisters are not "clocked" when they are placed in overpacks. Longitudinal weld locations are uncertain.

However, Efficient passive cooling means that some fraction of the welds (regardless of placement) will rapidly reach temperatures low enough to allow deliquescence.

Flattened canister temperature map, 0 yrs

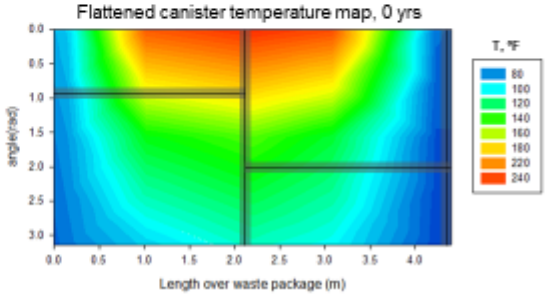

39

Used Fuel Disposition

Evolution of Surface Temperature:
Measured Data, Vertical Canister

Vertical Canister, Diablo Canyon

- **HOLTEC HISTORM 100, Version B**
  - 32 PWR, loaded with high-burnup fuel
  - Decay heat 20.1 kW at loading
- **Inspection after 2 years**
  - Dust samples collected and surface temperatures measured
  - Decay heat 17.1 kW at inspection

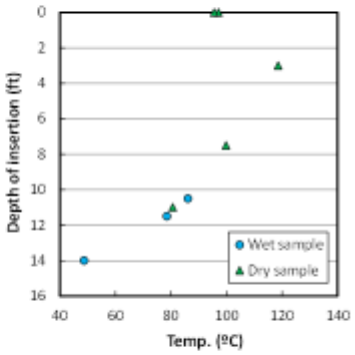

Lower ~3 feet of the canister already cool enough for deliquescence after 2 years *(remember that there is a side-penetrating baseplate weld on vertical canisters).*

40

Used
Fuel
Disposition

Brine Properties as a Function of Salt Load, T and RH

41

Used
Fuel
Disposition

Environmental Parameters for Pit Growth Model

Chen and Kelly (2010): Max pit size is a function of the maximum cathode current.

Max. cathode current

Brine conductivity

Brine layer thickness

Electrochemical term (from cathodic polarization curve)

$$\ln I_{c,max} = \frac{4\pi k W_L \Delta E_{max}}{I_{c,max}} + ln\left[\frac{\pi e r_a^2 \int_{E_{corr}}^{E_{rp}} (I_c - I_p) dE}{\Delta E_{max}}\right]$$

42

Used Fuel Disposition

Brine Properties

Brine layer thickness

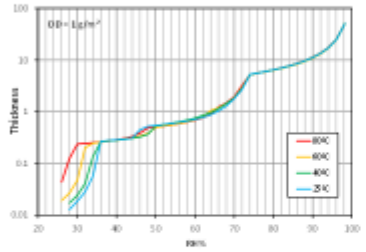

Brine Conductivity

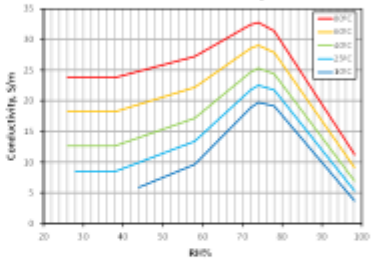

Thickness × Conductivity = (∝ Conductance?)

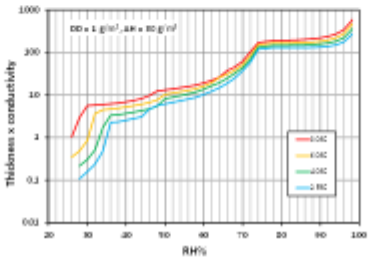

43

Used Fuel Disposition

Brine Properties

Effect of Salt Load

Dotted lines represent the maximum RH possible at the listed temperature

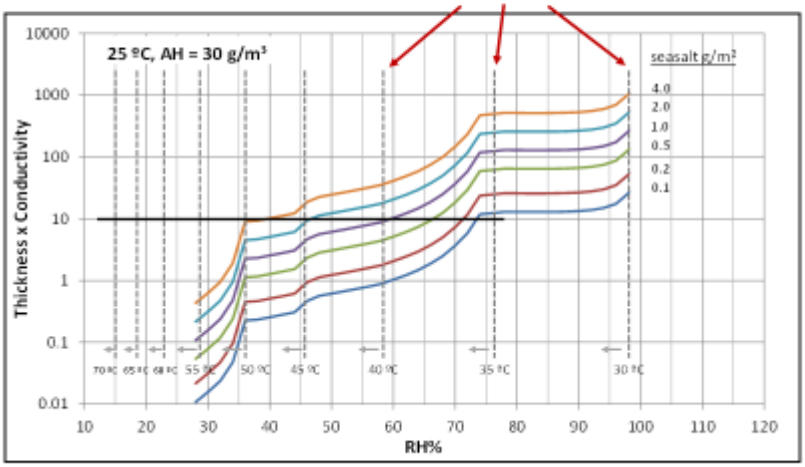

44

Used Fuel Disposition

Brine Properties

Electrochemical data? Measurements in progress.

Chloride concentration and pH change little below the point of halite saturation, but predicted chloride activities change greatly. Large changes in cathodic polarization curve?

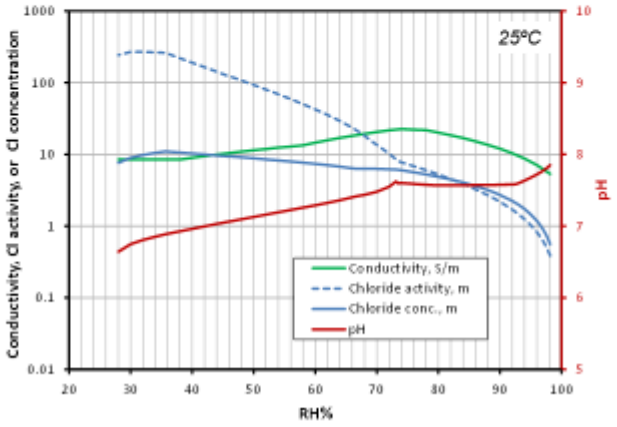

45

Used Fuel Disposition

Summary

- Interim storage systems commonly consist of welded 304 SS canisters in passively ventilated concrete/steel overpacks. Salt aerosols enter with airflow, and are deposited on canister surfaces.
- Chloride-rich sea-salt aggregates have been observed on canister surfaces at near-marine ISFSI sites, and over time are likely to build up to significant concentrations. Breaking waves and shoreward winds are likely important (Diablo—yes, Calvert and Hope Creek—no).
- Decay heat raises canister surface temperatures above ambient, but effective passive cooling means temperatures vary widely over the canister surface.
- Maximum AH values are consistently around 28-30 g/m^3, regardless of ISFSI location. However, mean yearly values are strongly controlled by latitude (and mean temperature).
- Combined canister surface temperature and AH data suggest that some parts of the canister surface become cool enough (<~65°C?) to allow salt deliquescence and corrosion soon after emplacement into storage.
- RH_L? For sea-salts, may be a function of salt load (minimum brine volume required). $MgCl_2$ data suggest it may be may be as low as ~15%, *if sufficient sea-salt is present.*

46

APPENDIX E: MAXIMUM PIT SIZE MODEL (R. KELLY)

CENTER FOR ELECTROCHEMICAL SCIENCE AND ENGINEERING

Department of Materials Science and Engineering

UNIVERSITY of VIRGINIA ENGINEERING

Prediction of Maximum Pit Size from Atmospheric Exposure of Metallic Materials

R.G. Kelly, M. Woldemedhin, J. Srinivasan, Z.Y. Chen

Department of Materials Science and Engineering

University of Virginia

SCC Workshop
Sandia National Laboratory
March 24-25, 2016
Albuquerque, NM

Most popular pit growth laws are power laws

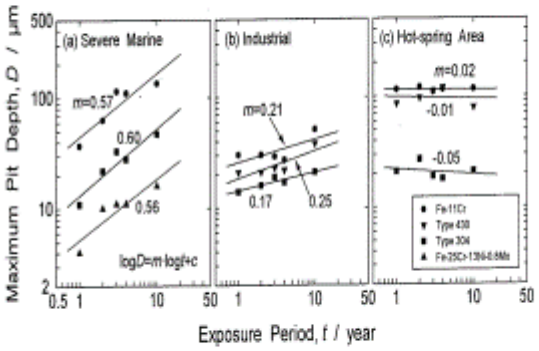

I. Muto et al., Proc. of Int. Symp. On Plant Aging and Life Pred. of Corr. Structures, May 1995, Sapporo, Japan

$d = At^m$

m = power law exponent

Exponents as high as 0.6

The problem with power laws for long-term prediction is the needed precision

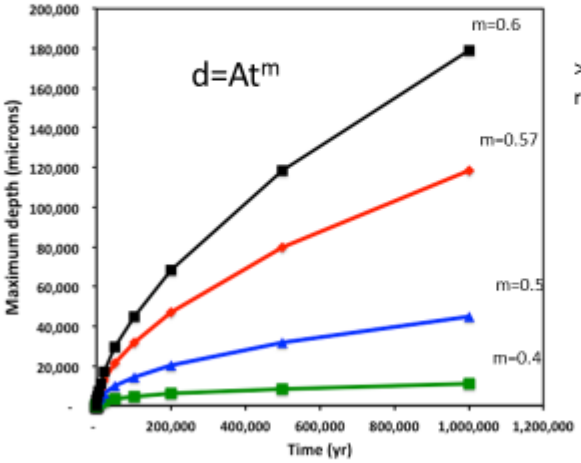

10 cm

> Factor of 40 for observed range of m

Similar sensitivity to A

A=45 from Muto fit for severe marine site for up to 10 y

It is an issue even at shorter times

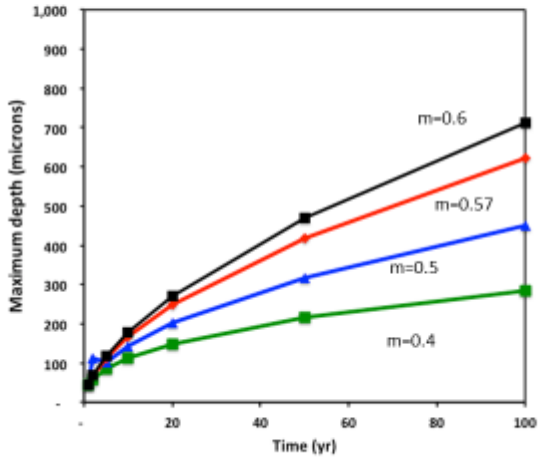

$d=At^m$

Limiting pit sizes are often seen for atmospheric exposures

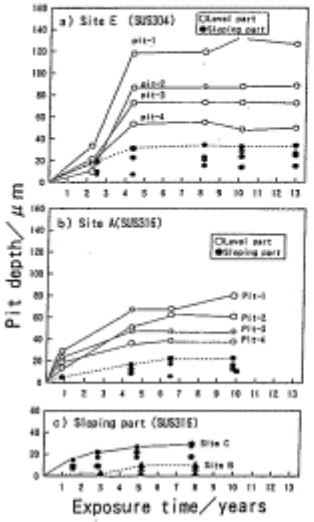

- Can take several years to reach plateau
- Value of plateau depends on alloy, environment

M. Nakata, N. Ono, Y. Usada, *Corrosion Engineering*, 46, 655-666 (1997)

Why would there be a limiting pit size?

- In service, materials are at their open circuit potential
- Under open circuit conditions, the conservation of charge dictates

$$\Sigma I_c = \Sigma I_a$$

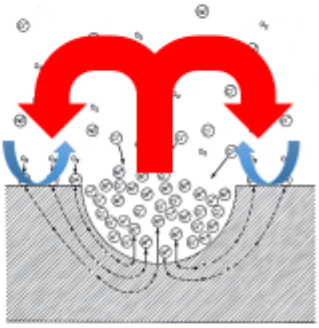

- The anodic and cathodic reactions are spatially separated during pitting
- As pits grow, more cathodic current is needed

Consider localized corrosion as a galvanic couple to define limits

- Cathode Current Capacity ($I_{cath,max}$)
  - The total cathodic current that a wetted surface *could* provide to support a growing crevice or pit
  - Provides **upper** bound for cathode current
- Anode Current Demand (I_{LC})
  - The total anodic current that an active localized corrosion site *requires* to maintain its critical chemistry
  - Provides **lower** bound for anode current for stable site

The combination of the material and environmental conditions will determine whether stable localized corrosion is **possible**

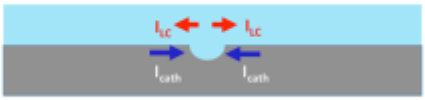

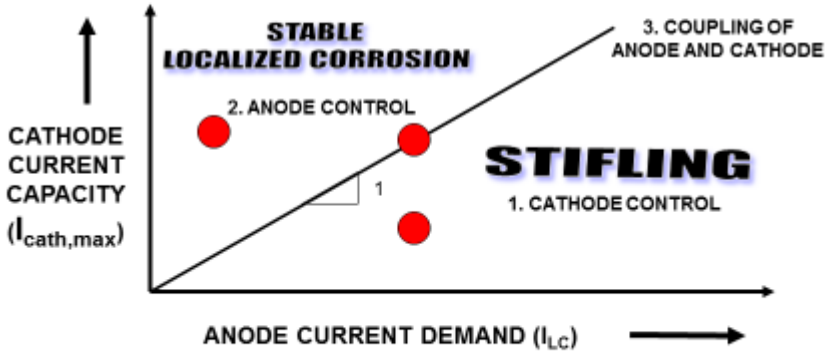

Cathode Current Capacity ≥ Anode Current Demand for stability

What limitations might exist at each electrode?

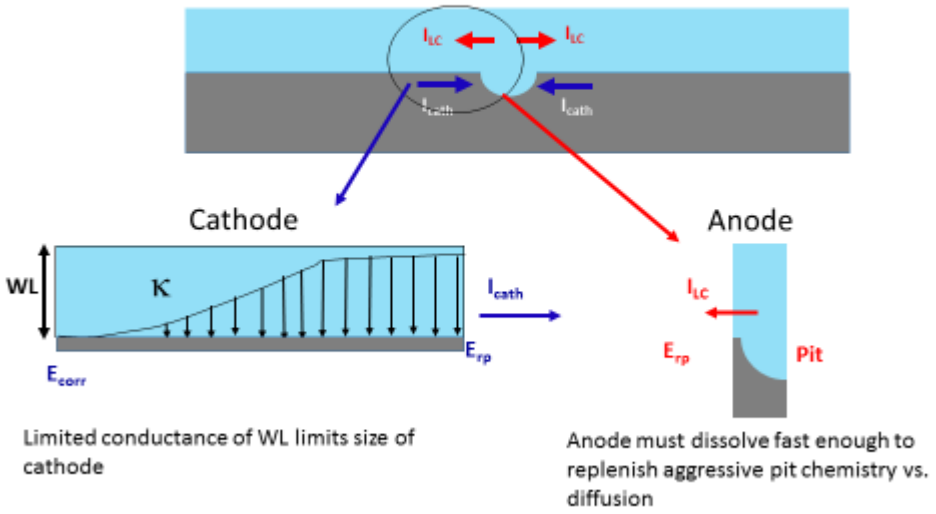

Limited conductance of WL limits size of cathode

Anode must dissolve fast enough to replenish aggressive pit chemistry vs. diffusion

Consider the cathode

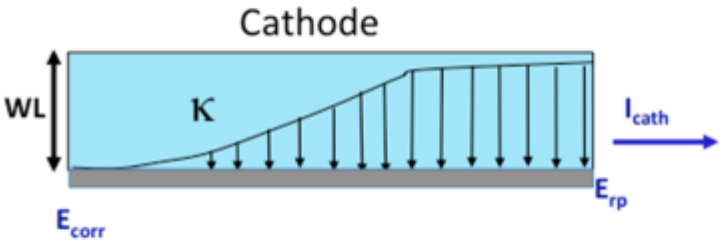

Goal is to calculate the HIGHEST value of I_{cath} possible given WL, κ, and cathodic kinetics = $I_{cath,max}$

Concept of an equivalent cathode

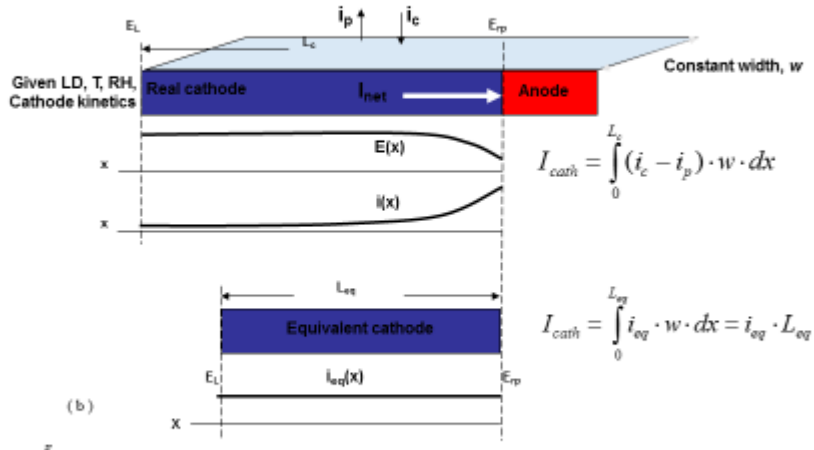

$$I_{cath} = \int_0^{L_c} (i_c - i_p) \cdot w \cdot dx$$

$$I_{cath} = \int_0^{L_{eq}} i_{eq} \cdot w \cdot dx = i_{eq} \cdot L_{eq} \cdot w$$

$$i_{eq} = \frac{\int_{E_L}^{E_{rp}} (i_c - i_p) \cdot dE}{E_L - E_{rp}}$$ = average current density over $E_L < E < E_{rp}$

Derivation of I_{cath} Equation for Circular Cathode

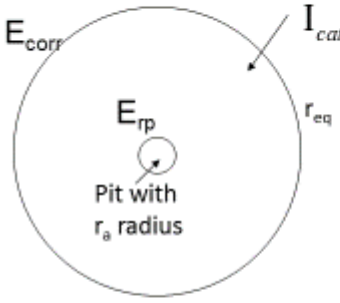

$$I_{cath,max} = i_{eq} \cdot \pi \cdot r_{eq}^2$$

$$i_{eq} = \frac{\int_{E_L}^{E_{rp}} (i_c - i_p) \cdot dE}{E_L - E_{rp}}$$

$$\Delta E = E_L - E_{rp} = \int_{r_a}^{r_{eq}} dV = \frac{i_{eq} \cdot r_{eq}^2}{2\kappa \cdot WL} \cdot \left[\ln\left(\frac{r_{eq}}{r_a}\right) - \frac{1}{2} \right]$$

$$\ln I_{cath,max} = \frac{4\pi \cdot \kappa \cdot WL \cdot (E_{corr} - E_{rp})}{I_{cath,max}} + \ln\left(\frac{\pi \cdot e \cdot r_a^2 \cdot \int_{E_{corr}}^{E_{rp}} (i_c - i_p) \cdot dE}{E_{corr} - E_{rp}}\right)$$

Z.Y. Chen and R.G. Kelly. *J. Electrochem. Soc.* 157 (2) C69-C78 (2010)

Comparison of I_{net} from FEM and Equation Calculation for Circular Cathode

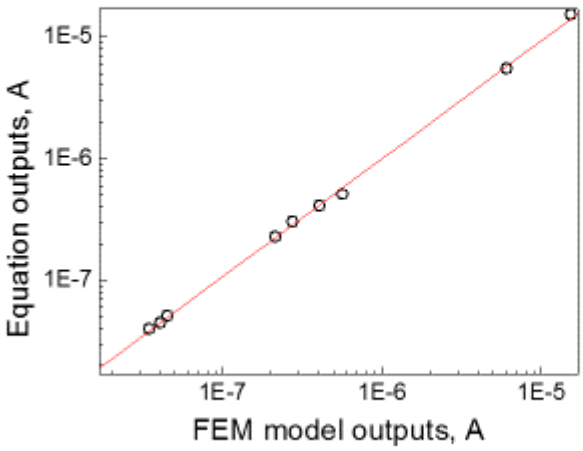

- r_a = 10 µm
- 316L
- 25 °C
- E_{rp} = -0.4 V
- $i_p = 10^{-4}$ A/m^2

Cathode conditions determined by ohmic drop and cathodic kinetics, as influenced by WL

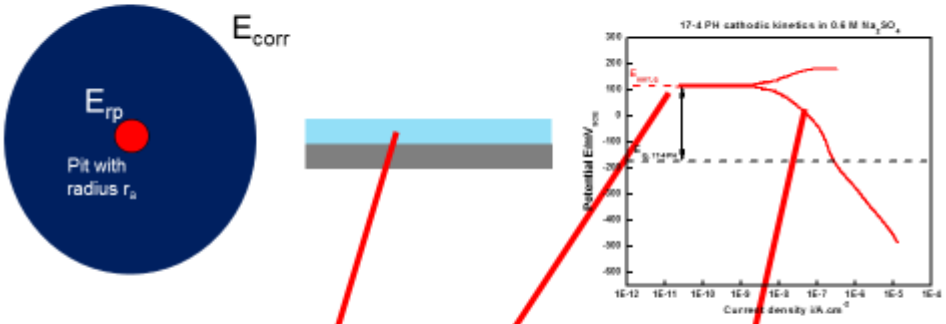

$$\ln I_{cath,max} = \frac{4\pi \cdot \kappa \cdot WL \cdot (E_{corr} - E_{rp})}{I_{cath,max}} + \ln\left(\frac{\pi \cdot e \cdot r_a^2 \cdot \int_{E_{corr}}^{E_{rp}} (i_c - i_p) \cdot dE}{E_{corr} - E_{rp}}\right)$$

Relate WL and κ to measurable parameters: RH and Loading Density (LD)

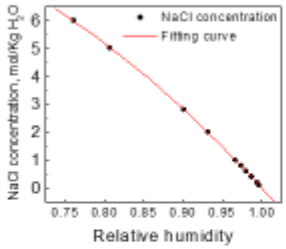

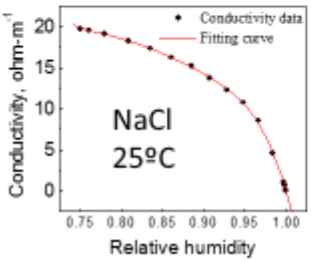

- At RH > DRH, equilibrium concentration of salt is determined by RH
- Mass of salt (LD) available then determines WL
- Conductivity determined by molality

$$WL = \frac{LD(1 + m_{Salt}(RH,T) \cdot MW_{salt})}{m_{salt}(RH,T) \cdot \rho(RH,T) \cdot MW_{salt}}$$

Create a $I_{cath,max}$ Surface for Circular Cathode of SS 316L

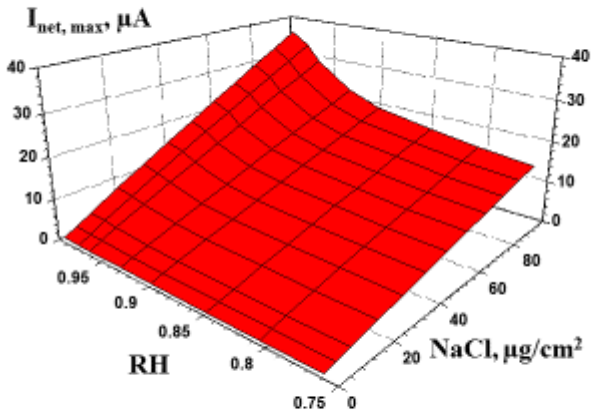

r_a = 10 µm and T = 25 °C

Why would the $I_{cath,max}$ expression be bounding?

- Assumes fixed chemistry and kinetics
  - pH increases with time, kinetics slow
- Assumes no particulate
  - Increases effective resistivity
- Assumes no limitations on cathode length
  - e.g., surface tension, surface curvature

Galvele pit stability product allows critical anode conditions to be determined

- Pit stability product (i•x) must be exceeded for stable localized corrosion:
  - i•x is required to maintain C^+ at base of pit
    - i =dissolution current density
    - x = depth of pit
- If $i \bullet x < (i \bullet x)_{crit}$, pit repassivates
- For 2-D, **I/r** is the pit stability product

$$I_{LC} = (I/r)_{crit} * r_{pit}$$

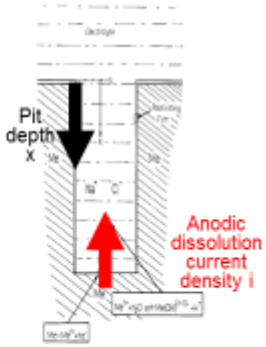

J.R. Galvele, JECS, 123(4), 1976

Is I_{LC} bounding?

- Yes, for hemispherical pit
  - Extendable to other geometries
- Measurement of $(i \bullet x)_{crit}$
  - Usually done for salt-film-covered surface
  - If salt film not required, $(i \bullet x)_{crit}$ would be < $(i \bullet x)_{sf}$
  - Degree of saturation required generally quoted as 60-80%

Individual expressions for I_{LC} and $I_{cath,max}(r_{pit})$ are combined to determine maximum pit size

$$\ln I_{cath,max} = \frac{A}{I_{cath,max}} + \ln(B \cdot r_{pit}^2)$$

$$I_{LC} = (I_A/r)_{crit}\, r_{pit}$$

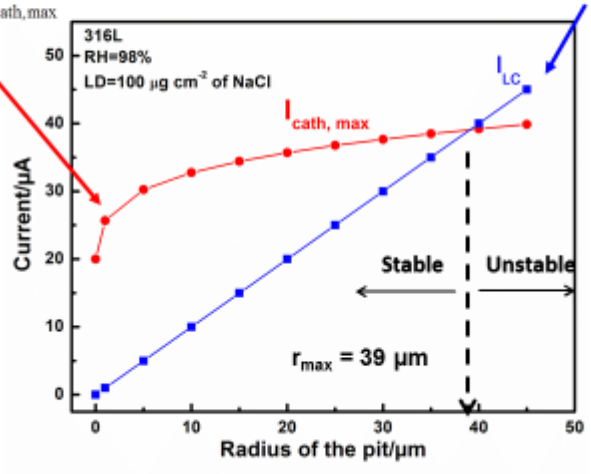

The crazy aunt in the basement is how to obtain critical parameters

- Salt loading density
  - Field measurements
  - Use as parameter in modeling
- RH dependence of concentration
  - Thank heavens for thermodynamics
- Cathodic kinetics
  - Given above, determine in appropriate solution, account for increased O_2 diffusion limited current at low WL
- Pit stability product
  - Artificial pit
- Repassivation potential
  - Artificial pit

Artificial pit measurements give both $(i \bullet x)_{sf}$ and E_{rp}

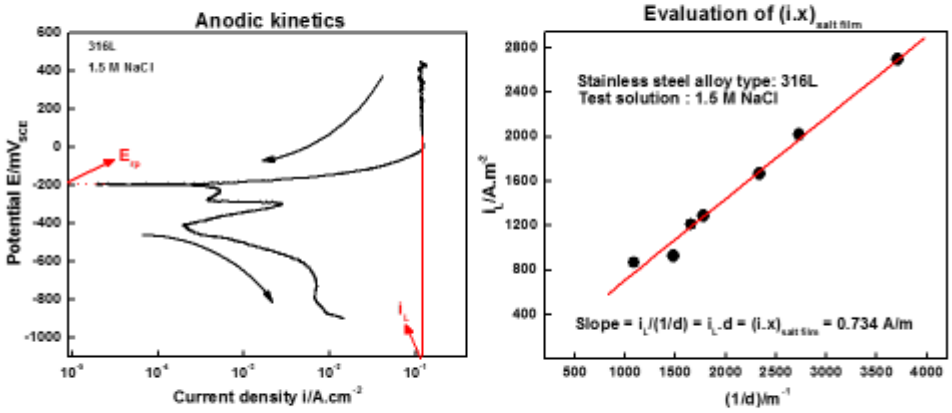

$$i_L = zFD\Delta C/d = (zFD\Delta C) \bullet (1/d)$$

$$(i^*x)_{crit} = f * (i^*x)_{salt\ film}$$

Initial comparisons to literature are encouraging for seacoast exposures

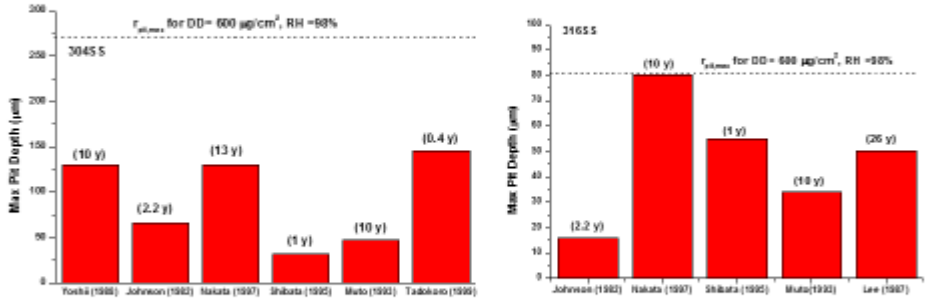

Marine atmosphere exposures for up to 26 y show limiting pit sizes

Z.Y. Chen and R.G. Kelly. *J. Electrochem. Soc.* 157 (2) C69-C78 (2010)

Approach to Validation

- Material and Environment
  - 316
  - Thin film of $FeCl_3$
- Experimental
  - Anodic kinetic parameters via artificial pit measurements
  - Cathodic kinetic parameters via **Cl-free** polarization curves
  - Plasma-cleaned 6.5 cm^2 surfaces exposed up to 7 days to thin layer of $FeCl_3$, assess pit dimensions with profilometry
- Computational
  - Calculate maximum cathode current using method of Chen et al.
  - Calculate anode current for hemispherical pit

M.T. Woldemedhin, M. E. Shedd, R. G. Kelly, *J. Electrochem. Soc. 161(8), 2014.*

Typical data from artificial pit measurements

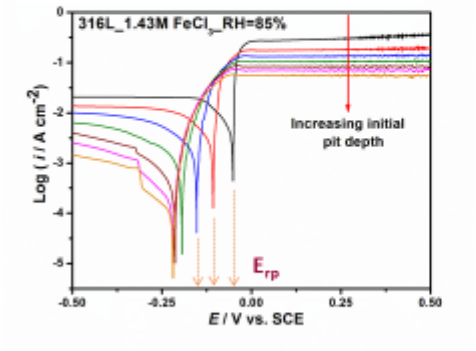

$$i_L d = nFDC_S = (ix)_{saltfilm}$$

Cathodic Kinetics of Fe^{3+} Reduction on SS

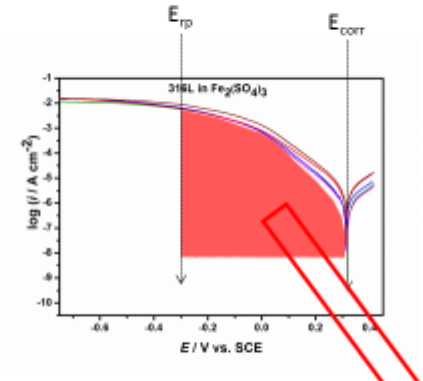

$$\ln I_{cath,max} = \frac{4\pi \cdot \kappa \cdot WL \cdot (E_{corr} - E_{rp})}{I_{cath,max}} + \ln\left(\frac{\pi \cdot e \cdot r_a^2 \cdot \int_{E_{corr}}^{E_{rp}} (i_c - i_p) \cdot dE}{E_{corr} - E_{rp}}\right)$$

Extract needed anodic parameters from artificial pit measurements

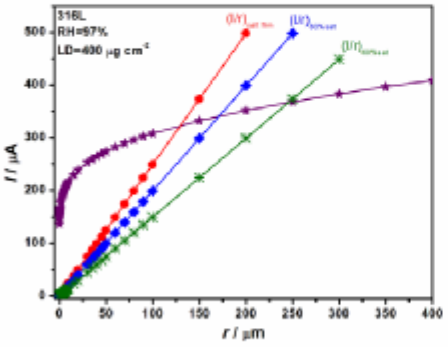

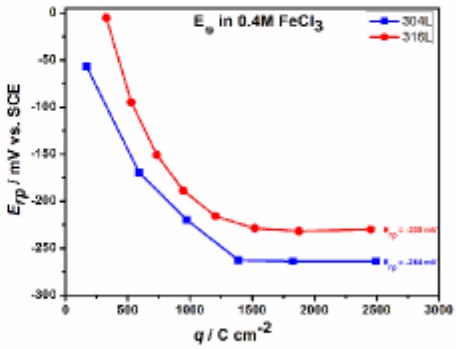

Maximum pit size calculation predicts bounds as a function of assumed degree of saturation required

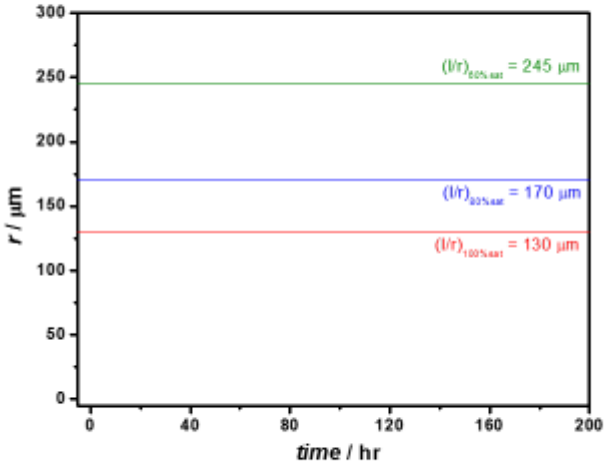

316L

Do the experiment:
RH=97%, LD=400 mg cm^{-2}, t up to 7 d

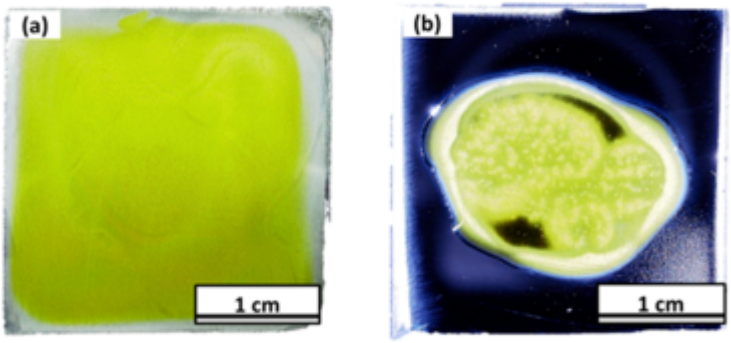

Plasma cleaned

Not

Hemispherical pits quickly reach a limiting size

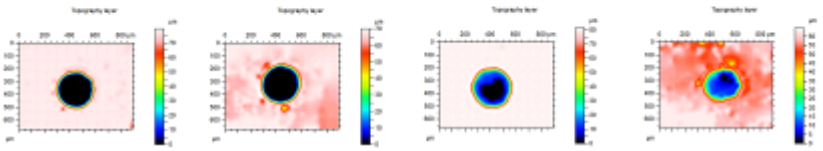

6 h

24 h

48 h

168 h

…… and don't grow under a salt film

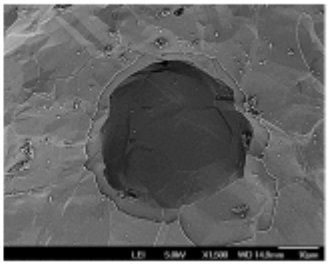

Maximum pit size calculation bounds experimental observations for thin film case

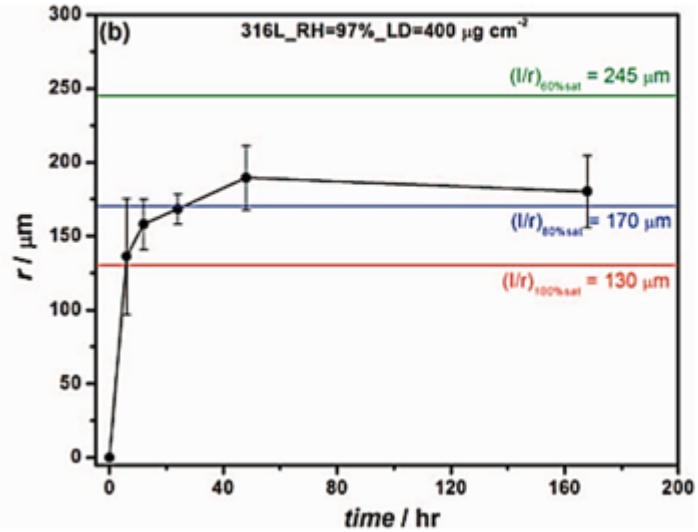

Exposure results are bounded by critical stability criteria of 70-80%

M.T. Woldemedhin, M. E. Shedd, R. G. Kelly, *J. Electrochem. Soc. 161(8), 2014.*

Pit density > 1 per $A_{cath,\,max}$ limits pit size, too

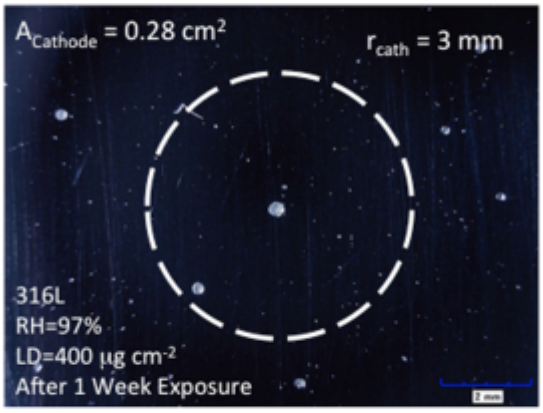

Use $I_{cath,max}$ equation to calculate R_{min} = minimum cathode size

Summary and Conclusions

- Maximum pit size approach determines a physical upper bound on the size of a hemispherical pit grown under a thin electrolyte film
- Critical parameters can be determined experimentally or via thermodynamics to allow application to atmospheric exposure
- Maximum pit size approach can be validated with thin $FeCl_3$ film data
- Demonstrates that even under these conditions, a salt film is not required for pit growth

Acknowledgements

- Office of the Undersecretary of Defense Technical Corrosion Collaboration via the USAFA Contract FA7000-10-2-0011.
- Center for Surface Technology, Rolls-Royce Corporation, Indianapolis, IN.

DISTRIBUTION

1 Dr. Peter Andresen
GE Corp Research & Development
1 Research Circle K1 3A39
Schenectady, NY 12309-1027
518 /387-5929

1 Dr. Robert G. Kelly
Dept. of Materials Science and Engineering
University of Virginia
Charlottesville, VA 22904-4745
434/982-5783

1 Dr. John R. Scully
Dept. of Materials Science and Engineering
University of Virginia
Charlottesville, VA 22904-4745
434/982-5786

1 Dr. Alan Turnbull
Electrochemistry and Corrosion Group
National Physical Laboratory
Teddington, Middlesex
TW11 0LW

1 James F. Dante
Southwest Research Institute

1	MS0888	David G. Enos	1852
1	MS0889	Coby L. Davis	1852
1	MS0747	Ken B. Sorenson	6223
1	MS0779	Charles R. Bryan	6225
1	MS0779	Sylvia J. Saltzstein	6225
1	MS0899	Technical Library	9536 (electronic copy)


Sandia National Laboratories